UNIVERSITY OF HAWAII
LIBRARY

The
PHILOSOPHICAL MAGAZINE

FIRST PUBLISHED IN 1798

Vol. 1 Eighth Series No. 8 August 1956

A Journal of Theoretical Experimental and Applied Physics

EDITOR
PROFESSOR N. F. MOTT, M.A., D.Sc., F.R.S.

EDITORIAL BOARD
SIR LAWRENCE BRAGG, O.B.E., M.C., M.A., D.Sc., F.R.S.
SIR GEORGE THOMSON, M.A., D.Sc., F.R.S.
PROFESSOR A. M. TYNDALL, C.B.E., D.Sc., F.R.S.

PRICE £1 0s. 0d.
Annual Subscription £10 10s. 0d. payable in advance

ALERE FLAMMAM.
Printed and Published by
TAYLOR & FRANCIS LTD.
RED LION COURT, FLEET STREET, LONDON, E.C.4

The Scientific Work of René Descartes

(1596–1650)

By

J. F. SCOTT, B.A., M.Sc., Ph.D.

With a foreword by H. W. TURNBULL, M.A., F.R.S.

This book puts the chief mathematical and physical discoveries of Descartes in an accessible form, and fills an outstanding gap upon the shelf devoted to the history of philosophy and science.

There is to be found in this volume the considerable contribution that Descartes made to the physical sciences, which involved much accurate work in geometrical optics and its bearing upon the practical problem of fashioning lenses, as also the deeper problems of light and sight and colour. The careful treatment that Dr. Scott has accorded to this work of Descartes is welcome, is well worth reading and will be an asset to all libraries. Publication is recommended and approved by the Publication Fund Committee of the University of London

212 *pages*, 7" × 10", *amply illustrated*

Price £1 - 0 - 0 net **First published July 1952**

Printed & Published by
TAYLOR & FRANCIS, LTD.
RED LION COURT, FLEET STREET, LONDON, E.C.4

CONTENTS OF No. 8.

Page

LXXI. The Propagation of Stress Pulses in Viscoelastic Solids. By H. Kolsky, Imperial Chemical Industries Research Department, Welwyn 693

LXXII. Creep of Alpha Uuranium During Irradiation with Neutrons. By A. C. Roberts, Research Laboratories of the General Electric Co. Ltd., Wembley, and A. H. Cottrell, Atomic Energy Research Establishment, Harwell 711

LXXIII. Scattering of Phonons and Electrons by Imperfections in a Metal. By K. Mendelssohn, F.R.S., and H. Montgomery, Clarendon Laboratory, Oxford 718

LXXIV. Columnar Recombination in Nitrogen. By E. H. Bellamy and W. R. Hogg, Department of Natural Philosophy, University of Glasgow 722

LXXV. The Low Frequency Spectrum of the Cygnus (19N4A) and Cassiopeia (23N5A) Radio Sources. By R. J. Lamden and A. C. B. Lovell, Jodrell Bank Experimental Station, University of Manchester. 725

LXXVI. The Thermal and Electrical Conductivity of Lithium at Low Temperatures. By H. M. Rosenberg, The Clarendon Laboratory, Oxford 738

LXXVII. The Thermal Expansion of Aluminium at Low Temperatures as Measured by an X-ray Diffraction Method. By B. F. Figgins, G. O. Jones and D. P. Riley, Department of Physics, Queen Mary College, London 747

LXXVIII. Soft X-Ray Spectroscopy of Solid Solutions of Aluminium and Magnesium. By B. Gale and J. Trotter (Communication from National Physical Laboratory) 759

LXXIX. Remanent Magnetism of some Dolerites, Basalts and Volcanic Tuffs from Tasmania. By Mary Almond and J. A. Clegg, Department of Physics, Imperial College of Science and Technology, London and J. C. Jaeger, Department of Geophysics, Australia National University, Canberra, A.T.C. 771

LXXX. Correspondence :—

- The Migration of Copper Atoms on the Surface of Silver. By R. B. Kehoe, R. C. Newman and D. W. Pashley, Physics Department, Imperial College, London 783
- Evidence for Direct Emission of a Pair of γ-rays from the Point of Decay of a K-Meson. By M. S. Sinha and N. C. Das, Bose Institute, Calcutta 785

LXXXI. Reviews of Books 788

***All communications for the Philosophical Magazine should be addressed, post-paid, to the Editors, c/o Messrs. Taylor and Francis, Ltd., Red Lion Court, Fleet Street, London, England.

LXXI. *The Propagation of Stress Pulses in Viscoelastic Solids*

By H. Kolsky ‡
Imperial Chemical Industries Research Department, Welwyn †

[Received December 28, 1955]

Abstract

The propagation of short mechanical pulses along rods of three polymers, polythene, polystyrene and polymethylmethacrylate, has been investigated experimentally. The pulses were produced by the detonation of small quantities of explosive at one end of a rod and a condenser microphone was employed to record the displacement of the opposite end. It is shown that if the response of the material to sinusoidal stresses over a wide frequency range is known, the pulse shapes can be predicted accurately by means of a numerical Fourier synthesis. Further, that where the damping loss is not too large and is constant over a wide frequency range, as it is for many polymers, a general solution of the problem can be obtained which gives the pulse shape for all such polymers and for all distances of travel. Some experiments on pulses through blocks of plastic are also described.

§ 1. Introduction

The mechanical behaviour of high polymers, such as rubbers and plastics, depends very markedly on the rate at which they are deformed and, in recent years, the stress–strain relations of these materials under dynamic loading has received considerable attention both experimentally and theoretically. For small deformations the relation between stress and strain can generally be expressed as a linear differential equation, involving the stress, the strain and their derivatives with respect to time, so that a stress which varies sinusoidally with time produces a sinusoidally varying strain. The phase difference between stress and strain is a measure of the internal friction of the material. The rather involved theory of linear viscoelastic behaviour has been ably summarized in books by Leaderman (1943) and Gross (1953) and relations derived in these will be used below. It is the purpose of this paper to describe some experiments on the propagation of pulses of short duration along rods of high polymers and to discuss the interpretation of the results in terms of the known viscoelastic properties of these materials. Some preliminary experiments have been described earlier (Kolsky 1954 a).

---

† Communicated by the Author.

‡ Now at Brown University, Providence, Rhode Island, U.S.A.

For nearly all high polymers it is found that the elastic modulus, i.e. the ratio between the stress amplitude and the strain amplitude for sinusoidal vibrations, increases very markedly with increasing frequency whilst the internal friction, which may be defined by the fractional energy loss per cycle $\triangle W/W$ or alternatively by the tangent of the phase lag, tan δ, between stress and strain, changes comparatively little, except in the region when the polymer is at a temperature close to the transition from rubber-like to glass-like behaviour.

If a plane sinuosoidal stress wave travels through a viscoelastic material and its amplitude is $\sigma_0 \cos pt$ at the origin, its amplitude at a distance x from the origin is $\sigma_0 \exp(-\alpha x) \cos p(t-x/c)$, where p is 2π times the frequency, α is the attenuation coefficient and c is the velocity of propagation of the wave, which is given by $(E/\rho)^{1/2}$ where E is the elastic modulus and ρ is the density of the medium. α is related to the loss factor tan δ by the equation

$$\alpha = \frac{p}{4\pi c}(\Delta W/W) = \frac{p}{2c}\tan\delta \text{ (see Kolsky 1953, p. 106).} \qquad . \quad (1)$$

Thus if tan δ is constant the attenuation α increases linearly with the frequency.

When a mechanical pulse is propagated through a viscoelastic solid it is dispersed, as the high frequency components travel faster and are attenuated more rapidly than those of lower frequency. A purely analytic approach to the problem of pulse propagation in a general viscoelastic solid leads to intractable mathematical expressions and several attempts have been made to treat the solid in terms of a simple model. This was first done by Thompson (1933) and subsequently by several other workers including Ricker (1943), Zverev (1950), Eubanks *et al.* (1952), Lee and Kanter (1953) and Glauz and Lee (1954). Whilst these treatments are undoubtedly of theoretical interest and may well have some practical application they suffer from the inherent limitation that the mechanical behaviour of most plastics and rubbers does not conform over more than a very limited frequency range to that of a simple mechanical model. This limitation is discussed fully by Leaderman (1943) and by the author (Kolsky 1953), and figs. 1, 2 and 3 are included here to illustrate the fact. Figure 1 shows the experimental results obtained in this laboratory by Hillier (1949) for the attenuation α and the phase velocity c of sinusoidal waves in a polythene filament. The dynamic measurements were made at frequencies between 1 kc/s and 16 kc/s. The point for ‘ zero frequency ’ was obtained for a stressing time of several seconds. Figure 2 shows the theoretical curves for two simple models, the Maxwell model which consists of a perfectly elastic spring in series with a dashpot which has Newtonian viscosity, and the Voigt model in which the spring is joined across the dashpot. The relations for velocity and attenuation in materials whose mechanical behaviour is given by such models have been discussed earlier (Kolsky 1953, Chap. V). The curves here are plotted non-dimensionally, τ being the characteristic time given by the ratio of the viscosity of the dashpot divided by the elasticity of the spring in each case. (For the Maxwell model τ is termed the *relaxation time* and for the Voigt model τ is the *retardation time*.) The scale for the vertical axis was fixed for the Maxwell curve by plotting

Fig. 1

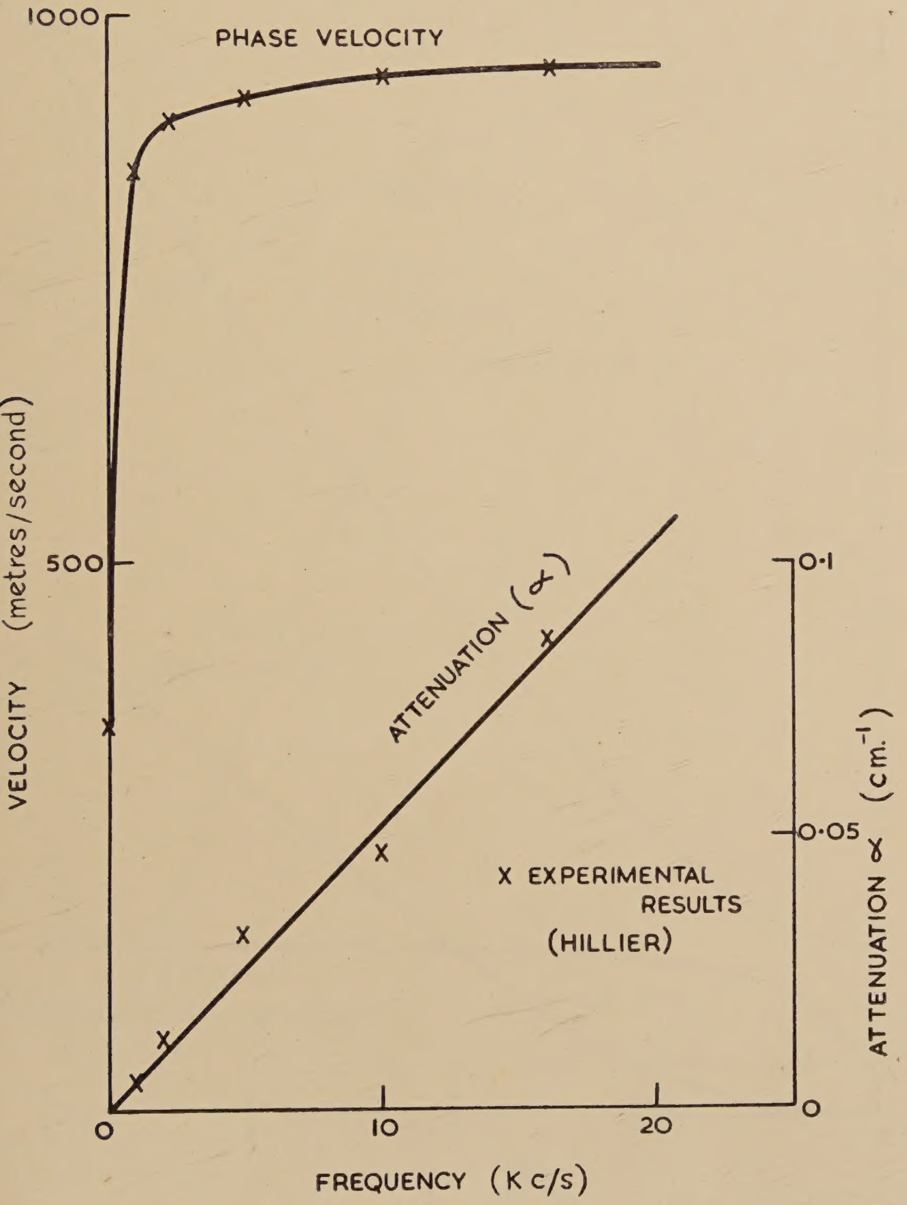

Experimental measurements of attenuation and velocity in polythene filaments at 10°c.

$\alpha/\alpha_{\max}$ and $c/c_{\max}$, whilst for the Voigt solid $c/c_{\min}$ is plotted and α is in arbitrary units. It may be seen that even over a very limited frequency range it is impossible to fit the observed behaviour of a polymer such as polythene to the dispersion curves obtained from such two element

Fig. 2

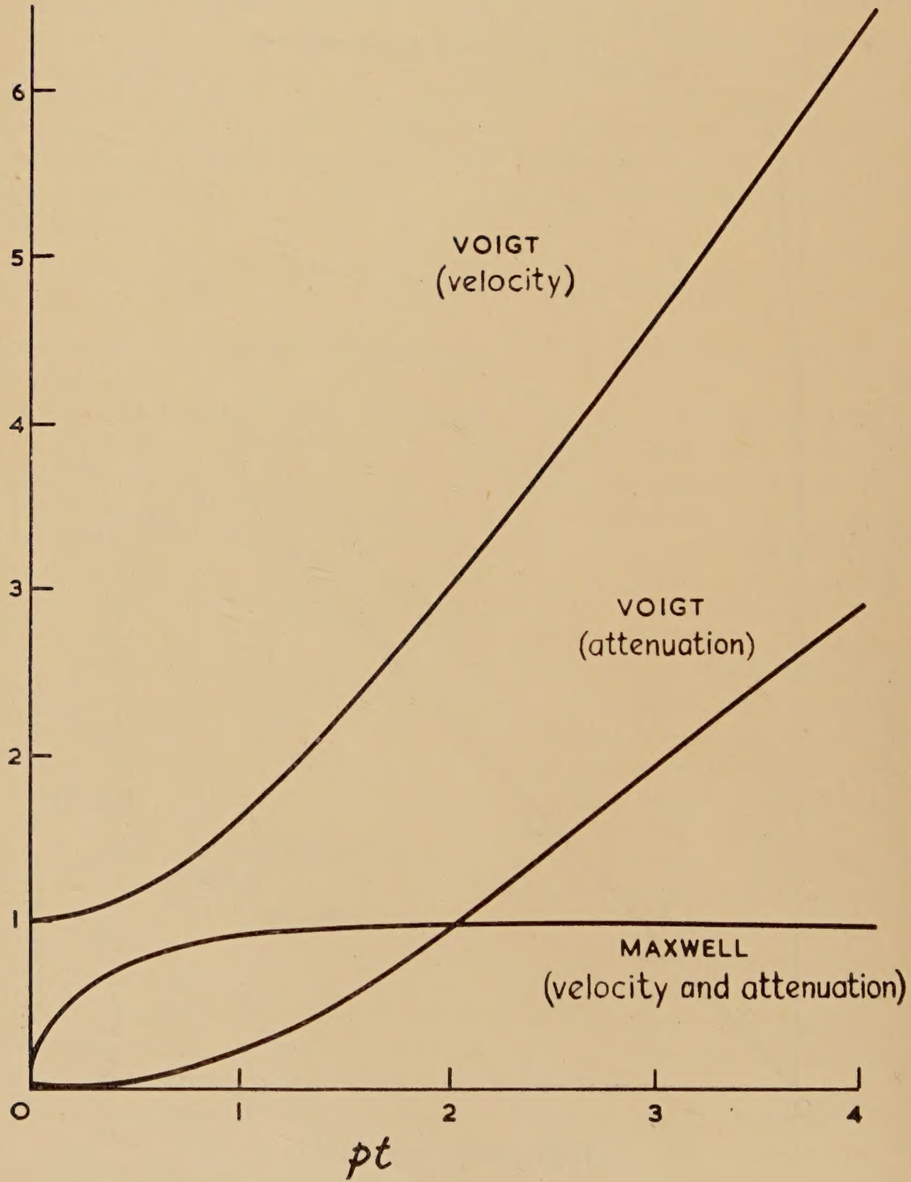

Velocity and attenuation for Maxwell and Voigt solids.

models. Figure 3 shows the corresponding curves for a simple three element model which is sometimes known as the *standard linear solid.* This model can be represented by a second spring in series with a Voigt model and its mechanical behaviour corresponds to the most general

Fig. 3

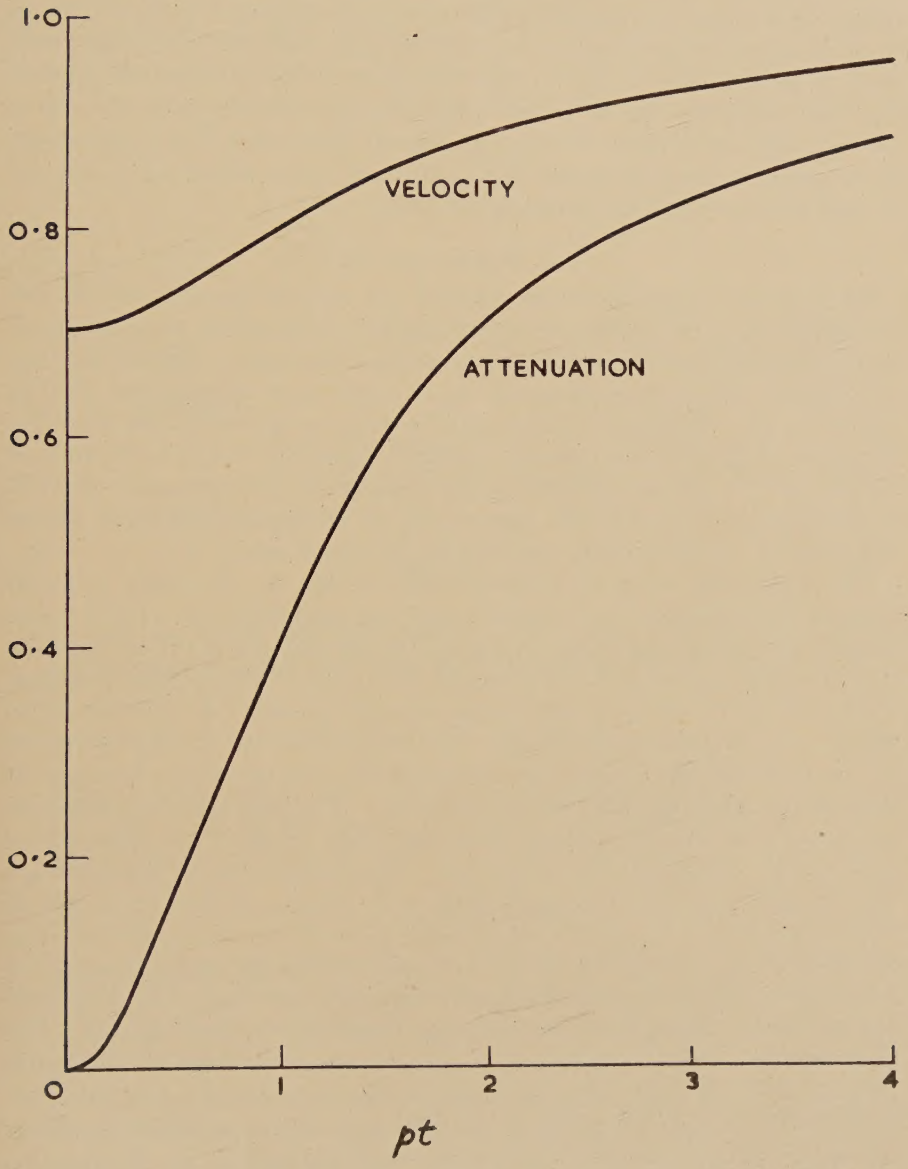

Velocity and attenuation in standard linear solid. Model corresponds to two equal springs in series, across one of which there is a dashpot.

linear equation in stress and strain involving only stress, strain and their first derivatives with respect to time. It may be seen from fig. 3 that such a model gives a somewhat better approximation to the behaviour of a real viscoelastic solid such as shown in fig. 1 but still can only be fitted over a limited frequency range.

In the work which follows it will be shown that it is possible, by numerical Fourier methods, to predict quite accurately the change in shape of a short mechanical pulse as it is propagated along a rod of viscoelastic material, using the measured elastic constants of the material such as those shown in fig. 1. Furthermore, if the assumption is made that the damping ($\tan\delta$) is not large and is constant over the whole relevant frequency range so that α is directly proportional to p, the shape of the pulse can be represented in a ' universal ' form which will apply for all high polymers and all distances of travel.

§ 2. EXPERIMENTAL

Most of the experiments were carried out on rods of material 1·25 cm in diameter and of lengths up to two metres. The pulses were produced by detonating small quantities of lead azide at one end of the rod and the attenuated pulses were detected by a condenser microphone at the opposite end. Once the pulse length becomes great compared with the diameter of the rod the relevant elastic constant is Young's modulus E and in the absence of attenuation the velocity of propagation is $(E/\rho)^{1/2}$. A few experiments were also carried out on propagation through blocks of plastic and these will be very briefly described later.

The apparatus is shown schematically in fig. 4. In order to avoid losses at the supports the specimen rod was suspended by long threads, and the explosive was placed in a recess at the end of a short anvil of the same material as the rod. The anvils, the ends of which were polished, were held on to the rods by a thin layer of grease. A nichrome wire which could be heated electrically was used to detonate the explosive and this also served the purpose of steadying the rod up to the moment of detonation, when the wire was blown away. The lead azide charges were up to 0·1 g in weight, a small silver acetylide primer ($\sim$1 mgm) being used to help detonation of the charge. The detector end of the specimen was covered with a thin graphite layer and this was earthed by means of a very fine wire. The insulated detector plate of the condenser unit was attached to a micrometer head and charged to 360 v through a 50 megohm resistance. The insulated plate was connected through the feed unit and a wide band amplifier to a high-speed cathode-ray oscillograph. The circuits were similar to those described by Davies (1948) and by the author (Kolsky 1949, 1954 b). The oscillograph trace was triggered by a photocell which received the light from the explosion, and a calibrated oscillator was used to provide a time trace on the oscillograph record. The records were obtained photographically, the camera being opened just before the charge was detonated.

Any movement of the end of the rod resulted in a change in the capacity of the condenser consisting of the detector plate and the earthed graphite layer at the end of the rod, and since the plate could only lose its charge through large resistances a sudden change in capacity resulted in a corresponding change in the potential of the plate. This change of potential was amplified and recorded on the oscillograph. When the displacement of the end of the rod is small compared with the separation between it and the detector plate, the change in voltage across the condenser becomes proportional to this displacement (cf. Davies 1948). Under these conditions the oscillograph gives a true record of the motion of the end of the rod, and by differentiating this displacement–time curve, the stress–time curve can be obtained. The relation used applies when the pulse length is great compared with the diameter of the rod and is

Fig. 4

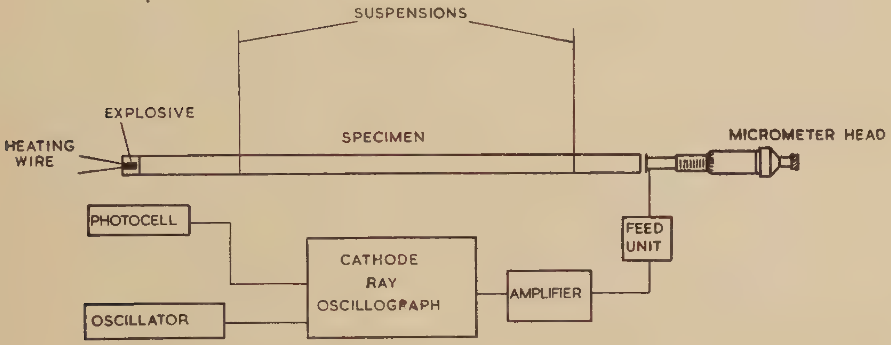

Experimental arrangement.

$$\sigma = \tfrac{1}{2}\rho c \frac{du}{dt} \quad . \quad . \quad . \quad . \quad . \quad . \quad . \quad . \quad . \quad (2)$$

where σ is the stress and u is the displacement at time t. Integrating eqn. (2) it can be seen that the total displacement U produced by the reflection of a pulse at the end of the rod is given by

$$\int \sigma \, dt = \tfrac{1}{2}\rho c U. \quad . \quad . \quad . \quad . \quad . \quad . \quad . \quad . \quad (3)$$

The left-hand side of the equation represents the momentum associated with the pulse. In order to measure the values of this momentum, explosive charges similar to those used in the later experiments were detonated against a small ballistic pendulum. The total movement U in each case could then be calculated from (3) and the condenser gap set in each experiment to be sufficiently wide for there to be virtual linearity between the voltage change and the displacement.

In the experiments, the compression pulse was reflected at the detector end of the specimen as a pulse of tension (since the end is free). This travels back to the firing end where it is once again reflected with a reversal of phase so that it again approaches the detector end as a pulse of compression. A second reflection then takes place resulting in a further movement in this end of the specimen. In between reflections the ends of the specimen are at rest and in the absence of attenuation of the pulse the ends would continue to move in jumps indefinitely (cf. Kolsky 1953, p. 46). If an oscillograph record is taken of the motion of the detector end during several reflections the shape of the pulse after it has traversed the rod once, three times, five times, etc. can be found and such records were used to determine the change in pulse shape for long distances of travel in the material. Figures 5, 6, 7 and 8 are oscillograph records which illustrate qualitatively how attenuation has affected the motion of the end of the rod in specimens of four different materials.

The first, fig. 5, is included for comparison and was obtained with a silver steel rod 1 metre in length and 1·25 cm in diameter. Thus each step in the trace corresponds to the pulse having traversed a distance of 2 metres of steel. The trace shows that there is very little change in the shape of the pulse even after 11 reflections when the pulse has travelled through 21 metres of the metal. It may be seen that after the sharp rise in each case there are some high frequency oscillations. These are produced by the dispersion of the pulse as a result of the effect of lateral inertia. This causes the high frequency components of the pulse to travel at a lower velocity than the low frequency ones. The effect of this geometric dispersion is thus in the opposite sense to that produced by the change in the elastic properties of high polymers which, as mentioned earlier, results in the velocity of propagation increasing with the frequency of the waves. The pulse produced by the explosive is initially about 2 microseconds in duration and in the 1·25 cm diameter steel rod, because of the effect of lateral inertia, the pulse is extended to a length of about 15 microseconds ; this is followed by a train of high frequency oscillations. Davies (1948) has discussed the effect fully and has shown that a pulse must be at least ten times as long as the diameter of the rod for it to be propagated without appreciable change in shape. In the present investigation this effect placed a lower limit on the length of pulse that could be studied, since it was necessary to ensure that the observed changes in the pulse shape were due to the properties of the material and not to inertia effects.

Figure 6 is a record of the movement of the end of a rod of polystyrene 1·25 cm in diameter and 50 cm in length. Polystyrene is a rather brittle glass-like polymer which has comparatively low internal friction (see Lethersich 1950). It may be seen that there is little change in the shape of the pulse as it travels back and forth along the rod although a slight rounding off of the steps occurs on the 6th and 7th reflections, showing a slight lengthening of the pulse. It may be noted that the oscillations which in steel follow the main pulse do not appear in this record. This is due to the attenuation by the plastic of the high frequency Fourier components which produce these oscillations.

Figure 7 shows the record obtained from a specimen, 40 cm. long, of another glass-like polymer, ‘ Perspex ’ (a form of polymethylmethacrylate). This material has a higher mechanical loss than polystyrene and it may be seen that as a result the steps in the record become progressively more gradual, the pulse length increasing considerably between each reflection. It may also be noted that the high frequency oscillations produced by lateral inertia effects are here completely absent.

Lastly fig. 8 was obtained with a specimen 20 cm long of the softer polymer polythene which has a high coefficient of internal friction and here the pulse is rapidly lengthened so that after a few reflections the motion of the end of the bar has become almost continuous.

In order to determine the shape of the pulse, after travelling through various distances in the material, rods of different lengths were used and the records for the first few reflections were measured. Wherever possible only the first and second reflections were used, since this enabled a larger and hence more accurate trace to be obtained and also made it possible to employ a condenser gap which was sufficiently large, compared with the total relevant movement of the end of the bar, for linearity to obtain. The measured displacement–time curves were differentiated numerically to give the shapes of the stress pulses. Figure 9 shows the pulse shapes for polythene after traversing 30, 60 and 90 cm and fig. 10 shows similar curves in ‘ Perspex ’ for travel distances of 120, 360, 600 and 840 cm. The attenuation in polystyrene was too low for reliable changes in pulse shape to be determined. The figures show that the pulses in both materials are asymmetrical in shape and that they continually lengthen and decrease in amplitude as they progress through the specimen. Since the area under each pulse is proportional to the momentum associated with it this area will remain constant as the pulse travels through the material. The dependence of the pulse shape on the viscoelastic properties of the medium is discussed in § 3.

As mentioned earlier, a few experiments were also carried out on the propagation of pulses in blocks of polymer. There is no dispersion due to lateral inertia in this case, so that the propagation of pulses of very much shorter duration can be investigated. Since, however, the pulse under these conditions is spreading out radially its amplitude is inversely proportional to the distance travelled. Furthermore, at distances from the source comparable with the pulse length changes in shape occur even in perfectly elastic media as the pulse travels out. The form of spherically divergent stress pulses has been discussed by several authors (e.g. Selberg 1952) and they show that the displacement u_r at distance r is represented by

$$u_r = \frac{c}{r} f'(r-ct) - \frac{c^2}{r^2} f(r-ct). \quad . \quad . \quad . \quad . \quad . \quad . \quad . \quad (4)$$

Thus for large r the first term on the right-hand side of the equation is predominant, whilst for small r the second term becomes important. The shape of the displacement–time curve at large distances from the source is thus the differential of the curve close to it. It is consequently

Fig. 9

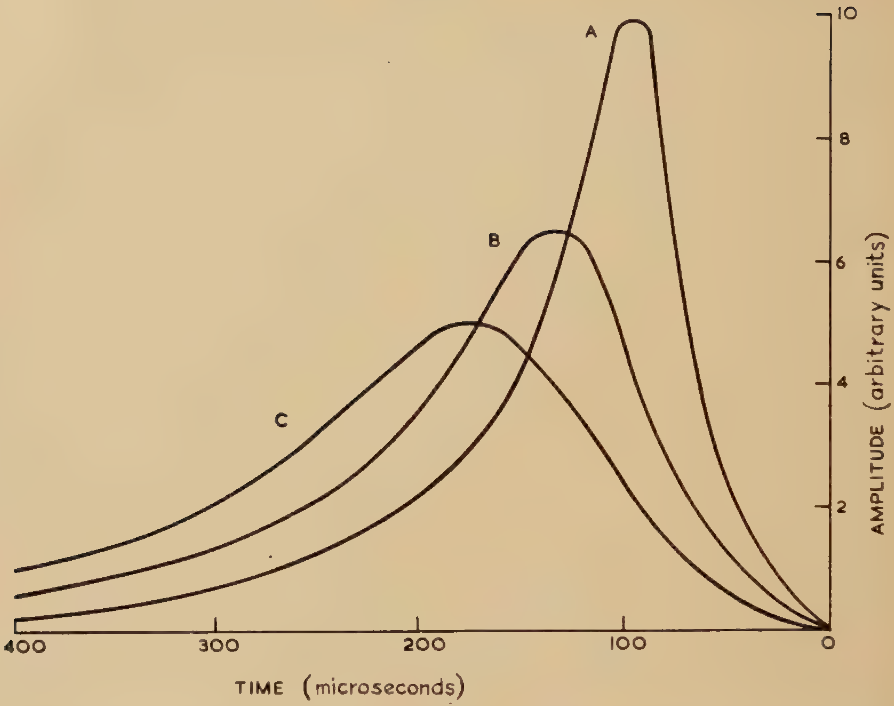

Experimental results for attenuation through different lengths of polythene rod at 15°c. A, 30 cm ; B, 60 cm ; C, 90 cm.

Fig. 10

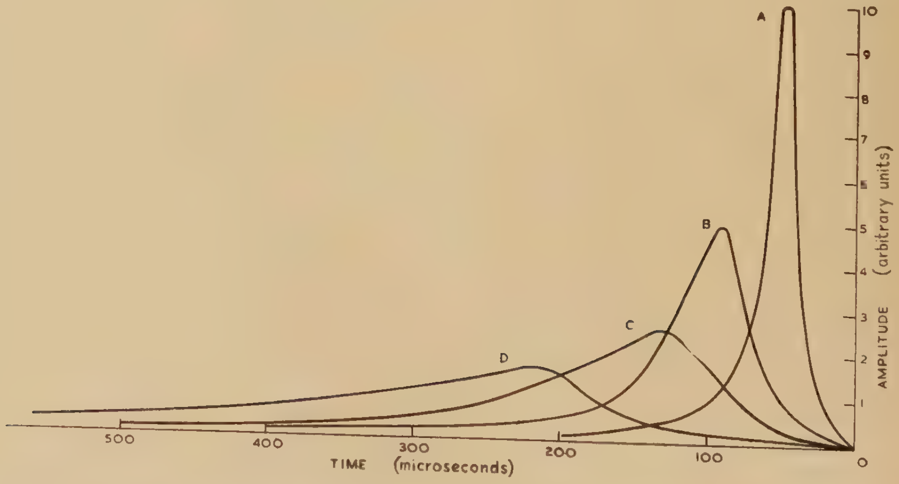

Experimental results for attenuation through different lengths of ‘ Perspex ’ at 15°c. A, 120 cm ; B, 360 cm ; C, 600 cm ; D, 840 cm.

Fig. 11

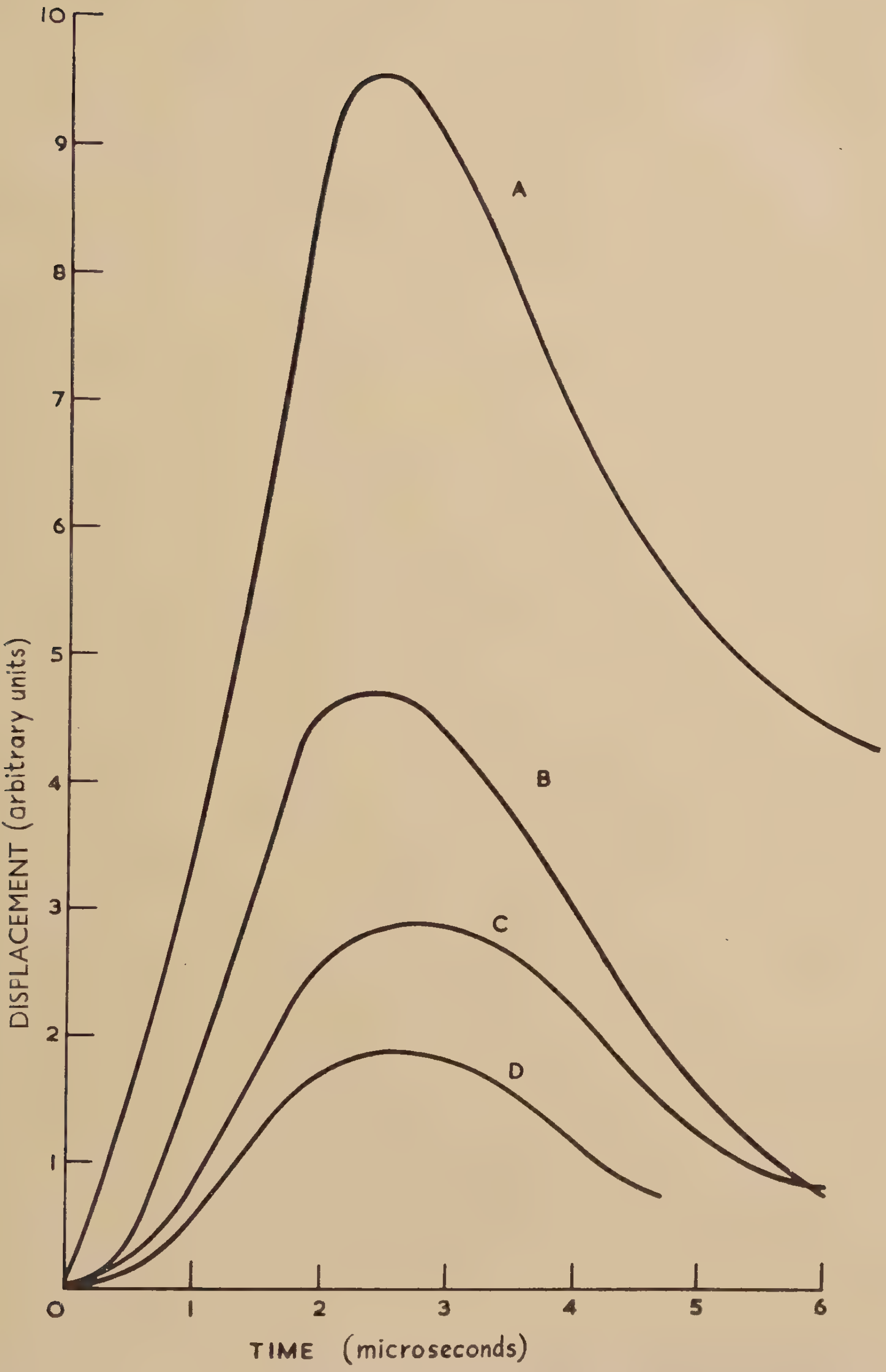

Displacement-time curves through blocks of polythene of different thicknesses at 15°c. A, 2·5 cm ; B, 5 cm ; C, 7·5 cm ; D, 10 cm.

difficult to separate the effects of attenuation by the medium from changes in pulse shape due to geometrical effects, but it was nevertheless considered worthwhile to carry out some experiments in order to see what qualitative changes occurred. The experimental arrangements were similar to those used in earlier work (Kolsky 1954 b) to investigate the propagation of pulses in elastic cylinders and most of the present experiments were carried out on cylinders of polythene. The displacement–time curves for four thicknesses of this material are shown in fig. 11 and it may be seen that in each case the displacement is tending to return to zero. This is to be expected from eqn. (4) since it is $f'(r-ct)$ which will be dominant at these distances of travel. It should be noted that the pulse lengths are here much shorter and increase more slowly than for propagation in rods of the material. This might be expected since we are dealing here with dilatation waves in which the relevant elastic constant is $(k+4/3\mu)$, where k is the bulk modulus and μ is the shear modulus of the material. k for polythene is considerably greater than μ and might be expected to be less sensitive to rate of loading. There will consequently be less dispersion due to the dependence of velocity of propagation on frequency. Further, the fraction of stored elastic energy which is dissipated in a stress cycle might be expected to be smaller so that there will be less attenuation due to damping for waves of this type.

§ 3. Discussion of Results

As mentioned earlier, it was intended to use the dynamic elastic constants of the plastics obtained from measurements with sinusoidally applied stresses for calculating the shape of the pulses after they had travelled some distance along rods of these materials. This can be done if a Fourier analysis of the initial pulse-shape is first carried out ; the appropriate changes in amplitude and phase of each Fourier component are then made and the pulse re-synthesised. Thus if the stress pulse at the origin is represented by the Fourier integral

$$\int_0^\infty A_p \cos pt \, dp$$

after travelling distance x it will be given by

$$\sigma(x,t)=\int_0^\infty A_p \exp(-\alpha x) \cos p(t-x/c) \, dp. \quad . \quad . \quad . \quad (5)$$

Thus if α and c are known over the relevant range of frequency, the new shape can be calculated.

In the experiments described in § 2 the pulse was originally very short (ca. 2 microseconds) compared with its length when measured (several hundred microseconds). Further, in the early stages of its progress down the bar two separate types of dispersion were present, viz. : attenuation by the material of the bar and dispersion due to lateral inertia effects.

In order to treat the problem theoretically, it therefore seemed reasonable to investigate the propagation of a pulse which was infinitely sharp at the origin and hence can be represented by a δ-function. In this case A_p is a constant and all that is required is a Fourier synthesis for any value of x.

In order to carry this out numerically the Fourier integral must be replaced by a Fourier series and it is desirable to choose a frame of reference which is moving with the pulse. If we take v as the velocity of the pulse we may write

$$\sigma(x,t)=\sum_{0}^{n} A \exp(-\alpha x) \cos np\left(t-\frac{x}{c}+\frac{x}{v}\right) \quad . \quad . \quad . \quad . \quad (6)$$

where t is now measured from the time at which the pulse arrives at the point at which it is observed, a distance x from the origin.

Equation (6) can be expanded in the form

$$\sigma(x,t)=\sum_{0}^{n} A_n \cos npt+\sum_{1}^{n} B_n \sin npt \quad . \quad . \quad . \quad . \quad . \quad (7)$$

where $$A_n=A \exp(-\alpha x) \cos npx(1/c-1/v)$$

and $$B_n=A \exp(-\alpha x) \sin npx(1/c-1/v).$$

A_n and B_n can be calculated for the terms in the series if the values of α and c are known at each frequency $np/2\pi$. v is a constant for the summation and must be chosen so that the pulse remains within the basic interval of the series. The value of v is not too critical in that a change in v results only in a shift of the pulse with respect to the chosen axes of reference; in the present work v was taken as the phase velocity at the basic frequency $p/2\pi$. The basic interval of the series is $2\pi/p$ and for accuracy this must be chosen sufficiently narrow for the pulse to occupy a large part of the time covered. On the other hand it must be sufficiently wide to preclude any appreciable part of the pulse falling outside this interval, or the periodicity assumption inherent in the use of a Fourier series is no longer justified. The numerical method which was employed for the Fourier synthesis is that due to Danielson and Lanczos (1942) and by using 32 terms for both the cosine and sine summations 64 ordinates of the final pulse could be calculated.

Using the data shown in fig. 1 the pulse shapes to be expected in polythene rods were determined. Two difficulties arise in comparing these with those found experimentally. First, the initial pulse is not infinitely sharp and secondly, as mentioned earlier, the dispersion due to inertia effects in the bar is important until the length of the pulse becomes several times the diameter of the bar. The result of both these effects is to make the pulse longer than that predicted by the calculation. For 1·25 cm polythene rods it was found that at large distances of travel the agreement was best when the calculated distance was about 10 cm greater than the actual distance travelled. Figure 12 shows a comparison between the pulse observed experimentally after travelling through 60 cm of polythene and that calculated for 70 cm.

In comparing the pulse shapes shown in figs. 9 and 10 it was found empirically that they were all approximately similar in shape. By this is meant that if the time scales are suitably extended or contracted and the amplitudes decreased or increased in the same ratio (so that the area under the curve remains constant) all the pulses approximate to the same shape. This result was surprising in view of the very different properties of the two plastics and it therefore seemed worth seeing whether there was any underlying reason for this similarity.

Fig. 12

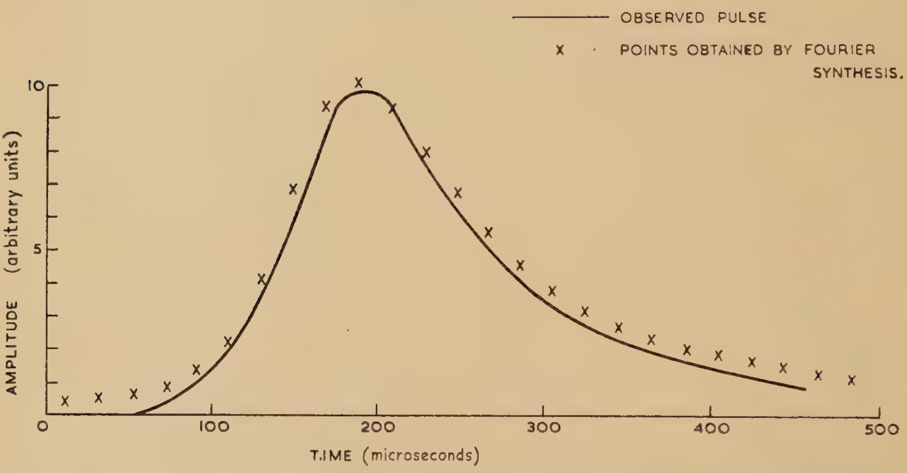

Comparison between observed pulse for 60 cm rod and curve calculated for 70 cm.

The observed similarity implies that if the stress pulse, after travelling a distance x_1 is expressed as

$$\sigma_1 = f(t) \quad \text{. . . . .} \quad (8)$$

at distance x_2 the stress will be given by

$$\sigma_2 = \frac{1}{m} f\left(\frac{t}{m}\right). \quad \text{. . . . .} \quad (9)$$

Choosing a frame of reference moving with velocity v as before, and using the expression for α from eqn. (1) we may rewrite eqn. (5)

$$\sigma_1 = A \int_0^\infty \exp(Kpx_1) \cos p\left(t - x_1\left[\frac{1}{c} - \frac{1}{v}\right]\right) dp \quad \text{. .} \quad (10)$$

where $K = -\tan \delta/2c$.

Now if we put $m = x_2/x_1$, the expression at x_2 may be written

$$\sigma_2 = \frac{A}{m}\int_0^\infty \exp(Kmpx_1) \cos mp\left(\frac{t}{m} - x_1\left[\frac{1}{c} - \frac{1}{v}\right]\right) d(mp). \quad \text{.} \quad (11)$$

This is of the form (9) if K and $(1/c-1/v)$ are either independent of p or can be expressed as a function of the product px. As mentioned earlier, for most polymers tan δ does not vary markedly over limited ranges of frequency whilst c increases with frequency. The relevant frequency range of the Fourier integral which effectively determines the pulse shape is only of the order of a decade or two and within this region tan δ will in general vary very little. Further, if tan δ is independent of frequency and small, the theory of linear viscoelasticity shows that

$$\frac{dE}{d(\ln p)}=\frac{2\tan\delta}{\pi}$$

$$E=E_0\left(1+\frac{2\tan\delta}{\pi}\ln\left[p/p_0\right]\right)$$

where E_0 is the modulus at a standard frequency p_0. Hence since

$$c=(E/\rho)^{1/2}$$

$$c\simeq c_0\left(1+\frac{\tan\delta}{\pi}\ln\left[p/p_0\right]\right). \quad . \quad . \quad . \quad . \quad . \quad . \quad . \quad (12)$$

Thus if tan δ is small c will not vary much over the relevant frequency range and K may be assumed to be constant. The same, however, does not apply to the expression $(1/c-1/v)$, since it is just the small variations of c which produce dispersion effects in the pulse. Since this expression is not constant the similarity condition will only hold if $(1/c-1/v)$ can be expressed as $f(px)$. This would, in general, not be possible, but from eqn. (12) we have

$$\frac{1}{c}\simeq\frac{1}{c_0}\left(1-\frac{\tan\delta}{\pi}\ln\left[p/p_0\right]\right)$$

and so if we take

$$\frac{1}{v}=c_0\left(1+\frac{\tan\delta}{\pi}\ln\frac{x}{x_0}\right) \quad . \quad . \quad . \quad . \quad . \quad . \quad . \quad . \quad (13)$$

where x_0 is a disposable constant, we have

$$(1/c-1/v)=\frac{\tan\delta}{c_0\pi}\ln\frac{px}{p_0x_0}. \quad . \quad . \quad . \quad . \quad . \quad . \quad . \quad . \quad (14)$$

which is of the required form. Equation (13) implies that the 'pulse velocity' v is not constant but decreases slowly as the pulse progresses.

It has thus been shown that if tan δ is constant and sufficiently small for its higher powers to be neglected, similarity will apply between the pulse shapes at different distances of travel through any one material. If we now use eqn. (14) to substitute for $(1/c-1/v)$ in eqn. (11) and take $K=-\tan\delta/2c_0$, we find that the properties of the material occur only in

Fig. 13

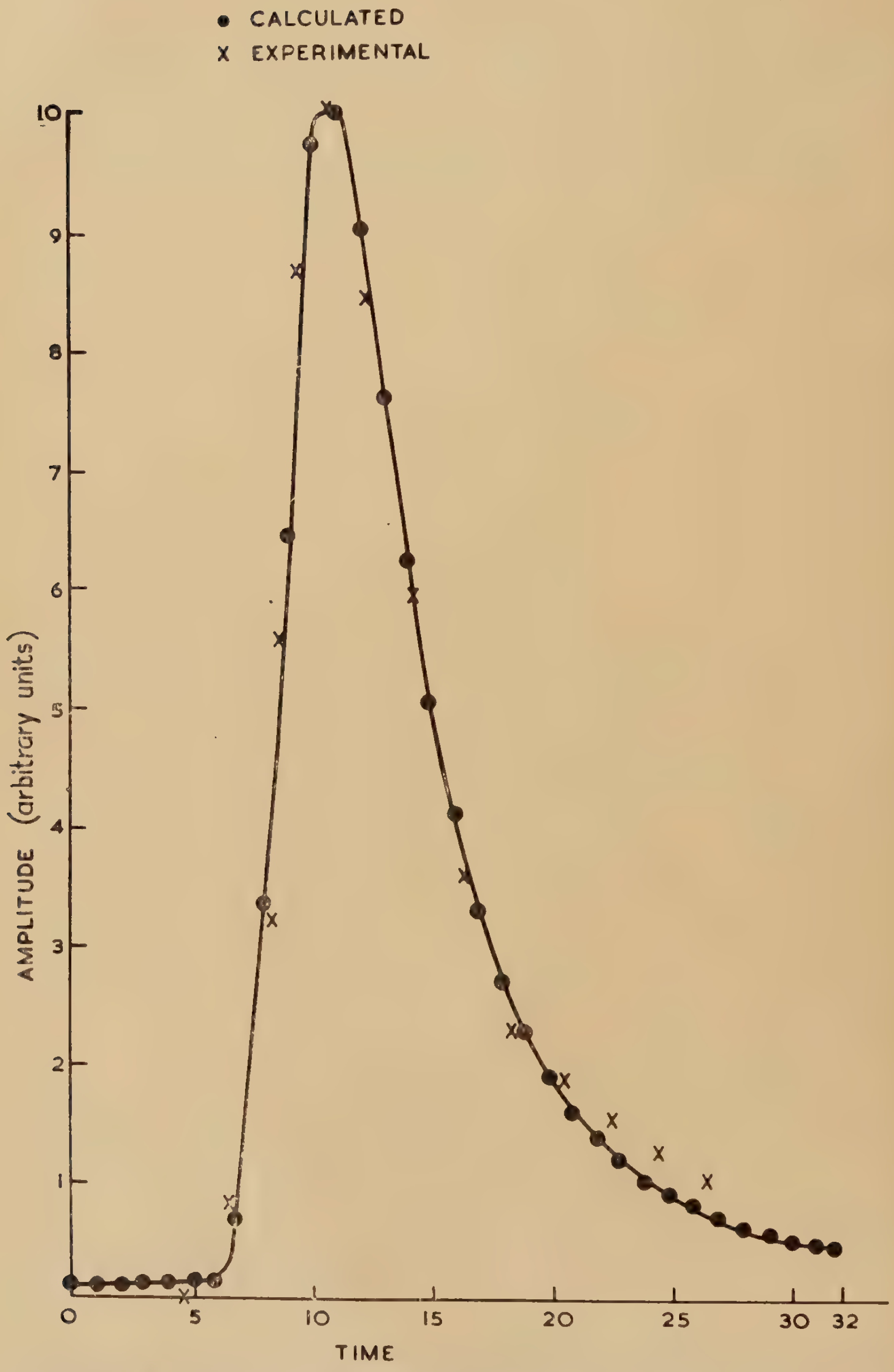

Experimental results for polymethylmethacrylate compared with universal pulse calculated by Fourier synthesis.

the form of the parameter $(x \tan \delta / c_0)$. Thus all linear viscoelastic materials which fulfil the assumptions made will give the same pulse shapes after suitably scaled travel distances and if the integral is evaluated it will give the pulse shape for all such viscoelastic materials and all distances of travel when the time scale is suitably chosen.

In order to calculate the shape of the generalized pulse the integral was replaced by the sum of a sine and a cosine Fourier series, as given in eqn. (7). The basic interval of the series was taken to correspond to $(4\pi x \tan \delta)/c$ (writing c for c_0), so that the basic value of p was $c/(2x \tan \delta)$. Figure 13 shows the central 32 of the 64 ordinates obtained from a numerical Fourier synthesis, the x axis being plotted in units of time given by $(\pi x \tan \delta)/16c$. It should be possible to fit this plot to a pulse in any polymer of the type postulated at any distance x if the value of $\tan \delta / c$ is known. The figure shows the remarkably good fit obtained with the pulse shape observed in polymethylmethacrylate after a distance of travel of 6 metres. The time scale here was fitted empirically, taking $(x \tan \delta / c)$ to be 100 microseconds. The value of c can be determined from the time of transit of the pulse across the rod (see fig. 6) and for this plastic the value is about 2300 metres/second. This makes the value of $\tan \delta$ about 0·04, which is in reasonable agreement with that found by Lethersich (1950) for torsional oscillations of this material at comparable frequencies.

§ 4. CONCLUSION

When mechanical pulses are propagated along rods of high polymers they change in shape as a result of two separate causes. First, the lateral inertia of the rods results in dispersion, and secondly, the variation of mechanical properties of the material produces dispersion and attenuation of the pulse. A theoretical investigation of the combined effects of the two types of dispersion would be of interest but would certainly involve heavy mathematical analysis. When, however, the length of the pulse is large compared with the diameter of the rod the effects of lateral inertia can be neglected and it has been shown that under these conditions the pulse shape can be accurately predicted from a knowledge of the variation of elastic modulus and damping with frequency. Further, that if the damping ($\tan \delta$) is constant and sufficiently small for powers higher than the first to be neglected, (i.e. $\tan \delta < 0{\cdot}1$), the effects of damping and velocity change can be combined into a single parameter and the results of pulse attenuation expressed in a non-dimensional form which applies to all such viscoelastic solids.

ACKNOWLEDGMENTS

The author wishes to express his thanks to Dr. F. C. Roesler for many valuable discussions on this work and to Mrs. P. M. Weaver for her help with the experiments.

REFERENCES

DANIELSON, G. C., and LANCZOS, C., 1942, *J. Franklin Inst.*, **233**, 365.

DAVIES, R. M., 1948, *Phil. Trans.* A, **240**, 375.

EUBANKS, R. A., MUSTER, D., and VOLTERRA, E. G., 1952, *Illinois Inst. of Techn. Tech. Rep.* No. 1, Contract No. N7onr–32911, Project No. NR 064 369.

GLAUZ, R. D., and LEE, E. H., 1954, *J. Appl. Phys.*, **25**, 947.

GROSS, B., 1953, *Mathematical Structure of the Theories of Viscoelasticity* (Paris: Hermann).

HILLIER, K. W., 1949, *Proc. Phys. Soc.* B, **62**, 701.

KOLSKY, H., 1949, *Proc. Phys. Soc.* B, **62**, 676; 1953, *Stress Waves in Solids* (Oxford: Clarendon Press); 1954 a, *Proc. 2nd Int. Congr. on Rheology*, p. 79 (London: Butterworths); 1954 b, *Phil. Mag.*, **45**, 712.

LEADERMAN, H., 1943, *Elastic and Creep Properties of Filamentous Materials* (Washington: Textile Foundation).

LEE, E. H., and KANTER, I., 1953, *J. Appl. Phys.*, **24**, 1115.

LETHERSICH, W., 1950, *Brit. J. Appl. Phys.*, **1**, 294.

RICKER, N., 1943, *Bull. Seism. Soc. Amer.*, **33**, 197.

SELBERG, H. L., 1952, *Arkiv. fysik*, **5**, 97.

THOMPSON, J. H. C., 1933, *Phil. Trans.* A, **231**, 339.

ZVEREV, I. N., 1950, *Appl. Math. Mech., Leningr.*, **15**, 295.

LXXII. *Creep of Alpha Uranium During Irradiation with Neutrons*

By A. C. Roberts † and A. H. Cottrell ‡ §

[Received May 24, 1956]

Abstract

During neutron irradiation at 100°c alpha uranium creeps slowly (e.g. 10^{-7} per hour) under external stresses of order of one-hundredth of the normal yield stress of the metal at that temperature. This effect is predicted as a consequence of the phenomenon of 'radiation-growth' which occurs in uranium, and is then confirmed by creep experiments on helical springs of natural uranium in a flux of $1{\cdot}3\times10^{12}$ thermal neutrons per cm^2 per sec. In addition to this steady-state creep, transient effects occur at the start of irradiation and when the neutron flux is removed.

§ 1. Introduction

There must be many ways in which the various processes that occur in uranium during irradiation in a nuclear reactor can affect its creep properties. Vacancies and interstitials, created by neutron collisions and knock-on processes along the tracks of fission fragments (Seitz 1949), may produce creep either directly, by migrating to crystal boundaries (Nabarro 1948), or indirectly, by helping dislocations to climb over obstacles in their glide planes. Thermal spikes, also created along fission tracks, may help dislocations to glide through obstacles. Internal stresses, for example created by the temperature gradients in the metal, may help in a more macroscopic manner to produce plastic deformation. After prolonged irradiations the concentration of new atoms created by fission becomes appreciable ; since these mostly differ radically from the uranium atom they may affect the mechanical properties of the metal strongly, especially by segregating to vital places such as crystal boundaries, dislocations and internal cavities.

Very little is known about such effects in practice, apart from a remark by Konobeevsky *et al.* (1955) to the effect that the creep of uranium is increased by a factor of 1·5 to 2 during irradiation.

In the work described below we have studied a particular effect which we anticipated might become large under certain circumstances. If a polycrystalline metal contains intergranular stresses large enough to bring its grains to the point of plastic yielding, it can give way plastically to an externally applied stress that is small compared with the yield strength of a uniformly stressed sample. During this plastic deformation most of the work is done by the internal stresses, and the external stress merely guides the local deformations so that their average, over the region under the external stress, has a non-vanishing component in the direction of that stress. This effect is of course familiar as a cause of deviations from Hooke's law at low stresses in polycrystalline solids. In such cases however the intergranular stresses exist only as an initial condition of the material and become compensated by differential plastic flow before the overall deformation has exceeded the order of magnitude of the initial elastic strains.

---

† Research Laboratories of the General Electric Company Ltd., Wembley; temporarily attached to Atomic Energy Research Establishment, Harwell.

‡ Atomic Energy Research Establishment, Harwell.

§ Communicated by the Authors.

The new feature about uranium is that under certain conditions the effect known as 'radiation growth' takes place. Each crystal changes its shape progressively along certain crystal axes during irradiation (Pugh 1955). In a polycrystal the mutual impingements of differently oriented grains undergoing radiation growth ensure a continual regeneration of internal stresses and it is possible that, in a creep experiment made under such conditions, these intergranular stresses may persist during the entire period of the experiment and the material may never become able to oppose its full yield strength to the applied stress.

§ 2. Creep due to Radiation Growth

When a free single crystal of alpha uranium is irradiated at temperatures in the range below 450°c it undergoes a deformation with strain velocity components given by

$$\begin{array}{c|ccc} & a & b & c \\ \hline a & -\dot{\epsilon}_g & 0 & 0 \\ b & 0 & +\dot{\epsilon}_g & 0 \\ c & 0 & 0 & 0 \end{array}$$

where a, b, and c, refer to the 100, 010, and 001, axes respectively, and $+\dot{\epsilon}_g$ signifies an elongation. The rate of growth reaches a maximum of about 4×10^{-9} sec^{-1} (for a thermal neutron flux of 10^{12} cm^{-2} sec^{-1}) at 200°c, and falls slowly at lower temperatures and more sharply at higher temperatures, reaching virtually zero at about 450°c. In polycrystals with certain preferred orientations the growths of the individual crystals produce an overall growth of the specimen, but this does not of course happen in randomly oriented polycrystals.

The various atomic processes postulated to explain radiation growth have been summarized by Pugh (1955), Paine and Kittel (1955) and Ball (1956).

Consider a random polycrystal. In the absence of applied stress, its overall dimensions do not change during irradiation. However, the variously oriented growth strains which occur in the individual grains produce intergranular stresses that reach the yield strength in a time

$$t_m \simeq \sigma_y / E\dot{\epsilon}_g, \qquad (1)$$

where σ_y is the appropriate yield strength of the crystal, i.e. the smallest stress needed to operate those plastic modes that are capable of accommodating the growth strains, and E likewise is the appropriate elastic constant. Typically, $\sigma_y \simeq 5\times10^4$ p.s.i. and $E \simeq 25\times10^6$ p.s.i. for uranium in the range 0–200°c. With the above value for $\dot{\epsilon}_g$, this gives $t_m \simeq 1$ week, which is short compared with typical times of irradiation in a reactor. Up to the time t_m the metal can accommodate its growth strains substantially by elastic deformation. Thereafter it must deform plastically. Evidence for this localized plastic deformation is provided by the 'wrinkling' which is observed on the surface of coarse-grained uranium after deformation (Pugh 1955) and by the numerous deformation twins observed inside the metal after irradiation (Konobeevsky *et al.* 1955, Paine and Kittel 1955, Leech and Eldred, private communication).

A precise calculation of the overall creep rate $\dot{\epsilon}_e$ to be expected when such a material is subjected to an applied stress σ during irradiation hardly seems possible. An estimate can be made by the following argument. When the stress σ is applied, an overall elastic deformation of order σ/E occurs. In addition, an overall plastic deformation of order σ/E also occurs due to the local plastic relaxations under the combined influences of the internal and applied stresses. Before the overall plastic deformation can continue further it is necessary for the internal stresses to re-establish their original distribution, and the time required for this must be of order t_m. Hence, during each interval t_m an increment σ/E of overall plastic deformation takes place, so that

$$\dot{\epsilon}_e \simeq \sigma/E\, t_m \simeq (\sigma/\sigma_y)\dot{\epsilon}_g. \qquad (2)$$

For example, with the above values of σ_y and $\dot{\epsilon}_e$, we expect a steady-state creep rate of 10^{-10} sec^{-1} under an applied stress of 1000 p.s.i. In the absence of irradiation, of course, there could be no appreciable steady-state creep in uranium at such low temperatures (e.g. 100°c) and stresses.

Two possible objections to this estimate are as follows:

(1) Since the growth strains have simple crystal symmetry it is conceivable that they could be accommodated by a set of plastic deformation modes that contains fewer than the number (i.e. 5) of independent modes needed to produce an arbitrary plastic deformation. In that case the inactive modes might be capable of supporting the applied stress without yielding, and the overall creep would cease after a deformation of order σ/E. However, it seems unlikely that the stress-continuity conditions

could be satisfied at the grain boundaries without producing more arbitrary states of plastic deformation there ; we thus expect that the full number of deformation modes is needed to accommodate the growth strains and that the overall creep will continue indefinitely during irradiation.

(2) Since the occurence of overall creep would require some grains to deform plastically more than others, it is possible that these would also work harden more, in which case a set of localized stresses could be built up to balance the applied stress. A transient radiation-creep effect would then be observed, but not a steady-state one. This possibility was pointed out to us by Makin and Bowen (private communication). However, the predominant form of hardening during such an experiment must undoubtedly be direct radiation-hardening (cf. Paine and Kittel 1955), and it is not clear that the differential work-hardening effect could be appreciable.

§ 3. EXPERIMENTAL METHOD

Because the interesting range of strain rates for testing the effect lies below 10^{-10} sec^{-1}, and because it is not easy to measure small deformations remotely on highly active material, the specimens were made in the form of helical springs to obtain a large deflection from a small strain.

Calcium-reduced rods of uranium, 6 mm dia., having the following composition,

	Fe	Cr	Ni	Mn	V	N_2
Parts per million :	200	100	15	7	7	150 (on surface)

were swaged into 1 mm wire, being annealed in vacuum at 500°c for 1 hour between alternate passes. The annealed wire was coiled into springs of 1 cm diameter. Each spring was supported horizontally by an alumina tube and heated by direct current to 720°c in high vacuum. At 720°c the current was taken off and the spring cooled to room temperature by allowing helium to enter the vacuum chamber. The spring was then heated again *in vacuo* to 450°c and allowed to cool slowly. This was a suitable treatment for randomizing the grain texture and produced a final grain size of 90 microns.

Each specimen consisted of a helical coil, about 20 turns and about 35 mm in length, with two arms formed by leading off the wire at each end outward along the axis of the coil for about 30 mm. Four rows of small aluminium dots were painted along the coil, parallel to the axis, to locate four orthogonal positions for measuring the length of the coil. The last turn at each end was not included in the measured length. The specimen was mounted vertically in a sealed cylinder of fused quartz in one atmosphere of helium and suspended (or supported in the case of a compression specimen) from a steel bridge. The load was applied axially, by the weight of the specimen itself (about 10 g) and by a lead weight fixed to the unattached arm.

Four such specimens were assembled as a unit and irradiated in BEPO at a thermal neutron flux of about $1{\cdot}3\times10^{12}$ cm^{-2} sec^{-1} and a temperature of 100°C (±10°C), which produced fissions at a rate of about 5×10^{-12} of all atoms per second. At weekly intervals (usually) the unit was withdrawn from the reactor and taken to a 2 ft. concrete enclosure for measurement. Here the lengths of the springs were measured in four positions, using a telescope sighted through a mirror.

A fifth specimen, for control, was set up in the laboratory at a temperature of 100°C under conditions which simulated those in the reactor.

§ 4. RESULTS AND DISCUSSION

Details of the loads, stresses and elastic deflections of the specimens are given in the table. The smallness of the loads used made it necessary to take account of the weight of the specimen itself, and the stresses σ in the specimens are calculated for the centre coil, using the formula

$$\sigma=(16PR/\pi d^3)\,[1+(d/4R)], \qquad . \quad . \quad . \quad . \quad . \quad . \quad . \quad (3)$$

where P is the load, R the radius of coil to centre of wire (0·45 cm) and d the diameter of wire (1 mm).

Loading of Specimens

Specimen	Number of turns	Half-weight of specimen (gm)	Applied load (gm)	Stress p.s.i.	Initial elastic deflection (mm)
A	24	5·6	0	190	0·09
B	23	5·8	21·8	950	0·5
C	22	5·9	49·5	1900	1·0
D†	17	4·0	0	140	0·06
Control	24	5·8	50·6	1940	1·0

† Compression specimen supported at the bottom; all others supported from the top.

The control specimen extended by 0·3 mm (i.e. $\frac{1}{3}$ of its initial elastic deflection) on raising its temperature to 100°C but thereafter remained constant over a period of several weeks at 100°C, during which time a few cycles between 20°C and 100°C were made to simulate the thermal treatment received by the other specimens. Only two creep measurements were obtained from the compression specimen because its silica container broke during the third week of irradiation; the creep deflection of this spring was zero after the first week and 0·5 mm (i.e. about 8 initial elastic deflections) after the second week. The results from the other three specimens are given in the figure.

Fig. 1

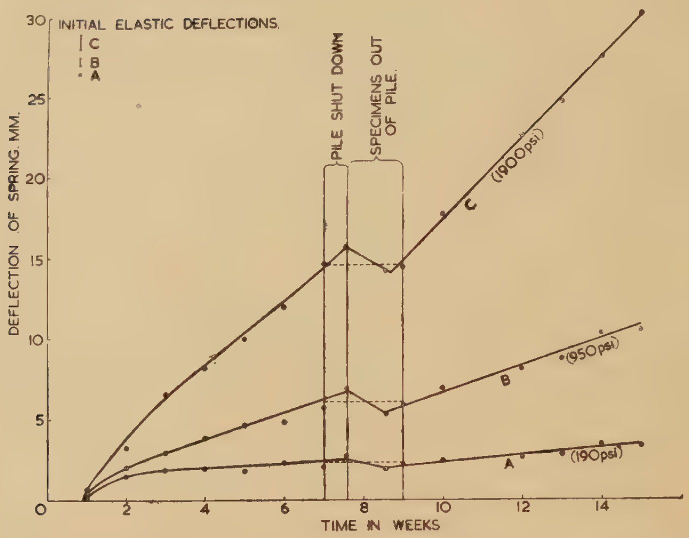

Creep of uranium springs during irradiation ($1{\cdot}3 \times 10^{12}$ thermal neutrons per cm^2 per sec) at 100°c. The stress values refer to mean skin stresses.

The results can be summarized as follows :

(1) Initially, for a period rather less than 1 week in duration, the creep was very small or entirely absent ; thus we deduce $t_m = 6(\pm 1)$ days, in agreement with the theoretical order of magnitude.

(2) Between the 1st and 3rd weeks of irradiation a transient creep occurred which produced the following deflections :

Specimen	Deflection (mm)	Deflection, in units of initial elastic deflection
A	1·6	17·7
B	1·6	3·2
C	2·4	2·4

(3) A steady-state creep occurred at the following rate :

Specimen	Rate of deflection (mm per week)	Rate of deflection, per week, in units of initial elastic deflection
A	0·105	1·16
B	0·75	1·5
C	2·0	2·0

These values were measured between the 3rd and 7th weeks of irradiation; later, slightly higher values were obtained. Taking $t_m = 6$ (± 1) days, the creep rate we deduce from eqn (2) is 1·16 ($\pm 0{\cdot}2$) elastic deflections per week. The theoretical order of magnitude estimate is thus confirmed, although the observed rate is not quite linear with stress.

(4) An interruption of the irradiation for two weeks (7th to 9th) caused the creep curve to be displaced along the time axis by the same amount. During the first part of this period the specimens were held in the pile, at zero power, and continued to creep. Afterwards they were held out of the pile and reversed their deformation.

There are several points for further investigation in the above results. The transient creep probably reflects the fact that the creep strain has to reach an appreciable fraction of σ_y/E before the steady-state distribution of internal stress is reached; initially, the rate of this transient may approach more nearly to $\dot{\epsilon}_g$ than $\dot{\epsilon}_e$. The behaviour during the period of interruption of irradiation is interesting, but it is not clear that holding the specimens in the pile under zero power can have an effect significantly different from that of holding them out of the pile. Further experiments are being made on this point. It is of course to be expected that the specimens would continue to creep for a period after the neutron flux is stopped, since the internal stresses which produce the creep persist until they are relaxed by creep. The reversal of creep which occurs afterwards is unexpected; possibly it is related to changes in elastic constants which are known to occur (Sansom, Hancock and Barnes, private communication) in uranium after irradiation.

ACKNOWLEDGMENTS

During the course of this work we had the benefit of useful discussions with Dr. W. M. Lomer, Mr. R. S. Barnes, Dr. A. T. Churchman, Dr. M. J. Makin, Mr. L. M. Wyatt and Dr. J. H. Bowen. Dr. M. Levy helped with a preliminary experiment, and Mr. O. C. Rock helped with the present one.

REFERENCES

BALL, J. G., 1956, *J. Inst. Metals*, **84**, 239.

KONOBEEVSKY, S. T., PRAVDYUK, N. F., and KUTAITSEV, V. I., 1955, *Geneva Conf. on Atomic Energy*, Paper No. 681.

NABARRO, F. R. N., 1948, *Report on Strength of Solids* (London: Physical Society), p. 75.

PAINE, S. H., and KITTEL, J. H., 1955, *Geneva Conf. on Atomic Energy*, Paper No. 745.

PUGH, S. F., 1955, *Geneva Conf. on Atomic Energy*, Paper No. 443.

SEITZ, F., 1949, *Disc. Faraday Soc.*, No. 5, 271.

LXXIII. *Scattering of Phonons and Electrons by Imperfections in a Metal*

By K. Mendelssohn, F.R.S. and H. Montgomery
Clarendon Laboratory, Oxford †

[Received February 1, 1956]

Heat transport in superconducting metals is a complex phenomenon, and many details still await a quantitative explanation. K_n, the thermal conductivity in the normal state (restored by a weak magnetic field), is due almost entirely to conduction electrons, unless the metal is very impure. K_s, the thermal conductivity in the superconducting state, is more complicated; however, recent experiments (Mendelssohn and Renton 1953, 1955, Laredo 1955) suggest that at low temperatures K_s is mainly due to phonons. In comparison with the normal metal the effect of the latter is much enhanced. This is because in a superconductor with falling temperature, the electrons are rapidly losing their entropy and can neither conduct heat nor scatter phonons.

The wavelengths of phonons are much longer than those of electrons. One may thus expect that the scattering effects of various crystal imperfections will be quite different in the two states. The following examples are taken from a general investigation of heat conduction in lead specimens, and they serve to contrast the effects produced by strain and by chemical impurity respectively.

A polycrystalline specimen of lead, containing 0·5 At % of Thallium, was annealed carefully, and its electrical and thermal conductivities measured between 1° and 4°K. The latter results are shown in curves 1 and 2 of fig. 1. Without removing it from the cryostat, the specimen was bent slightly and restraightened. The measurements were then repeated, the specimen being cooled to helium temperatures on the day after the strain had been introduced. Curve 2 shows that K_n was unaffected by this treatment, and the same was true of the electrical conductivity. However, curve 3 shows that the strain had reduced K_s by a factor of six at 1°K, and by a smaller proportion at higher temperatures.

Changing the amount of impurity in the specimens has the reverse effect. Figure 2 shows the conductivities of two annealed single crystals, one of pure lead, and the other containing 1 At % Bismuth. Although K_n and also the electrical conductivity was decreased by a factor of 100 on alloying, the two specimens had almost the same value of K_s below 1·4°K. Other measurements showed that K_s is similarly insensitive to the introduction of thallium or tin as impurity, provided that the solid solubility limit is not exceeded. Laredo (1955) found a closely similar behaviour in alloys of tin with indium. It should be noted that the effects described here cannot be caused by small frozen-in magnetic fields, since compensation of the earth's field as the specimens passed through their transition temperatures did not influence the results.

---

† Communicated by Dr. K. Mendelssohn, F.R.S.

Fig. 1

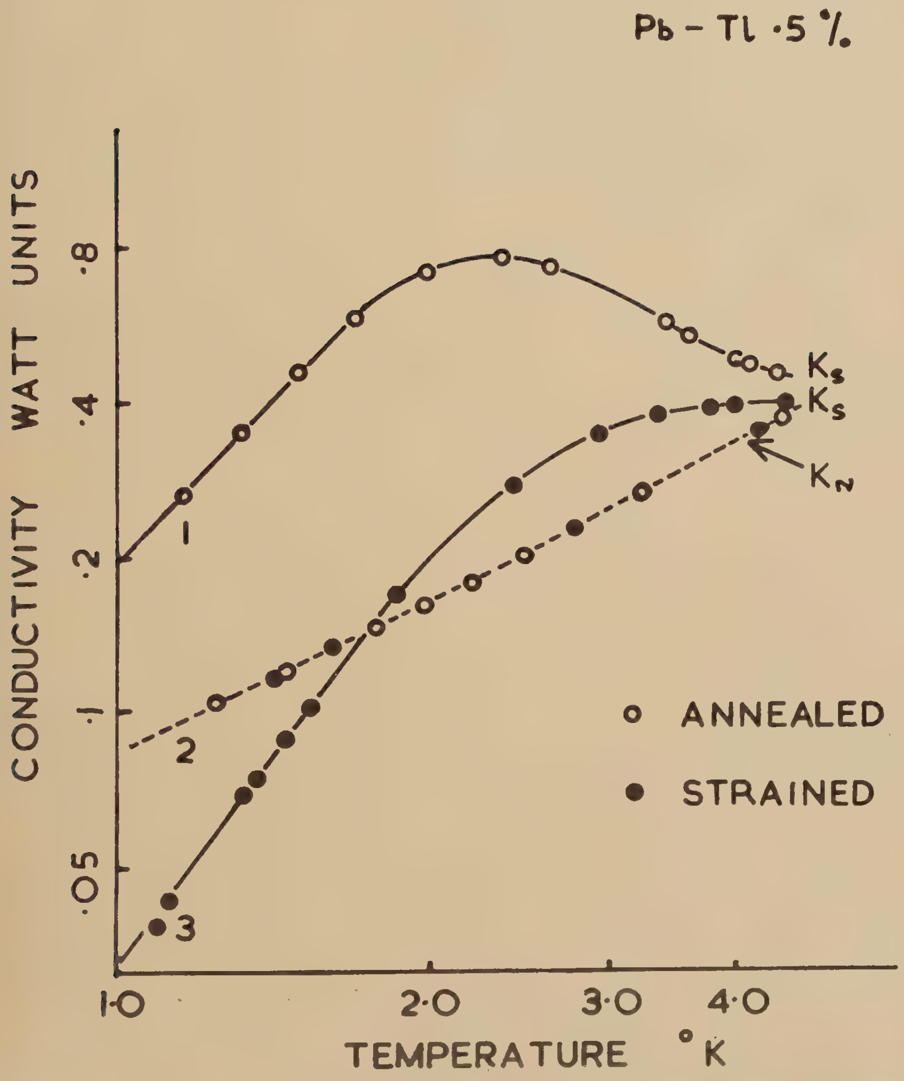

Logarithmic plot of the heat conductivity K_n in the normal and K_s in the superconductive state of an annealed and subsequently strained specimen of lead with 0·5 At % thallium.

Thus at sufficiently low temperatures, K_s is sensitive to strain but not to impurity, while K_n is sensitive to impurity but not to strain. A suggested explanation of this behaviour is as follows. Owing to their long wavelengths, the phonons are not scattered by impurity atoms, which scatter the electrons very strongly. When the specimen is plastically deformed at room temperature, dislocations are produced. Electrons are scattered less effectively by dislocations than by point defects or

Fig. 2

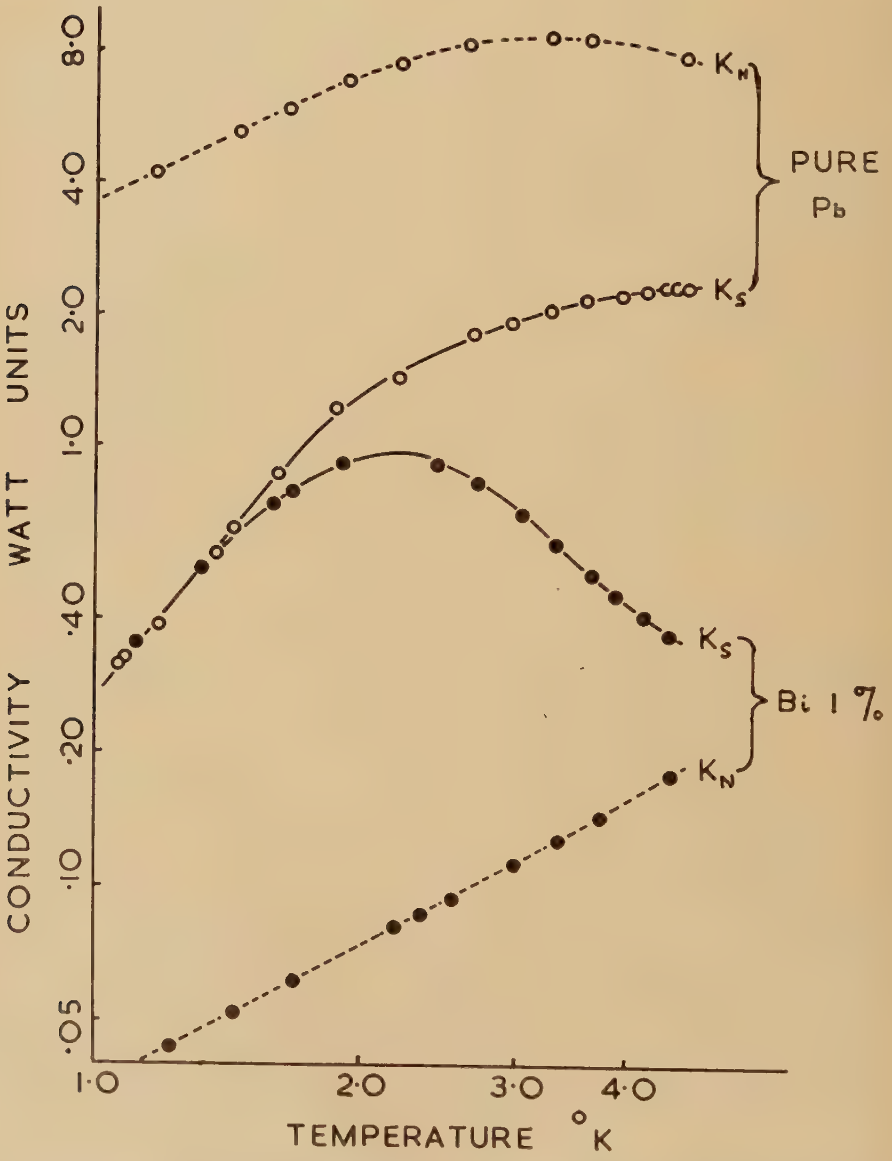

Logarithmic plot of the heat conductivity K_n in the normal and K_s in the superconductive state of single crystals of pure lead and lead with 1 At % bismuth.

impurities (van Bueren and Jongenburger 1955). Hence K_n is unaffected by the deformation of the specimen at room temperature, but the dislocations produced scatter the phonons strongly and K_s is much reduced.

These experiments support the view that phonon conduction is at low temperatures predominant in superconductors. Moreover the use of a superconductive metal demonstrates the nature of the different scattering processes in unusually simple circumstances. A full account of the general survey of dilute lead alloys will be published in due course. It is interesting to note that Kemp *et al.* (1956) have recently drawn similar conclusions from work on non-superconducting alloys, where the phonons are scattered partly by defects but mainly by conduction electrons.

Thanks are due to Dr. J. M. Makin, of A.E.R.E., Harwell, for help and advice in making the single crystals.

REFERENCES

VAN BUEREN, and JONGENBURGER, 1955, *Nature, Lond.*, **175,** 344.
KEMP, KLEMENS, STEEDHAR, and WHITE, 1956, *Proc. Roy. Soc.* A, **233,** 480.
LAREDO, 1955, *Proc. Roy. Soc.* A, **229,** 473.
MENDELSSOHN, and RENTON, 1953, *Phil. Mag.*, **44,** 776 ; 1955, *Proc. Roy. Soc.* A, **230,** 157.

LXXIV. *Columnar Recombination in Nitrogen*

By E. H. Bellamy and W. R. Hogg
Department of Natural Philosophy, University of Glasgow†

[Received November 16, 1955 ; and in revised form May 8, 1956]

Under normal conditions of use, pulse ionization chambers function by virtue of the collection of free electrons liberated by the incident radiation. It is sometimes found, especially under conditions of high gas pressure, that the recorded pulse is smaller than the initial ionic burst and this loss of pulse height is generally attributed to capture of electrons by electronegative impurities in the gas resulting in the formation of negative ions which, owing to their much smaller mobility, are not collected within the short collection times used.

It is generally considered that direct electron–positive ion recombination will not occur in such a chamber in view of the small values of electron–positive ion recombination coefficients found by the earlier measurements of these coefficients. Preferential recombination in free electron gases is also expected to be negligible under all practical conditions (see for example Wilkinson 1950, where the problem of recombination is discussed in general). However, measurements of the electron–positive ion recombination coefficient in nitrogen by the micro-wave method (Biondi and Brown 1949) yielded a value 10^4 times greater than the earlier measurements. It is therefore possible that direct electron–positive ion columnar recombination may occur, although no immediate estimate of the effect can be made since columnar recombination has been treated theoretically only for the case of recombination after negative ion formation. Preferential recombination is not expected to be important even allowing for the higher recombination coefficient.

We have observed a loss of pulse height from α-particles in a high pressure nitrogen-filled gridded ionization chamber. Attempts to eliminate this by gas purification were unsuccessful. The variation of pulse height with gas pressure in this chamber is shown in the figure, where it is seen that full electron collection occurs below a total pressure of 2·5 atmospheres. Commercial ‘ oxygen free ’ nitrogen was passed slowly into the thoroughly outgassed chamber through a coil immersed in liquid oxygen which removed condensable impurities. Traces of oxygen were removed inside the chamber by an electrically heated copper spiral which had been previously reduced in a hydrogen atmosphere.

To examine this loss of pulse height in more detail, three collimated polonium α-sources were mounted at distances of 13·5, 8·9 and 3·2 cm from the collector. The latter two were fixed on metal rods and could be removed from the counting volume while the chamber was in operation. The voltages on the rods were adjusted to give full electron collection at low pressures. At 10 atmospheres, it was observed that the pulse heights from all three sources had decreased to the same value. This result shows that electron capture was not occurring in transit to the collector plate and that the loss of pulse height must be attributed to direct preferential or columnar recombination between electrons and positive ions.

---

† Communicated by the Authors.

It may also be noted that Stafford (1948) found a decrease in pulse height from protons in a pulse ionization chamber filled with purified hydrogen at pressures up to 90 atmospheres. This author attributed the effect to preferential recombination.

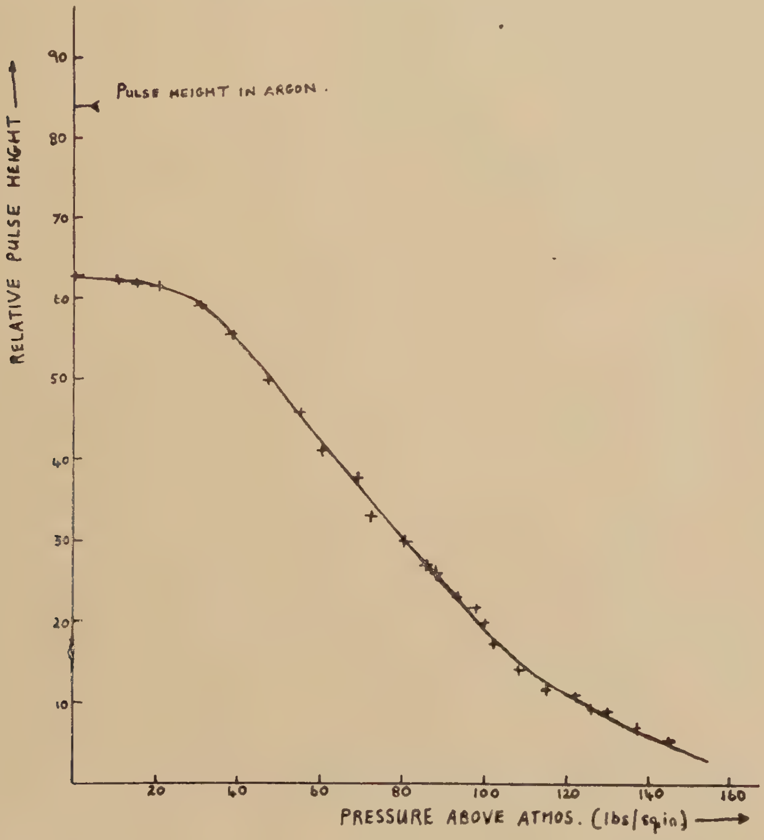

To distinguish between preferential and columnar recombination, the effect of columnar ionic density was examined. The chamber pressure was increased to 20 atmospheres, where pulses from polonium α-particles were not observed, and pulses were observed from electrons liberated in the chamber by γ-rays from a strong ^{60}Co γ-ray source, and also from protons produced by the ^{14}N (n, p) ^{14}C reaction when the chamber was irradiated with 2·5 MeV neutrons from the d(d, n) ^{3}He reaction. No loss of pulse height was noticed from these pulses.

The above experiments seem to establish that the loss of pulse height cannot be attributed either to loss of electrons by negative ion formation or to preferential recombination and suggest that the effect may therefore reasonably be associated with columnar electron–positive ion recombination.

The absence of columnar recombination in argon (full electron collection from α-particle tracks have been obtained in this chamber filled to 40 atmospheres with argon) may be explained in terms of the higher electron temperature in argon.

We wish to acknowledge the collaboration of Dr. F. C. Flack in the attempts to obtain full electron collection from α-particles at high gas pressures by purification of the nitrogen.

REFERENCES

BIONDI, M. A., and BROWN, S. C., 1949, *Phys. Rev.*, **76,** 1697.
STAFFORD, G. H., 1948, *Nature, Lond.*, **162,** 771.
WILKINSON, D. H., 1950, *Ionization Chambers and Counters* (Cambridge: University Press).

LXXV. *The Low Frequency Spectrum of the Cygnus* (19N4A) *and Cassiopeia* (23N5A) *Radio Sources*

By R. J. Lamden and A. C. B. Lovell
Jodrell Bank Experimental Station, University of Manchester †

[Received February 8, 1956]

Abstract

The intensities of the radio sources in Cygnus (19N4A) and Cassiopeia (23N5A) have been measured at frequencies of 16·5, 19·0, 22·6 and 30·0 Mc/s by using the 218-foot aperture transit radio telescope at Jodrell Bank. The main feature of the results is the abrupt fall in intensity of both sources at frequencies below 22 Mc/s. Possible causes of this behaviour are discussed and it is shown that the effect is probably due to absorption of the radiation in an interstellar Hɪɪ region of average density and extent.

§ 1. Introduction

Measurement of the intensity of the extraterrestrial radio sources is difficult at low frequencies because of interference from long distance ionospheric scatter signals. At the present time the published measurements extend to a low frequency limit of 22·6 Mc/s (Hey and Hughes 1954) at which the intensities of the Cygnus and Cassiopeia sources were still increasing. Measurements at still lower frequencies are desirable because it is in this low frequency region that the possible theories of the mechanism of generation of the radio noise differ in their predictions (for example, see Twiss 1954). An attempt has therefore been made to extend the lower frequency limit by using the narrow beam of the Jodrell Bank 218-foot transit radio telescope to alleviate the interference trouble, and the paper describes the results of measurements on 16·5, 19·0, 22·6 and 30·0 Mc/s.

§ 2. Apparatus

The primary feed for the radio telescope consisted of a dipole with reflector. The frequency range 16·5 to 22·6 Mc/s was covered in a single array by the use of adjustable telescopic tubing, but a separate array was necessary for the 30 Mc/s measurements. This primary feed was matched through a halfwave trombone to approximately 300 feet of low loss pressurized concentric cable running to the receiver situated outside the

---

† Communicated by the Authors.

bowl of the telescope. The loss in this cable was determined at each frequency by a comparison of noise diode measurements at the receiver input and at the aerial. The transfer loss included in the final reduction of the results contained an allowance for the various impedances which were measured at each frequency with an impedance bridge. The direction of the beam of the transit telescope could be adjusted for the observation of Cygnus or Cassiopeia by altering the tilt of the mast carrying the primary feed and impedance measurements were made in both positions of the mast so that a correction could be made for any changes in intensity which might arise from differing impedances in the two positions.

The receiver was a superheterodyne with an intermediate frequency of 465 kc/s. A narrow band width of 4 kc/s was used to assist in the selection of a band with minimum interference. The overall time constant was 4 seconds and the signal output was measured on a pen recording milliammeter.

Since the direction of the beam of the telescope could be adjusted by the operation of a winch controlling the tilt of the aerial mast, it was, in principle, possible to make observations on Cygnus and Cassiopeia during the same night. However, the beam was too broad to give a complete record of the successive transit of each source except on 30 Mc/s, and at the lower frequencies it was advisable to observe the sources on separate nights. Even with the relatively narrow beam of the telescope it was found that observations could be made only during the summer months when Cygnus and Cassiopeia were in transit during darkness. Under these conditions the 30 and 22·6 Mc/s measurements were straightforward, but the difficulties were severe on 19 Mc/s and 16·5 Mc/s, and only a small percentage of the total number of runs was sufficiently clear of interfering signals to be used in the analysis.

§3. RESULTS

The final series of measurements were made between May 1st and August 12th, 1955. A sample of the records obtained is shown in fig. 1 which is a facsimile of the 30 Mc/s recordings on August 11–12, 1955. Both sources show scintillations, an effect which was so severe on some of the lower frequency records that measurement of the deflection was impossible. Hence, a certain number of records had to be rejected on this account in addition to those rejected because of obscuration by interfering signals. The power input P at the receiver necessary to give the deflections as measured from the records similar to fig. 1 was determined by calibrating with a noise diode at the receiver input. The intensities of the radio sources S were then obtained from $S=(2P/A)\,\alpha$ where A is the collecting area of the radio telescope, and α the overall transfer loss referred to in § 2 above. The factor 2 is included so that the results refer to both planes of polarization. The details of the results are given in table 1 and are included in figs. 2 and 3.

Table 1

Date 1955	Frequency Mc/s	Intensities watts/m²/c.p.s. × 10^{-23}		Ratio Cygnus/ Cassiopeia
		Cassiopeia (23N5A)	Cygnus (19N4A)	
Aug. 2 to Aug. 12	30·0	45·0	24·0	0·53
May 1 to May 24	22·6	46·0	24·4	0·53
May 30 to June 11	19·0	27·2	18·9	0·69
June 26 to July 19	16·5	<11	14·5	> 1·0

§ 4. ERRORS

Random errors amounting to a few per cent arise in the noise diode calibration, and in the measurement of the transfer loss α from aerial to receiver. However, these errors are small compared with two major sources of error discussed below.

(i) In order to obtain the true deflection due to the source in this type of total power experiment it is necessary to extrapolate the background radiation in records of the type illustrated in fig. 1. In the case of Cassiopeia little difficulty arises since the source lies in a region where the background is uniform. The errors in determining the deflection of Cassiopeia are therefore small and arise mainly from the uncertainty in estimating the mean contour through the scintillations. Cygnus, however, lies on a steep slope of the galactic background and the uncertainty as to the extrapolation of this background would, under normal conditions, invalidate this type of experiment, particularly on the lower frequencies where the beam width becomes appreciable. The difficulty is illustrated in fig. 4 which shows the record of Cygnus on 22·6 Mc/s for May 18th, 1955. Fortunately the occurrence of scintillations which are well marked in this record, coupled with a knowledge of the time of transit, enable the extrapolation to be made. Even so this represents the chief source of random error in the experiment which is estimated to be about ±10%.

(ii) The second principle source of error is a systematic one arising from uncertainty as to the actual collecting area A of the transit telescope at these low frequencies. The physical area of the aperture is 3500 m², but the effective collecting area is considerably less than this for a variety of reasons, such as the inefficiency of the primary feed and the transmission

Fig. 2

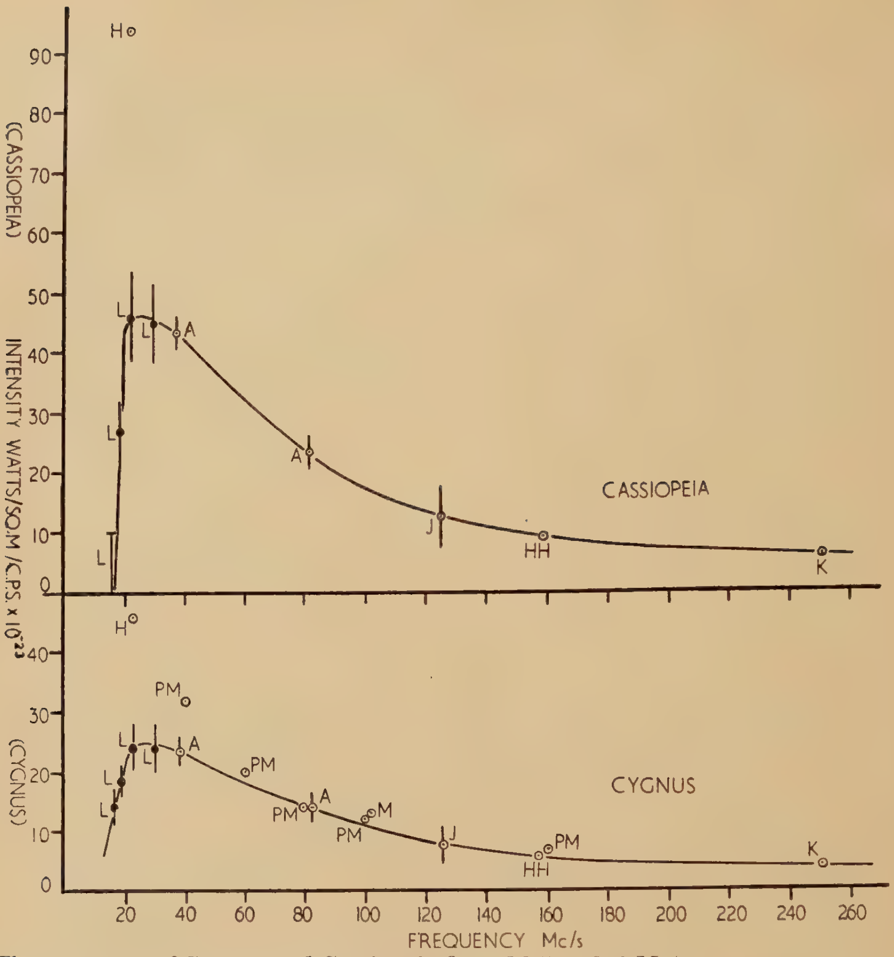

The spectrum of Cygnus and Cassiopeia from 16·5 to 250 Mc/s.
L=Lamden and Lovell (this paper). A=Adgie (1955). H=Hey and Hughes (1954). J=Jennison (Jodrell Bank, unpublished). HH=Hanbury Brown and Hazard (1951 b). M=Mills (1952). PM=Piddington and Minnett (1952). K=Kraus, Ko and Matt (1954).

Fig. 3

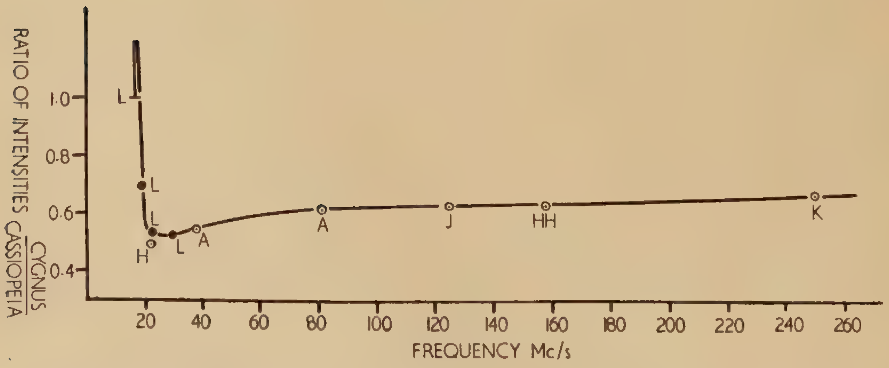

The ratio of intensities of Cygnus and Cassiopeia from 16·5 to 250 Mc/s. (Key as for fig. 2.)

loss through the wire reflecting surface. The estimated gain of the telescope as a function of wavelength has been given by Lovell (1954), and Hanbury Brown and Lovell (1955) based on unpublished calculations by Clegg. The only experimental check on the power gain was made by Hughes (1949) using a transmitter in an aircraft as a source at 72 Mc/s. These results were in close agreement with the above predictions. On 158·5 Mc/s Hanbury Brown and Hazard (1951 a) established that the beam width as determined by measurements on the radio sources was in close agreement with the calculated value. The effective collecting areas were 1560 m^2 on 72 Mc/s and 1000 m^2 on 158·5 Mc/s. On this basis the collecting area on 20 Mc/s should be 2330 m^2, assuming the same type and efficiency of the primary feed. The actual primary feed in the present experiments consisted of a single dipole with reflector, instead of the array used in the 72 Mc/s and 158·5 Mc/s work and measurement of its polar diagram showed that the fraction of the power falling within the telescope reflector was 0·48 instead of 0·8 for the arrays. This, together with several other smaller factors, such as the change in gain with tilt of the mast, have been considered in detail by Lamden (1955). The conclusion is that the effective collecting area in the present experiments varied from 1000 m^2 on Cygnus at 30 Mc/s to 1200 m^2 on Cassiopeia at 16·5 Mc/s. The appropriate values have been assumed in the reduction of the chart readings to source intensities as described in § 3, but it is considered that these values may be in error by as much as ±20% and they are the source of the predominant uncertainty in the results given in table 1.

These considerations apply only to the absolute values of intensity. In the measurements of the ratio of the intensities of Cygnus and Cassiopeia this error is common, and the uncertainty is the random error considered in (i) of ±10%. In the case of Cassiopeia on 16·5 Mc/s no deflection could be measured and the value given therefore represents an upper limit for the intensity.

§ 5. COMPARISON WITH PREVIOUS RESULTS AND DISCUSSION OF THE SPECTRUM

There are no published measurements in the critical region below 22·6 Mc/s with which the results can be compared. The sudden fall off which is the main feature of the present experiment will be discussed in § 6. In this section the influence of the 22·6 and 30 Mc/s measurements on the nature of the spectrum at these higher frequencies will be considered.

As a result of their measurements on 22·6 Mc/s Hey and Hughes (1954) considered that the spectrum of Cassiopeia between 20 and 200 Mc/s could be represented by a law of the form $I \alpha f^{-1 \cdot 2}$. The spectrum of Cygnus was similar although a fall off in intensity was indicated at frequencies below 50 Mc/s. Since the publication of these results the present measurements on 22·6 and 30 Mc/s have been made, and also those of Adgie (1955) on 38 Mc/s for which an accuracy of ±10% is claimed. All the measurements have therefore been replotted in figs. 5 and 6 on a log–log scale for comparison with the spectrum derived by Hey and Hughes which is shown as a full line (i.e., $I \alpha f^{-1\cdot 2}$). It is obvious that it is not possible to reconcile the various measurements in this region of the spectrum and the present position can be summarized as follows :

Fig. 5

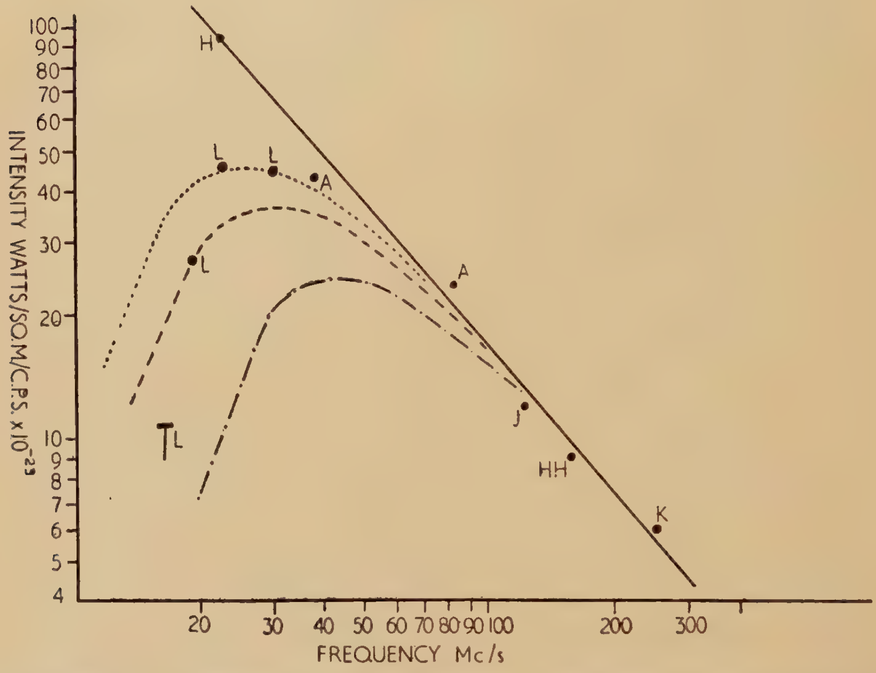

The spectrum of Cassiopeia on a log–log scale. The experimental points are those of fig. 2. The full line is $I \alpha f^{-1\cdot 2}$, and the broken curves show the calculated effect of absorption in an H II region with values of $\int N^2 ds$ as follows :

— · — · — · — 6×10^{21} cm^{-5}.
———————— 3×10^{21} cm^{-5}.
. . . . $2\cdot 04 \times 10^{21}$ cm^{-5}.

(i) In the region between 50 and 300 Mc/s the conclusion of Hey and Hughes that the spectrum can be represented by a law of the form $I \alpha f^{-1\cdot 2}$ would appear to be justified.

(ii) In the region between 20 and 50 Mc/s the continuation of this law can be justified only if the present results, and those of Adgie are rejected in favour of those of Hey and Hughes (and of Piddington and Minnett 1952) in the case of Cygnus.

(iii) If the new results (Lamden and Lovell ; Adgie) are preferred, the indication is that the spectrum changes from an $f^{-1\cdot 2}$ law above 50 Mc/s to a law of the form $I \alpha f^{-0\cdot 6}$ between 20 and 50 Mc/s.

It seems unlikely that the discrepancy can be resolved until further independent measurements are made between 20 and 50 Mc/s. On the other hand it may be mentioned that the most probable interpretation of the results (see § 6) implies a change of slope at the higher frequency, and moreover that this change in the case of Cygnus was already anticipated in the work of Hey and Hughes.

Fig. 6

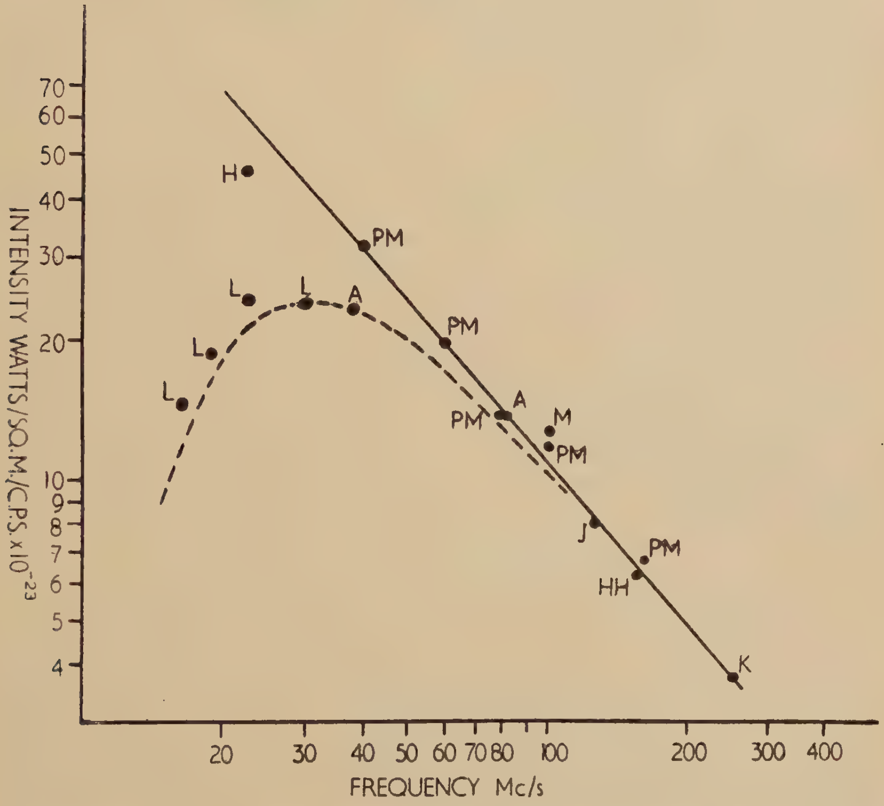

The spectrum of Cygnus on a log–log scale. The experimental points are those of fig. 2. The full line is $I \propto f^{-1\cdot 2}$ and the broken curve is the calculated effect of absorption in an HII region with $\int N^2 ds = 3 \times 10^{21}$ cm^{-5}.

§ 6. THE FALL OF INTENSITY BELOW 22·6 Mc/s

The primary result of the experiments described in this paper is the abrupt fall in intensity of both sources below 22 Mc/s. The measurements on the four frequencies were made with the same apparatus and hence this sudden change in slope is uninfluenced by any underestimate of systematic errors which might affect the discussion in § 5 above. It is clear from figs. 5 and 6 that, whatever values for the intensity are preferred on 22·6 Mc/s and above, the slope of the spectrum changes from one with an exponent negative in the region $-0{\cdot}13$ to $-1{\cdot}2$, to a positive exponent. In the case of Cygnus the law below 22·6 Mc/s appears to be of the form $I \alpha f^{+1{\cdot}6}$ and for Cassiopeia $I \alpha f^{+4{\cdot}4}$. The value of the exponent in the latter case remains in some doubt because it was possible to set only an upper limit to the intensity of Cassiopeia on 16·5 Mc/s. At the same time, fig. 3 shows that there is a significant change in the ratio of the intensity of the two sources. From 250 to 22·6 Mc/s the ratio Cygnus/Cassiopeia decreases slowly from 0·66 to 0·52. Between 22·6 and 16·5 Mc/s the ratio increases sharply and probably rises above unity in the neighbourhood of 16·5 Mc/s. Some possible reasons for this behaviour will be discussed below.

(*a*) THE EFFECT OF THE IONOSPHERE

The effect of absorption in the ionosphere must be considered as a possible cause of the fall of intensity below 22·6 Mc/s. Calculations of the absorption to be expected in a radio wave traversing the ionosphere have been made by several workers, and for the case at present under consideration the treatment by Jaeger (1947) is appropriate. In the experiment the sources were observed at transit and the zenith angle was 6° for Cassiopeia and 14° for Cygnus. The error introduced by considering the case of a radio wave incident vertically will therefore be small compared with the effect under investigation. In this case it can be shown that for a wave of frequency f making a single passage of a Chapman region with critical frequency f_c, the absorption is given by

$$4{\cdot}34\,\frac{\nu_m H}{c}\left(\frac{f_c}{f}\right)^2 \Phi\left(\frac{f_c}{f}\right) dB$$

where H is the scale height, c the velocity of light, ν_m the collision frequency at the height of maximum ionization, and Φ is a function tabulated by Jaeger (1947). For the night time F_2 layer in the summer the appropriate values of H and ν_m are 35 km (Martyn 1954) and $1{\cdot}6 \times 10^3\ \text{sec}^{-1}$ (Mitra 1952) approximately, thus the absorption is

$$0{\cdot}8\left(\frac{f_c}{f}\right)^2 \Phi\left(\frac{f_c}{f}\right) dB.$$

The maximum values of the critical frequency f_c for the F_2 layer during the runs on the various frequencies have been obtained from the Slough data. These are shown in table 2 together with the absorption calculated from the above formula.

Mitra and Shain (1953) have determined the absorption by the F_2 region of 18·3 Mc/s radio waves in the southern hemisphere using the extra-terrestrial radio emissions. Although their curve of variation with frequency has a different shape from the one calculated from Jaeger's theory, the general agreement of absolute values between theory and experiment is reasonable. Hence the above calculation of the absorption can be applied to the present experiment with confidence. In this calculation the maximum value of f_c during the course of the individual experiments has been taken, and it is therefore very improbable that the ionospheric absorption at any time exceeded 0·5 *dB*. Moreover, the differential absorption between the 22·6 Mc/s runs and those on 19·0 and 16·5 Mc/s is only ~0·1 *dB* and hence the influence of the ionosphere on the sharp fall in intensity must be negligible.

Table 2

Wave (f) Mc/s	Critical Frequency f_c of F_2 layer (Slough) Mc/s	(f_c/f)	$(f_c/f)^2$	$\Phi(f_c/f)$ (Jaeger)	Absorption *dB*
30·0	7·3	0·24	0·06	4·22	0·20
22·6	6·9	0·30	0·09	4·26	0·31
19·0	6·0	0·32	0·10	4·31	0·34
16·5	5·4	0·33	0·11	4·31	0·38

(*b*) *Absorption in Interstellar* HII *Regions*

The effect of HII regions on the extra-terrestrial radio emissions have been considered by a number of workers [for example, Piddington (1951), Scheuer and Ryle (1953)], and the possibility that absorption in these regions might be the cause of the fall off in intensity at low frequencies will be considered in this section. The absorption of a radio wave of frequency ν traversing an HII region containing N_e electrons per cm³, has been investigated by Smerd and Westfold (1949). By making certain simplifying assumptions Scheuer and Ryle (1953) have shown that the absorption coefficient K_ν can be written as

$$K_\nu = 0{\cdot}177\ T_e^{-3/2}\ \nu^{-2}\ N_e^2$$

where T_e is the kinetic temperature in the region. In the following calculation we also make the conventional assumption that $T_e = 10^4$°K so that

$$K_\nu = 0{\cdot}177 \times 10^{-6} \nu^{-2} N_e^2.$$

The optical depth

$$\tau_\nu = \int_0^\infty K_\nu\, ds$$

$$= 0{\cdot}177 \times 10^{-6}\ \nu^{-2} \int_0^\infty N_e^2\, ds.$$

The ratio of intensities before and after absorption is given by

$$I = I_0 \exp(-\tau_\nu) = I_0 \exp\left\{-0{\cdot}177 \times 10^{-6}\, \nu^{-2} \int_0^\infty N_e^2 ds\right\}$$

and hence the influence of absorption in the region can be calculated as a function of ν for given values of

$$\int_0^\infty N_e^2\, ds.$$

There is some diversity of opinion as to the extent and electron density in the average HII region. Values of $N_e = 10\ \mathrm{cm}^{-3}$ in clouds of extent 4 parsecs would appear to be common, in which case $\int N_e^2\, ds = 1{\cdot}2 \times 10^{21}\ \mathrm{cm}^{-5}$. According to Oort (1952) the average HII cloud might contain as many as 20 electrons/cm³, and extend for 5 parsecs, in which case $\int N_e^2\, ds = 6{\cdot}0 \times 10^{21}\ \mathrm{cm}^{-5}$. As a basis for comparison we have assumed a value of $\int N_e^2\, ds = 3{\cdot}0 \times 10^{21}\ \mathrm{cm}^{-5}$ and calculated the absorption I/I_0 as a function of ν. The results are compared with the experimental points for Cassiopeia and Cygnus in figs. 5 and 6 respectively. The assumption made is that, without absorption, the spectrum of the form $I \alpha \nu^{-1{\cdot}2}$, well established at frequencies above 50 Mc/s, would extend to the low frequency region between 16 and 50 Mc/s.

It will be seen that the theoretical curves show very good agreement with the experimental results, particularly in the case of Cygnus, and leave little doubt that the behaviour of the low frequency spectrum can be satisfactorily explained as an effect due to absorption of the radiation in an average HII cloud. Moreover, the nature of the calculated absorption curve is very sensitive to the value assumed for $\int N_e^2\, ds$, as illustrated in fig. 5 where the curves for $\int N_e^2 ds = 2{\cdot}0 \times 10^{21}$, $3{\cdot}0 \times 10^{21}$ and $6{\cdot}0 \times 10^{21}\ \mathrm{cm}^{-5}$ are plotted. These indicate that the Cassiopeia absorption must have occurred in a region with $\int N_e^2\, ds$ in the neighbourhood of 2 to $4 \times 10^{21}\ \mathrm{cm}^{-5}$, with even closer limits set in the case of Cygnus.

(c) *Effects due to Mechanism of Generation in the Radio Sources*

A number of suggestions have been made in an attempt to explain the generation of the radio frequency energy in sources such as Cassiopeia and Cygnus and it is necessary to explore the possibility that any of these ideas might explain the fall off below 22 Mc/s.

(i) *Thermal mechanisms.* A thermal mechanism would produce an intensity varying as a function of ν between ν^0 and ν^2 depending on the optical depth of the emitting region. The extreme case of a black body emitter (ν^2) is not incompatible with the slope of the observed spectrum below 22 Mc/s. At higher frequencies, however, the observed slope is in opposition to that predicted. This is illustrated in fig. 7 where the thermal spectrum is fitted at 60 Mc/s. On these grounds alone the thermal mechanism can be eliminated from the list of possibilities. There are, of course, many other reasons in support of this elimination, particularly the exceedingly high equivalent temperatures ($\sim 10^8$ to 10^{9}°K) required to explain the observed intensity.

(ii) *Emission by relativistic electrons.* Emission by relativistic electrons interacting with local magnetic fields has been considered by a number of authors (e.g. Alfvén and Herlofson 1950). In particular Twiss (1954) has considered the effect of resonant reabsorption in the source, which becomes important below a certain critical frequency. He shows that this critical

Fig. 7

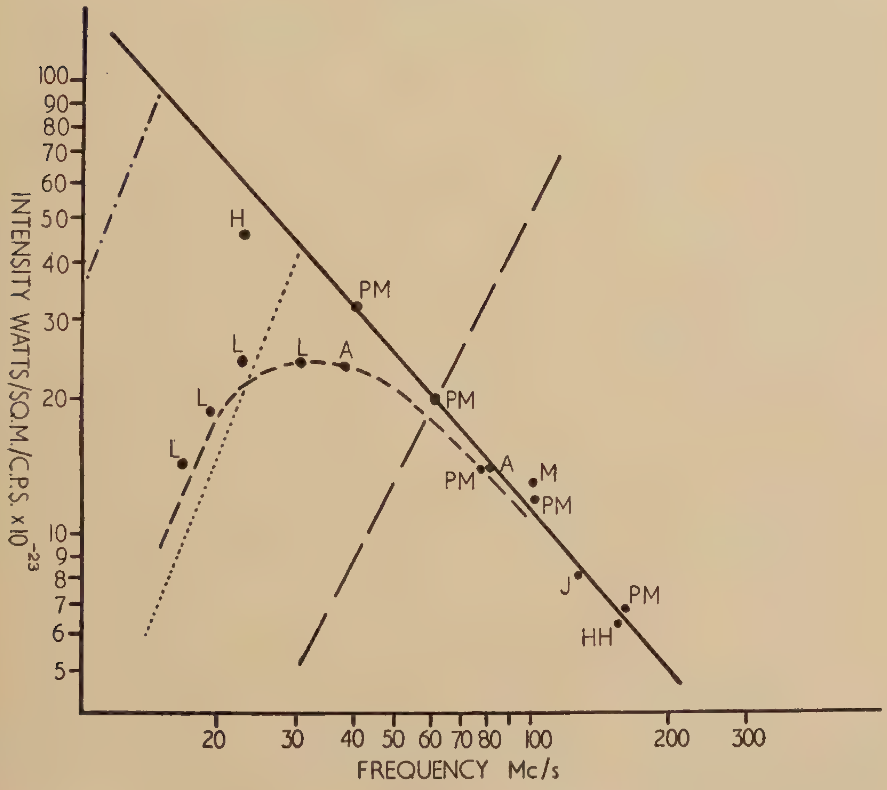

The spectrum of Cygnus on a log–log scale for comparison with the predictions of various theories. The experimental points are those of fig. 2. The full line is $I \alpha f^{-1 \cdot 2}$.

– – – – – – Hɪɪ region absorption as in fig. 6 with $\int N^2 ds = 3 \times 10^{21}$ cm^{-5}.

—— —— —— Thermal spectrum $I \alpha f^2$ fitted at 60 Mc/s.

. . . . Resonant reabsorption of the emission by relativistic electrons with critical frequency 30 Mc/s according to the model proposed by Twiss.

— · — · — · — Resonant reabsorption of the emission by relativistic electrons with critical frequency 15 Mc/s according to the model proposed by Twiss.

frequency should be 10 Mc/s for Cassiopeia and 15 Mc/s for Cygnus, after which the emission falls off as $\nu^{5/2}$. This approximates to the observed behaviour of the spectrum, except that the predicted critical frequencies are too low. The predicted curve for the most favourable case of Cygnus is shown in fig. 7, for two values of ν_c of 15 Mc/s and 30 Mc/s. It is seen that for $\nu_c = 30$ Mc/s the model proposed by Twiss would give reasonable agreement with the observed spectrum. However, it would seem to be out of the question that ν_c could be as high as 30 Mc/s, since the magnetic field (B) required for $\nu_c = 15$ Mc/s approaches the upper limit required by energy considerations, and $\nu_c \alpha B^{7/2}$. The case of Cassiopeia, where the predicted value of $\nu_c = 10$ Mc/s, is even less favourable. It is therefore unlikely that the observed cut off can be caused by resonant reabsorption in the source, and that such an effect, if it exists, is obscured by the cut off at higher frequencies due to other reasons.

(iii) *Plasma phenomena.* A further possibility is that the emission originates from some organized phenomenon such as plasma oscillations in the source. In this connection Jaeger and Westfold (1949) have studied the effect of shock phenomenon and have shown that the intensity distribution will show a cut off at the plasma frequency. In the absence of any precise quantitative theory it is difficult to make comparisons with the observations, although it seems that any plasma shock phenomenon would produce a cut off which is more abrupt than that actually observed.

(iv) *Conclusion.* The various possibilities considered in this section are summarized in fig. 7 together with the experimental points for Cygnus. The only agreement is with the prediction that the fall off is caused by absorption in an HII region of average density and extent. If further work with other radio sources confirms that the low frequency effect is due to this HII absorption then a new technique is available for the measurement of the density, or extent, of these regions in the direction of the radio sources.

ACKNOWLEDGMENTS

We are indebted to Mr. R. Hanbury Brown, Mr. R. D. Davies and many other colleagues at the Jodrell Bank Experimental Station for helpful discussions. One of us (R.L.) was in receipt of a D.S.I.R. Maintenance Grant during the course of this work.

REFERENCES

ADGIE, R., 1955, *I.A.U. Symposium on Radio Astronomy at Jodrell Bank* August, 1955.

ALFVÉN, H., and HERLOFSON, N., 1950, *Phys. Rev.*, **78,** 616.

HANBURY BROWN, R., and HAZARD, C., 1951 a, *Mon. Not. Roy. Ast. Soc.*, **111,** 357 ; 1951 b, *Ibid.*, **111,** 576.

HANBURY BROWN, R., and LOVELL, A. C. B., 1955, *Vistas in Astronomy* (Pergamon Press), **1,** 542.

Hey, J. S., and Hughes, V. A., 1954, *Nature, Lond.*, **173,** 819.
Hughes, V. A., 1949, *M.Sc. thesis* (University of Manchester).
Jaeger, J. C., 1947, *Proc. Phys. Soc.*, **59,** 87.
Jaeger, J. C., and Westfold, K. C., 1949, *Aust. J. Sci. Res.*, **2,** 322.
Kraus, J. D., Ko, H. C., and Matt, S., 1954, *Astrophys. J.*, **59,** 439.
Lamden, R. J., 1955, *M.Sc. thesis* (University of Manchester).
Lovell, A. C. B., 1954, *Discovery*, **15,** 185.
Martyn, D. F., 1954, *Physics of the Ionosphere* (London : Physical Society).
Mills, B. Y., 1952, *Aust. J. Sci. Res.*, **5,** 266.
Mitra, S. K., 1952, *The Upper Atmosphere* (Royal Asiatic Society, Bengal).
Mitra, A. P., and Shain, C. A., 1953, *J. Atmos. Terr. Phys.*, **4,** 204.
Oort, J. H., 1952, *Astrophys. J.*, **116,** 233.
Piddington, J. H., 1951, *Mon. Not. Roy. Ast. Soc.*, **111,** 45.
Piddington, J. H., and Minnett, H. C., 1952, *Aust. J. Sci. Res.*, **5,** 17.
Scheuer, P. A. G., and Ryle, M., 1953, *Mon. Not. Roy. Ast. Soc.*, **113,** 3.
Smerd, S. F., and Westfold, K. C., 1949, *Phil. Mag.*, **40,** 831.
Twiss, R. Q., 1954, *Phil. Mag.*, **45,** 249.

LXXVI. *The Thermal and Electrical Conductivity of Lithium at Low Temperatures*

By H. M. ROSENBERG
The Clarendon Laboratory, Oxford.†‡

[Received January 14, 1956]

ABSTRACT

The thermal and electrical conductivity of two specimens of lithium has been measured in the range 2° to 90°K. At the lowest temperatures the ideal electrical resistivity is found to vary as $T^{3\cdot5}$ and the lattice scattering term for the electronic thermal resistance is $1\cdot8\times10^{-4}T^2$. These results and the value of the Lorenz number are compared with current theories.

§ 1. INTRODUCTION

UP till now the only heat conductivity measurements at low temperatures on the alkali metals have been by Berman and MacDonald (1951) on sodium. They also measured the electrical resistance of their specimens and for this they used a different apparatus. The present work gives the results of electrical and thermal measurements on high purity lithium in which both sets of measurements were taken in the same apparatus. the specimen not having to be handled between the electrical and thermal readings. This prevents any damage occurring to the specimen and hence the electrical and thermal conductivities can be more confidently compared. The general experimental technique has been described previously (Rosenberg 1955). The electrical resistance of the alkali metals at low temperatures has been measured by MacDonald and Mendelssohn (1950).

§ 2. THE SPECIMENS

The lithium was distilled into a stainless steel capillary‡ since the molten metal attacks glass. The capillary was 0·83 mm internal diameter and 1·1 mm outside diameter. Two specimens were made. One, Li 1, had copper thermal contacts hard-soldered into small holes drilled in the capillary so that the copper was in direct contact with the lithium. The second, Li 2, had copper contacts soldered on to the outside of the stainless steel tube and relied on the wall of the tube to provide electrical and thermal contact with the lithium. The second method was found

---

† Communicated by Dr. K. Mendelssohn, F.R.S.

‡ I am very grateful to Mr. G. W. Horsley of Metallurgy Division, A.E.R.E., Harwell, for preparing the specimens.

to be very satisfactory in spite of the low thermal and electrical conductivities of the stainless steel. These are so small that they can be neglected when calculating the conductivities of the lithium.

§ 3. The Electrical Conductivity

Figure 1 shows the variation of the electrical resistivity with temperature from 90°K down to 2°K for the two specimens. It can be seen that their resistance becomes effectively constant below about 9°K. This constant resistance is called the residual resistance and is caused by the scattering of the electrons by physical and chemical defects in the metal.

Fig. 1

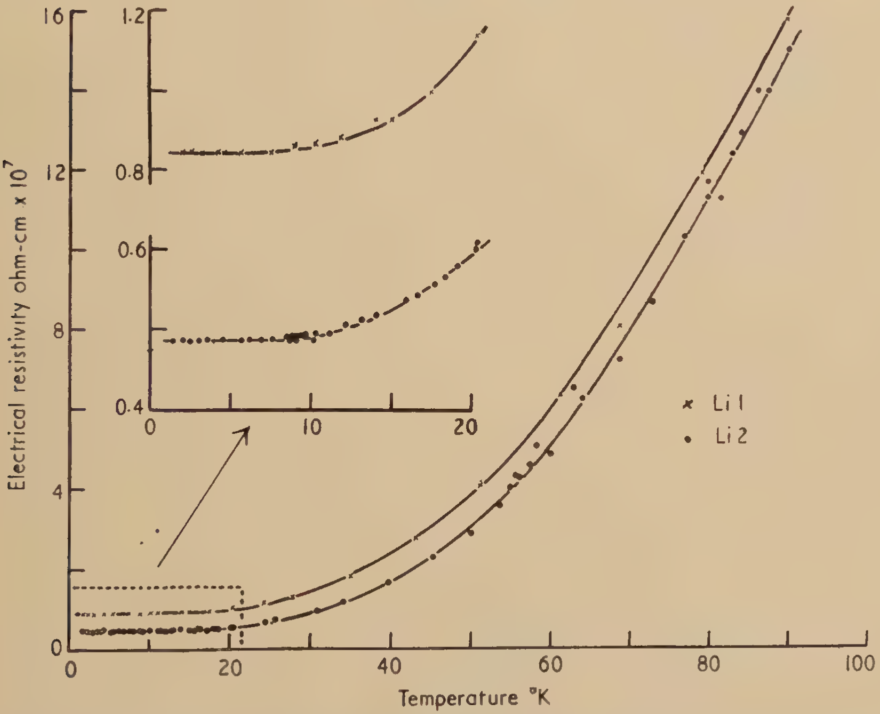

The total electrical resistivities of the two lithium specimens from 2° to 90°K. The inset shows the low temperature end of the graph on a larger scale.

Its value thus depends on the strain and purity of the sample. The graphs show that the residual resistance of Li 1 is about double that of Li 2. This is probably due to the copper wires, which were in contact with the lithium, contaminating the metal slightly, hence increasing the residual resistance. The room temperature resistivity of the specimens is $8 \cdot 98 \times 10^{-6}$ ohm cm for Li 1 and $9 \cdot 17 \times 10^{-6}$ ohm cm for Li 2. This is slightly higher than the values given in standard tables ($8 \cdot 5$ to $8 \cdot 75 \times 10^{-6}$ ohm cm). The ratio of residual to room temperature resistance is 10^{-2} for Li 1 and 5×10^{-3} for Li 2. Thus Li 2 has a very similar ratio to those specimens measured by MacDonald and Mendelssohn (1950).

By subtracting the constant residual resistance from the measured resistivity values, the so-called ‘ ideal ’ resistance is obtained. This is the resistance due to the scattering of the electrons by the thermal vibrations of the lattice and it should be independent of the purity of the specimen. A graph of this ideal resistivity on a logarithmic scale is shown in fig. 2. It can be seen that the values for the two specimens are practically identical and that up to about 65°K the graph is linear indicating that the ideal resistivity is of the form BT^n. For Li 2, n has the value 3·52 up to ~30°K and 3·4 up to ~65°K. For Li 1 n has approximately the same values but since there are fewer experimental points the accuracy is not so high. These values are considerably less than that of $n=4{\cdot}5$ found by MacDonald and Mendelssohn (1950).

Fig. 2

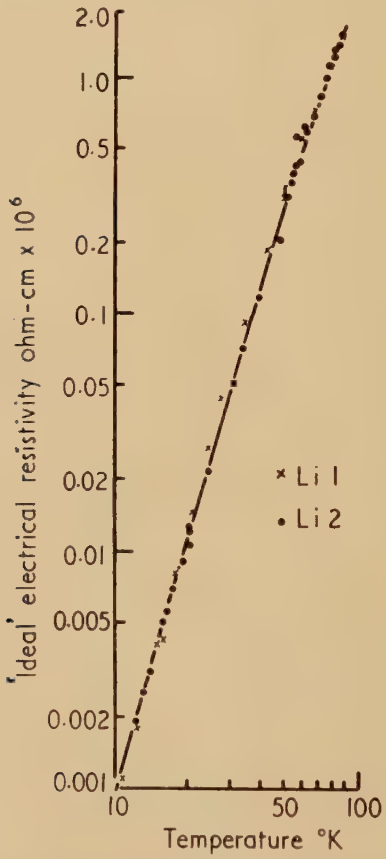

The ‘ ideal ’ electrical resistivity of the two lithium specimens from 10° to 90°K plotted on a logarithmic scale. It will be noted that this resistivity has almost the same value for both specimens.

The modern theory of electrical conductivity was first developed by Bloch (1928, 1930) and later modifications by various authors are given by Ziman (1954). At low temperatures where $T<\theta/12$, where θ is the Debye characteristic temperature, i.e. below 30°K for lithium, the ideal resistivity should be proportional to T^5. In spite of the discrepancy in the value of n found between this work and that of MacDonald and Mendelssohn (1950), both agree in the fact that down to 10°K, at least, n is considerably less than 5. Whilst future work with purer samples (in which the resistance would not become constant until much lower temperatures) might yield the value $n=5$ in a lower temperature range there would still remain the theoretical difficulty as to why such a very low temperature was necessary in order to obtain the correct theoretical value.

Fig. 3

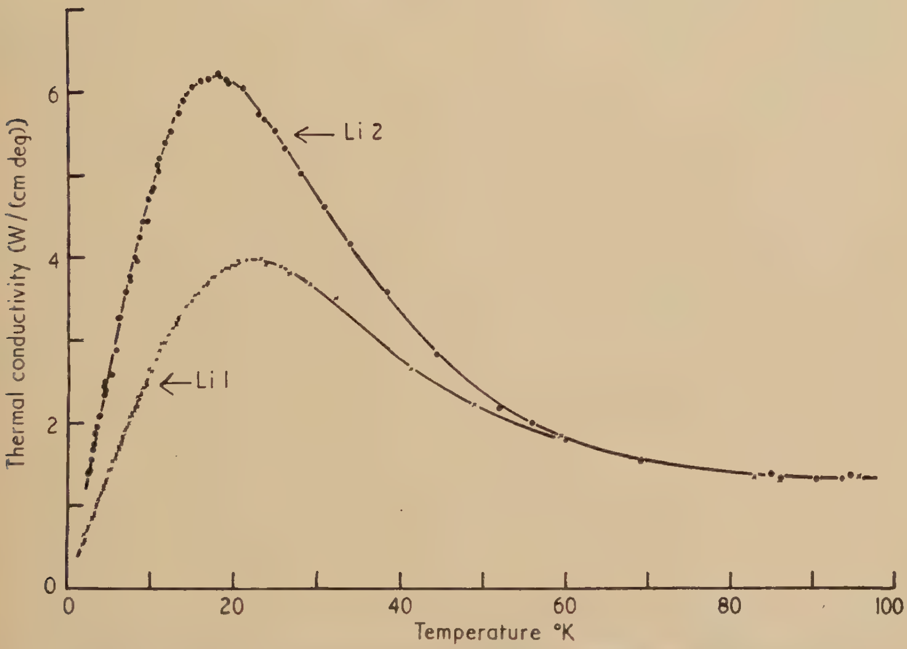

The thermal conductivity for the two lithium specimens from 2° to 90°K.

Because the resistivity does not obey a T^5 law in the low temperature region any attempts to calculate a characteristic temperature θ for the lattice vibrations from the Grüneisen (1933) formula will give a value of θ which is temperature dependent. At 90°K this is about 360°K and at 20·3°K it is 258°K, both in satisfactory agreement with Mendelssohn and MacDonald (1950). At 11·1°K the value of θ is 231°K, which is below that of Mendelssohn and MacDonald as is to be expected since the resistivity of our specimen varied with a lower power of T. Ziman (1954) suggests that θ should increase slightly as the temperature is decreased from $T=\theta/15$ to $T=0$°K. The present work does not give any evidence for such a trend.

§ 4. THE THERMAL CONDUCTIVITY

The thermal conductivity of the two specimens in the range from 2° to 90°K is shown in fig. 3. This shows that both have the same conductivity down to about 60°K and that below this temperature Li 2 has the higher value thus showing the same behaviour as the electrical conductivity. Both have a maximum in the thermal conductivity at about 20°K although that for the purer sample, Li 2, is at a slightly lower temperature than that for Li 1. This is in accord with the theory. Below this maximum the conductivity decreases linearly through the origin.

The modern theory of the thermal conductivity of metals is outlined by Olsen and Rosenberg (1953) and is developed further by Ziman (1954). It is also dealt with in detail by Klemens (1956). Analogous to the electrical resistance, the thermal resistance W can be considered as the sum of two separate independent resistances, W_i, the resistance due to the scattering of the electrons by the lattice vibrations which should be independent of the sample, and W_0 the resistance due to the scattering of the electrons by impurities which will depend on the purity of the sample. W_0 is of the form β/T and at temperatures below about $\theta/10$, W_i is of the form αT^2. Thus we have for the total thermal resistance, $W=\alpha T^2+\beta/T$. A graph of WT against T^3 should therefore give a straight line with a slope of α and an intercept on the WT axis of β. Such graphs are shown in fig. 4 (up to 20°K) and in fig. 5 for a larger temperature range. The values of α and β are given in the table. It will be noted that two values of α are given, one for temperatures up to 20°K and the other for temperatures up to 30°K. This second value of α is the same for both specimens, whereas the first value although slightly higher than the second value is not quite the same for both.

	$\alpha\times10^4$ (up to 20°K)	$\alpha\times10^4$ (up to 30°K)	β
Li 1	1·84	1·68	3·63
Li 2	1·76	1·68	1·88

The value of β is connected with the residual electrical resistance R_0 through the Wiedemann–Franz law by the relation $R_0/\beta=L_0$, where L_0 is the Lorenz constant which has a value $2{\cdot}45\times10^{-8}$. Values for R_0/β come out to be 2·45 and $2{\cdot}49\times10^{-8}$ for Li 1 and Li 2 respectively, in good agreement with the theory.

Agreement between the observed values of α and theoretical calculations, however, are not so satisfactory, for whilst these experiments show that a T^2 law is obeyed quite accurately, the coefficient, α does not have the value to be expected from theory. The value of α should be given by the relation $\alpha=GN^{2/3}/K_\infty\theta^2$, where N is the number of conduction electrons per atom, K_∞ is the limiting thermal conductivity at high temperatures and G is a numerical factor which, according to Klemens (1954) has the value 64. Assuming $\theta=340$°K (Smith, to be published), $K_\infty=0{\cdot}8$ watt units

Fig. 4

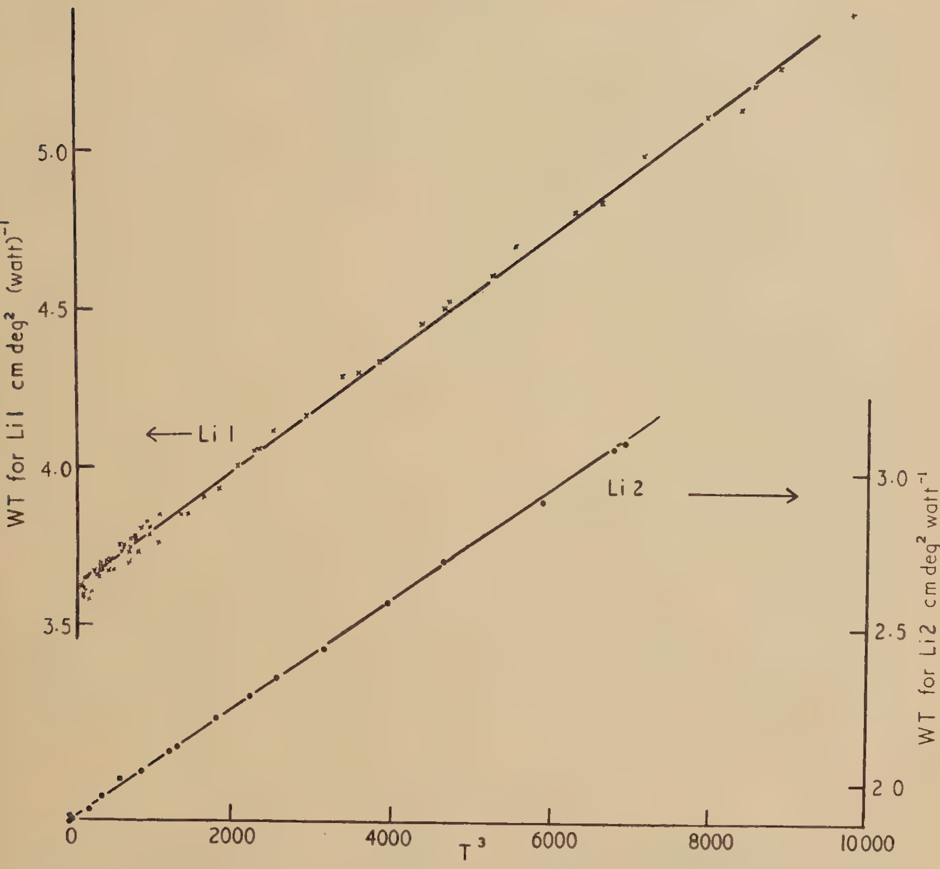

A plot of WT against T^3 (where W is the thermal resistance) for the two lithium specimens in the range up to 20°K.

Fig. 5

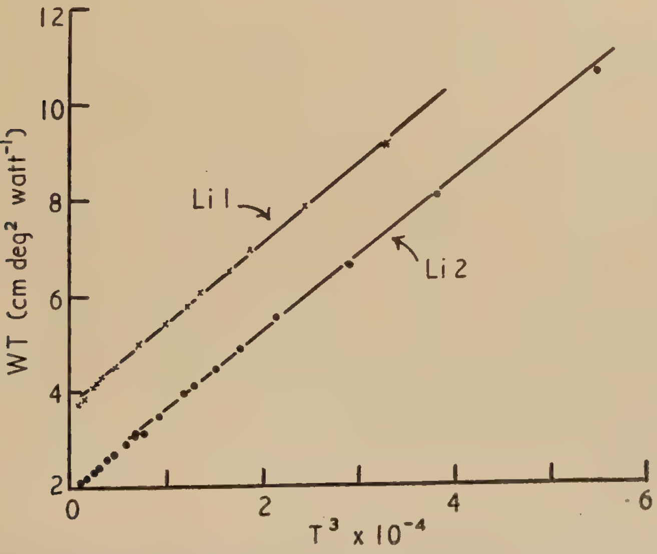

A plot of WT against T^3 for the two lithium specimens in the range up to 30°K.

and $N=1$, this gives a value for α of $6{\cdot}9\times10^{-4}$ which is nearly four times the experimental value. If on the other hand we enforce agreement with the experimental value of α, this means that either θ is about double its specific heat value† or that $N=0{\cdot}1$ electrons per atom. We can of course manipulate both θ and N at the same time in order to get agreement but in the absence of further theoretical guidance there seems to be no point in doing this. Thus, as in the case of sodium (Berman and MacDonald 1951) and other metals (e.g. Hulm 1950) the theoretical value of α does not agree with experiment.

The fact that α changes slightly with temperature as is shown in the table is probably due to the fact that θ for lithium also changes with temperature (Smith, to be published) in the low temperature region. This type of behaviour is demonstrated in the very marked changes found in the value of α for cadmium (Rosenberg, to be published) which are associated with changes in θ.

Although the absolute value of α as calculated theoretically may not be correct, it has been suggested (Rosenberg 1955) that the function $F=\alpha K_\infty\theta^2$ might be a useful parameter since the value of F is found to be approximately the same for all the metals of a given chemical group. Taking θ as 340°K the value for F for lithium comes out to be 14·6. This compares quite well with the value of 16·4 for sodium calculated from the measurements of Berman and MacDonald (1951) and using $\theta=180$°K. Due to uncertainties in the values of K_∞ and more especially of θ (which occurs squared) the agreement between the values of F for the two metals is as good as can be expected.

§5. THE LORENZ NUMBER

The Lorenz number, L, defined by the relation $L=KR/T$ is shown in fig. 6. At high and at very low temperatures L should for theoretical reasons tend to the value of $2{\cdot}45\times10^{-8}$ and in between, its value should decrease and pass through a minimum at some intermediate temperature. The amount of this decrease and the position of the minimum depends on the purity of the specimen. Makinson (1938) gives curves showing how L should depend on temperature and purity. He defines the purity by the parameter $R_0/4A$, where R_0 is the residual resistance and $A=R'\theta/T'$, R' being the resistivity at a temperature T' which is greater than $0{\cdot}6\,\theta$. The value of $R_0/4A$ is approximately 0·002 for Li 1 and 0·001 for Li 2.

At the lowest temperature both curves approach the value $2{\cdot}45\times10^{-8}$ quite accurately. They pass through a minimum at about 45°K ($0{\cdot}13\,\theta$) and by 90°K they are rising fairly steeply towards the limiting value again. In accord with the theory Li 2, the purer specimen, has the deeper minimum. When the values of L are compared quantitatively with

---

† Blackman (*Proc. Phys. Soc.* A, **64**, 681, 1951) has suggested that a special value of θ, $\theta_l\sim1{\cdot}5\,\theta$ should be used which only depends on the longitudinal phonons, since according to the Bloch theory these are the only phonons capable of interacting with electrons.

Makinson's calculations, however, the agreement is not so satisfactory. The highest purity for which Makinson gives a curve is for $R_0/4A = 0{\cdot}0038$, i.e. slightly less pure than Li 1; he calculates that the minimum value of L should be at about $0{\cdot}15\,\theta$ in fair agreement with Li 1, but that the value of L should be $0{\cdot}44 \times 10^{-8}$ instead of the experimental value of $1{\cdot}64 \times 10^{-8}$. Thus the experimental value of L is about four times the theoretical value. That this is so is not surprising, since, as has been mentioned earlier, it is known that the 'ideal' thermal conductivity predicted by the theory is about four or five times less than that observed experimentally, and this of course will be reflected in calculations of the Lorenz number, to give a value of L that is too low, particularly in the region where the 'ideal' conductivity is predominant. It should be noted that no anomalies in the curve for L, such as have been reported by Berman and MacDonald (1951) for sodium, have been found in the case of lithium.

Fig. 6

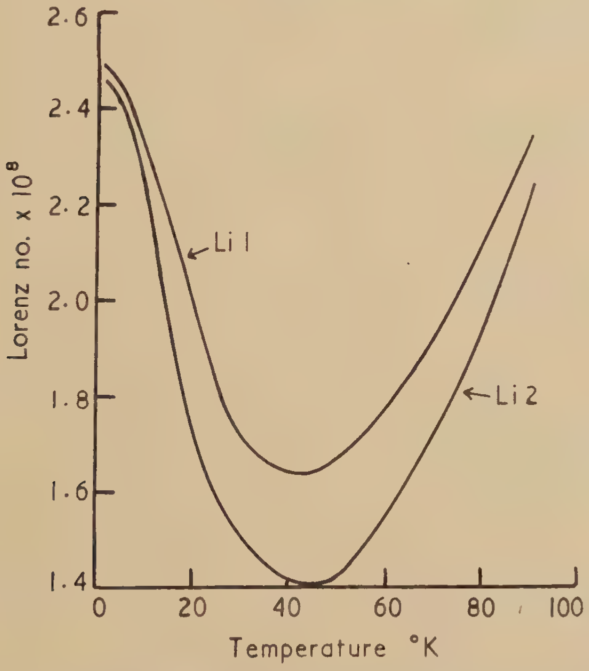

A graph of the Lorenz number, L, for the two lithium specimens in the range from 2 to 90°K.

The experiments which have been described show that whilst the results do agree qualitatively with theoretical calculations the numerical agreement is by no means satisfactory. In the case of sodium, Ziman (1954) has shown that agreement between theory and experiment can be achieved when one takes into account umklapp processes in the interaction between electrons and lattice vibrations. Such agreement does not appear to be possible in the present case, certainly not in the range below 20°K, since in this region the probability of scattering due to umklapp processes will not be very large. It is known that, unlike sodium, lithium cannot be considered a free-electron metal (e.g. see Seitz 1940) and that its effective electron mass is about 1·5 times the free electron mass. Nevertheless, this in itself is not sufficient to produce disagreement. The discrepancy must lie in the details of the energy distribution function, particularly near the Fermi surface, since it is those properties such as electrical and thermal conductivities and paramagnetic susceptibility, which depend on the nature of the energy levels at the Fermi surface, which are most seriously at fault when they are calculated theoretically. Whilst for most metals a more exact calculation is at present not possible, it is to be hoped that in the case of lithium the problem will not prove so intractable.

ACKNOWLEDGMENTS

I should like to thank Dr. K. Mendelssohn, F.R.S., for his interest in this work, and Mr. J. A. Carruthers and Miss J. N. Lomer for assistance in taking some of the measurements.

Note added in proof.—Further work on the alkali metals has now been published by MacDonald, White and Woods (1956).

REFERENCES

BERMAN, R., and MACDONALD, D. K. C., 1951, *Proc. Roy. Soc.* A, **209,** 360.
BLOCH, F., 1928, *Z. Phys.*, **52,** 555 ; 1930, *Ibid.*, **59,** 208.
GRÜNEISEN, E., 1933, *Ann. Phys. Lpz.*, **16,** 530.
HULM, J. K., 1950, *Proc. Roy. Soc.* A, **204,** 98.
KLEMENS, P. G., 1954, *Proc. Phys. Soc.* A, **67,** 194 ; 1956, *Handbuch der Physik*, **14,** 198.
MACDONALD, D. K. C., and MENDELSSOHN, K., 1950, *Proc. Roy. Soc.* A, **202,** 103.
MACDONALD, D. K. C., WHITE, G. K., and WOODS, S. B., 1956, *Proc. Roy. Soc.* A, **235,** 358.
MAKINSON, R. E. B., 1938, *Proc. Camb. Phil. Soc.*, **34,** 474.
OLSEN, J. L., and ROSENBERG, H. M., 1953, *Advances in Physics*, **2,** 28.
ROSENBERG, H. M., 1955, *Phil. Trans. Roy. Soc.* A, **247,** 441.
SEITZ, F., 1940, *Modern Theory of Solids* (New York : McGraw-Hill), p. 354.
ZIMAN, J. M., 1954, *Proc. Roy. Soc.* A, **226,** 436.

LXXVII. *The Thermal Expansion of Aluminium at Low Temperatures as Measured by an X-ray Diffraction Method*

By B. F. Figgins, G. O. Jones and D. P. Riley
Department of Physics, Queen Mary College, London†

[Received January 26, 1956]

Abstract

The accurate determination of lattice cell dimensions by means of x-ray diffraction methods has been applied to the measurement of thermal expansion at temperatures down to 20°K. In the first results, obtained with aluminium, the ultimate sensitivity in the determination of values of $\Delta a/a$ (where a is the lattice parameter) is estimated to be about 5×10^{-6}. The value of $(a_{110}-a_{20})/a_{273}$ obtained is $0{\cdot}613\times10^{-3}$. The results represent a tendency for the Grüneisen γ to increase at the lowest temperatures.

§ 1. Introduction

Until the recent experiments of Bijl and Pullan (1954, 1955) and Rubin *et al.* (1954), few measurements had been made of the thermal expansion of solids at temperatures lower than about $0{\cdot}3\ \Theta$, in spite of the importance of the expansivity in the theory of lattice dynamics (see for instance Bijl and Pullan 1955, Barron 1955). In the first instance, values of the expansivity are significant since they define the value of the Grüneisen 'constant' $\gamma\ (=\alpha V/C_v\kappa)$, where α is the (volume) expansivity, C_v and V the specific heat and volume, and κ the compressibility in any given case. The Grüneisen theory of thermal expansion implies a simple relation between the value of this constant and the sum of the exponents in the attractive and repulsive terms of the interatomic potential, for central forces between atoms of the Mie-Lennard Jones type. However, the Grüneisen theory cannot be valid at very low temperatures, and deviations must occur analogous to those which have to be considered in the rigorous theory of specific heats when the assumption of a Debye frequency spectrum is discarded. Accurate experimental determination of the expansivity at low temperatures would thus allow an independent line of attack upon many problems of lattice dynamics.

In the region of temperature of greatest interest the values of expansivity lie between 10^{-6} and 10^{-5}, so that the difficulties of accurate measurements are bound to be serious. Indeed, the results obtained in the latest such measurements, by Bijl and Pullan using a capacitative device and by Rubin *et al.* and Nix and MacNair (1941) using an interferometric method, and the much earlier results of Keesom *et al.* (1926) and Ebert (1928) who used comparator methods, are in such disagreement that it is still an open question how the quantity $\alpha V/C_v\kappa$ varies at the lowest temperatures.

---

† Communicated by the Authors.

We have adopted the X-ray method because it has the following advantages :

(i) It determines the size of the crystal unit cell directly. From the point of view of comparison with theory this would appear to be more significant than the use of a macroscopic dimension which might be affected by the grain boundaries of a polycrystalline solid.

(ii) It is an absolute method; most other methods have by their nature to make use of a reference standard at the temperature of the specimen.

(iii) It is immune to errors, which might be difficult to eliminate in other methods, arising indirectly from the effects of temperature gradients upon other parts of the apparatus. The X-ray camera, in which the film is at room temperature throughout, is of course quite unaffected by such errors.

No accurate measurements of lattice parameters by X-ray methods have previously been made over a range of temperatures below 90°K, and so we now discuss our experimental method and accuracy in some detail.

§ 2. EXPERIMENTAL METHOD

The method used was to take a Debye–Scherrer photograph of a wire of aluminium (stated by Messrs. Johnson, Matthey to be of 99·99% purity) whose temperature could be varied between room temperature and 20°K. The specimen was mounted below the liquid hydrogen container of a miniature hydrogen liquefier-cryostat (Jones 1955) in a small copper block to which it was thermally anchored with silicone grease (see figs. 1 and 2). A reservoir in the copper block could be filled with liquid hydrogen by condensation. The temperature could be maintained constant within 0·04° near 20°K, and more closely at higher temperatures, by adjusting the current through a heater wound on the block or the rate of a small flow of hydrogen gas through the reservoir. Limitations of space made it most convenient to use a (copper–constantan) thermocouple for the measurement of temperature. This was calibrated at 20·4°, 63·2°, 90°K and the steam-point, and the data of Simon (1922) Adams (1926) and Scott (1941) used for interpolation. It was estimated that the temperature difference between the middle and ends of the specimen must be less than 0·02° at 20°K and still smaller at higher temperatures. The heating to be expected as a result of absorption of X-rays is negligible.

The camera was a modified version of a Hilger and Watts 19 cm diameter instrument. Since rotation of the specimen in the cryostat would be difficult, a stationary polycrystalline wire was used. In order to obtain photographs exhibiting no preferred orientation and minimum spottiness, this was cold-rolled to 0·3 mm diameter from an original (drawn) diameter of 0·5 mm. Using an even effective focus on the x-ray tube of about 1 mm × 1 mm as viewed in projection, the lines thus obtained were sharp and exhibited little intrinsic broadening. Some slight unevenness of lines of the highest Bragg angle, θ, was apparent but did not hinder accurate measurement.

Fig. 1

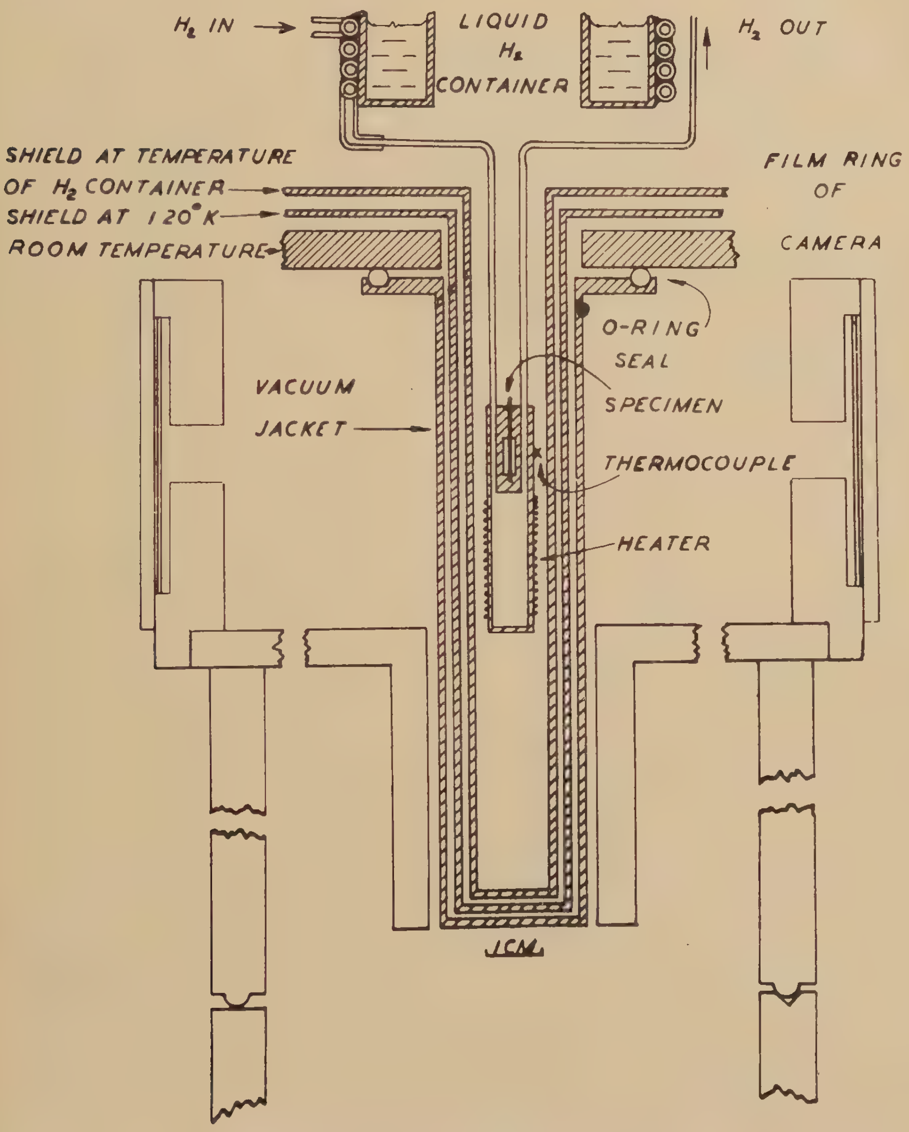

Diagram illustrating the method of mounting the specimen.

The specimen was surrounded by two copper radiation shields maintained at suitable temperatures (see fig. 2). Sections of these shields were replaced by thin aluminium foil (about 10 μ thickness) to allow passage of the scattered beam, gaps being left for the direct beam.

Fig. 2

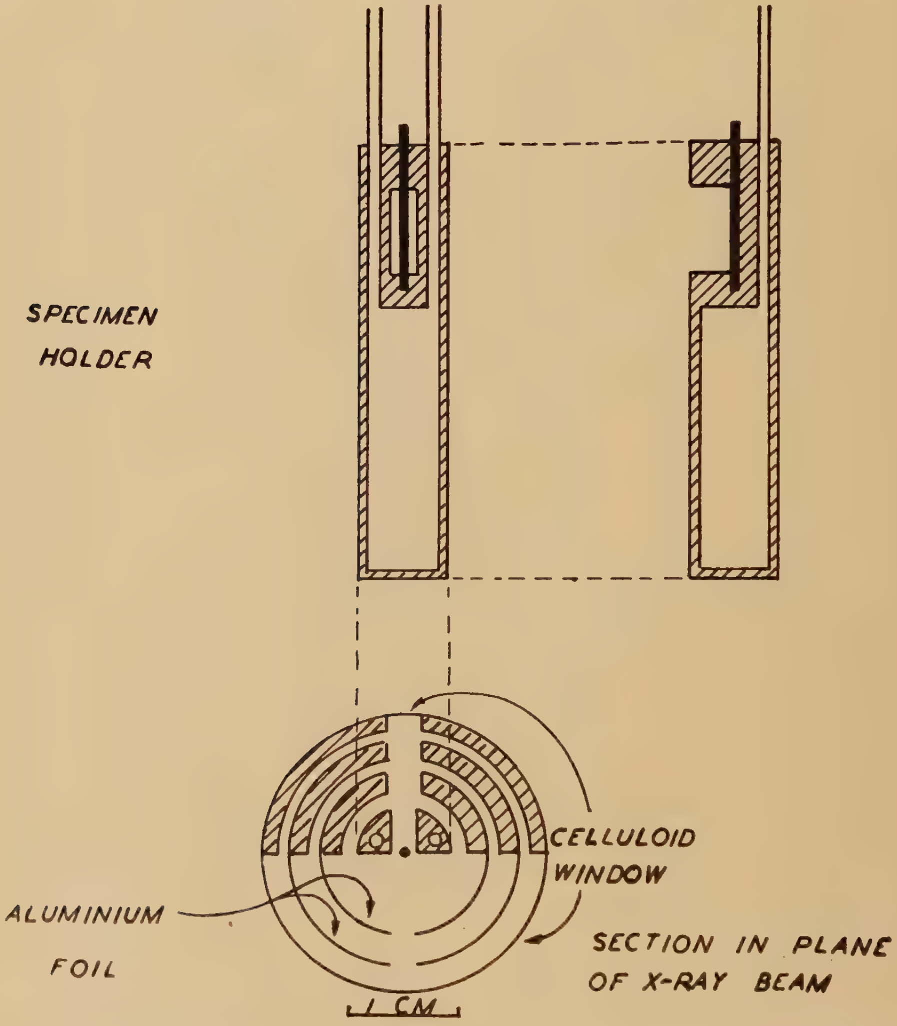

Section of specimen mount, showing the shielding arrangement.

The vacuum jacket carried a ' window ' of thin celluloid. The cooling block was constructed to allow the angular range down to $\theta \gtrsim 45°$ to be covered in the back-reflection region.

The specimen holder was attached rigidly via the body of the liquefier to the x-ray tube and table. The centring of the specimen in the camera and the aligning of the camera in the x-ray beam, once performed, did not need to be disturbed when the film was changed. The film ring was independent mechanically of the specimen–liquefier assembly and was located on a plane, hole and slot mounting on three legs. In this way it could be easily removed for loading and replaced.

§ 3. ACCURACY OF MEASUREMENT OF UNIT CELL DIMENSIONS

The Debye–Scherrer method of recording ‘ powder ’ lines from a cylindrical specimen on a co-axial cylindrical film is capable of great precision in the measurement of unit cell dimensions (see Edmunds *et al.* 1955). The van Arkel (1926) method of mounting the film was employed. In this mounting, the x-rays enter the camera through a hole punched in the film. If the hole is too large, appreciable errors can be introduced which are probably due to non-uniform variations in linear dimensions of the film during and after processing. The effect was investigated and a size of hole chosen which rendered such errors negligible. Our conclusion that the advantages of the van Arkel mounting need not be nullified by effects of this sort is in agreement with the earlier opinions of Lipson and Wilson (1941).

The geometry of our arrangement permitted the recording of 11 lines from the aluminium specimen with CuK radiation: $19(\alpha_1, \alpha_2)$, 24β, $20(\alpha_1, \alpha_2)$, 27β, $24(\alpha_1, \alpha_2)$, 32β, $27(\alpha_1, \alpha_2)$, in order of increasing θ. The $27\alpha_1$ line occurs at the Bragg angle of $\theta \gtrsim 83°$, which is high enough for precision investigation to be possible, and was always well defined and easily measurable. The $19\alpha_1$ line occurs at $\theta \gtrsim 56°$ and defines the lower end of the angular range covered. The knife-edges, whose shadow on the film provides the measuring standard, were at $\theta \gtrsim 74°$. The van Arkel mounting obviates the need for accurate calibration of the camera; the knife-edge angle was, nevertheless, known to an accuracy of about $\pm 0{\cdot}01\%$ by direct measurement on a goniometer table.

There are five categories of error which may be discerned in the determination of an accurate lattice parameter by the Debye–Scherrer method:

(*a*) random observational errors in the measurement of line positions on a film;

(*b*) subjective observational errors, similarly;

(*c*) systematic errors inherent in the method of a kind that are zero or small at $\theta = 90°$ (eccentricity, absorption, specimen-height);

(*d*) subjective errors in a graphical extrapolation;

(*e*) systematic errors which do not vanish at $\theta = 90°$ (refraction, uncertainty of wavelength standards).

The method used to minimize errors of types (*b*) and (*c*) was that of graphical extrapolation to $\theta = 90°$ of the apparent values of a derived from the 11 lines measured. The extrapolation function employed was

$\frac{1}{2}(\cos^2\theta/\sin\theta+\cos^2\theta/\theta)$, as recommended by Nelson and Riley (1945). It was clear, from an examination of the plot of a against this function of θ, that a satisfactory linear extrapolation of low slope was thereby obtained over the whole range in each case. There was, as usual, some scatter about the straight line of points due to the weaker lines or to α_2 lines.

A subjective error in extrapolation (type (d)) is therefore possible but its effect is not serious. If, as undoubtedly should be the case, the greatest weight is given to the $27\alpha_1$ line, even an unlikely choice of extrapolation line produces an alteration of only 0·00001 Å in the chosen value for a. This is due to the small slope of the line and the fact that 11 points have to be considered in choosing it. We can therefore say that the intrinsic reliability of the extrapolation process itself as applied to results derived from a single set of data (i.e. one film, once measured) is ±0·00001 Å in terms of maximum deviation; the probable error is, of course, less than this.

The effect of random observational errors (type (a)) is probably the ultimate limiting factor in the attainment of accuracy if, as is the case here, the extrapolation procedure itself is satisfactory. We have found that the precision of measurement of line positions is greatly aided if the cursor, or eyepiece graticule, is ruled with *two* thin vertical lines *ca* $\frac{1}{3}$ mm apart, rather than with a single line. The Hilger film-measuring rule, used with low magnification (*ca* 2×), was found to give measurements of high reproducibility. Twenty separate readings were taken on each of the two $27\alpha_1$ lines on a typical film by displacing the cursor to the left and right alternately between each reading; the measurements were made in two runs of 10 with an interval between them. The mean absolute deviations obtained were 0·004 mm and 0·006 mm. The vernier reads direct to 0·05 mm and, with the magnification used, readings could be interpolated to 0·01 mm; the reliability of this procedure was checked against a cathetometer reading direct to 0·01 mm. Over a 5 cm range (the separation of the two $27\alpha_1$ lines on the film), the accuracy of the rule, according to the manufacturers, is at least 0·005 mm. It would therefore appear that, in terms of mean absolute deviation, the accuracy of measurement of the distance separating the $27\alpha_1$ lines is about 0·007 mm, i.e. $[(0{\cdot}004)^2+(0{\cdot}006)^2]^{1/2}$. This corresponds to a mean absolute deviation (or average error) in a of *ca* 3×10^{-5} Å in the unit-cell dimension a.

The best check on the above analysis of errors is provided by an examination of the results obtained, with our standard procedures, from three films referring to the same temperature of the specimen. The 3 exposures were taken independently at various times in the course of the investigation; one film was measured thrice, and the other two films twice, as separate operations starting from the beginning; a separate extrapolation was performed for each of the 7 sets of measurements. The results are given in table 1 and refer to a temperature of 85·7°K.

Table 1. Extrapolated Values of a for Aluminium at 85·7°K

Film	Measurement and extrapolation	a in Å
A	1	4·03310
	2	4·03311
	3	4·03314
B	1	4·03311
	2	4·03311
C	1	4·03308
	2	4·03312

Mean value: a $=4{\cdot}03311$ Å
Mean absolute deviation $=1{\cdot}0\times10^{-5}$ Å
Standard deviation $=1{\cdot}7\times10^{-5}$ Å

N.B. The correction for refraction has *not* been included.

It will be observed that the mean absolute deviation of these actual results is better than the figure arrived at above; it is probably fortuitously good as a similar analysis of less extensive results at 20·4°K leads to a mean absolute deviation of twice the above value, as shown in table 2.

Table 2. Extrapolated Values of a for Aluminium at 20·4°K

Film	Measurement and extrapolation	a in Å
A	1	4·03183
	2	4·03184
	3	4·03186
B	1	4·03180
	2	4·03181

Mean value: a $=4{\cdot}03183$ Å
Mean absolute deviation $=1{\cdot}8\times10^{-5}$ Å
Standard deviation $=2{\cdot}1\times10^{-5}$ Å

N.B. The correction for refraction has *not* been included.

It may reasonably be concluded from the above figures that the standard deviation of measurements of the lattice parameter measured at any given temperature on the particular wavelength scale adopted does not exceed about 0·00002 Å. The effect of temperature fluctuations is quite negligible, being *ca* 5×10^{-7} Å in a.

To each of the extrapolated values for a, there should be added the constant correction for refraction, which is 0·00003 Å. All measurements refer to a scale of length defined by the following choice of wavelengths (Lonsdale 1955):

$$\mathrm{CuK}\alpha_1:\ \lambda=1{\cdot}54051\ \text{Å}$$
$$\mathrm{CuK}\alpha_2:\ \lambda=1{\cdot}54433\ \text{Å}$$
$$\mathrm{CuK}\beta:\ \lambda=1{\cdot}39217\ \text{Å},$$

and, particularly, by the first.

In considering volume changes in a crystal lattice, systematic errors of type (e) are clearly of no importance as they cancel out on subtraction. Uncertainties concerning the wavelengths, or the relevance of wavelengths based on the *peaks* of spectral lines (whereas Debye–Scherrer lines are measured more nearly at their centres of gravity), are of significance only in an absolute sense. Again, the importance of all systematic errors is greatly reduced if the purpose of the investigation is the observation of differences rather than absolute measurements. We have, nevertheless, attempted to reach as high a degree of absolute precision as our experimental arrangement permits. That our estimation of average error cannot be seriously wrong is demonstrated by a comparison of our result at 25°C with those obtained in other investigations of varying degrees of precision (table 3).

Table 3. Lattice Parameter a for Aluminium at 25°C

Observers	a in Å
Figgins, Jones and Riley	4·04963
Ievins and Straumanis (1936)	4·04963
Smakula and Kalnajs (1955)	4·04960
Jette and Foote (1935)	4·04958
van Bergen (1941)	4·04958
Wilson (1941)	4·04953

N.B. All results include the correction for refraction and refer to a scale of length defined by $\lambda\mathrm{CuK}\alpha_1=1{\cdot}54051$ Å; where necessary results at the nearest observed temperature are converted to values at 25°C by allowing for thermal expansion.

§ 4. RESULTS AND DISCUSSION

The results obtained are summarized in table 4 in which the actual temperatures of runs are listed and the number of measurements made in each case.

Table 4

Temperature (°K)	No. of photographs	No. of measurements	Mean a in Å (including refraction)
20·4	2	5	4·03186
32·3	1	2	4·03191
44·4	1	3	4·03201
55·1	1	2	4·03219
66·0	1	2	4·03239
75·0	1	2	4·03271
85·7	3	7	4·03314
106·2	1	2	4·03412
115·2	1	2	4·03462
125·0	1	2	4·03528
298·7 (25·5°C)	1	3	4·04968

In fig. 3 mean values of a are plotted against temperature. The radius of the circles representing the experimental points corresponds to 0·00002 Å which, as we have stated, is about the standard deviation of our individual results at a given temperature. It will be seen that they lie on a smooth curve with the expected consistency. Greater weight has been given to the more numerous results obtained at 20·4° and 85·7°K in drawing the curve.

In fig. 4 the present results, together with those of Bijl and Pullan (1955)† are compared with the curve which would be followed by a Grüneisen solid, that is, a solid for which $\alpha V/C_v\kappa$ (or γ) is constant. Since Bijl and Pullan measured changes in the length of a specimen and not the absolute value of lattice parameter, we have used our value of a at 110°K as a reference for this comparison.

In plotting the curve for the Grüneisen solid we have employed the expression $\Delta a = a_{273}\gamma\Delta U/3(V/\kappa)$, using $a_{273} = 4{\cdot}04736$ Å (present investigation) and $\gamma = 2{\cdot}17$. The values of U used are due to Giauque and Meads (1941). Allowance has been made for the variation in V/κ according to the Grüneisen theory, as done by Bijl and Pullan (1955). Their results and ours, as represented on the figure, are thus directly comparable.

It will be seen that the results at the lowest temperatures diverge from those of Bijl and Pullan. In order to make a comparison between the experimental results and the conclusions of the Grüneisen theory we have to remember that it is the slope *at a given temperature* of any one of these curves which is directly related to the value of γ, if γ is defined as $\alpha V/C_v\kappa$.

---

† We understand from Dr. Bijl that he is publishing an Erratum to his paper (Bijl and Pullan 1955) including amended results for aluminium. The present comparison is made with these latest values.

If the slope of the experimental curve at low temperatures is greater than that of the curve for the Grüneisen solid, the results represent an increase in γ at low temperatures above the high temperature value, and *vice versa*.

Fig. 3

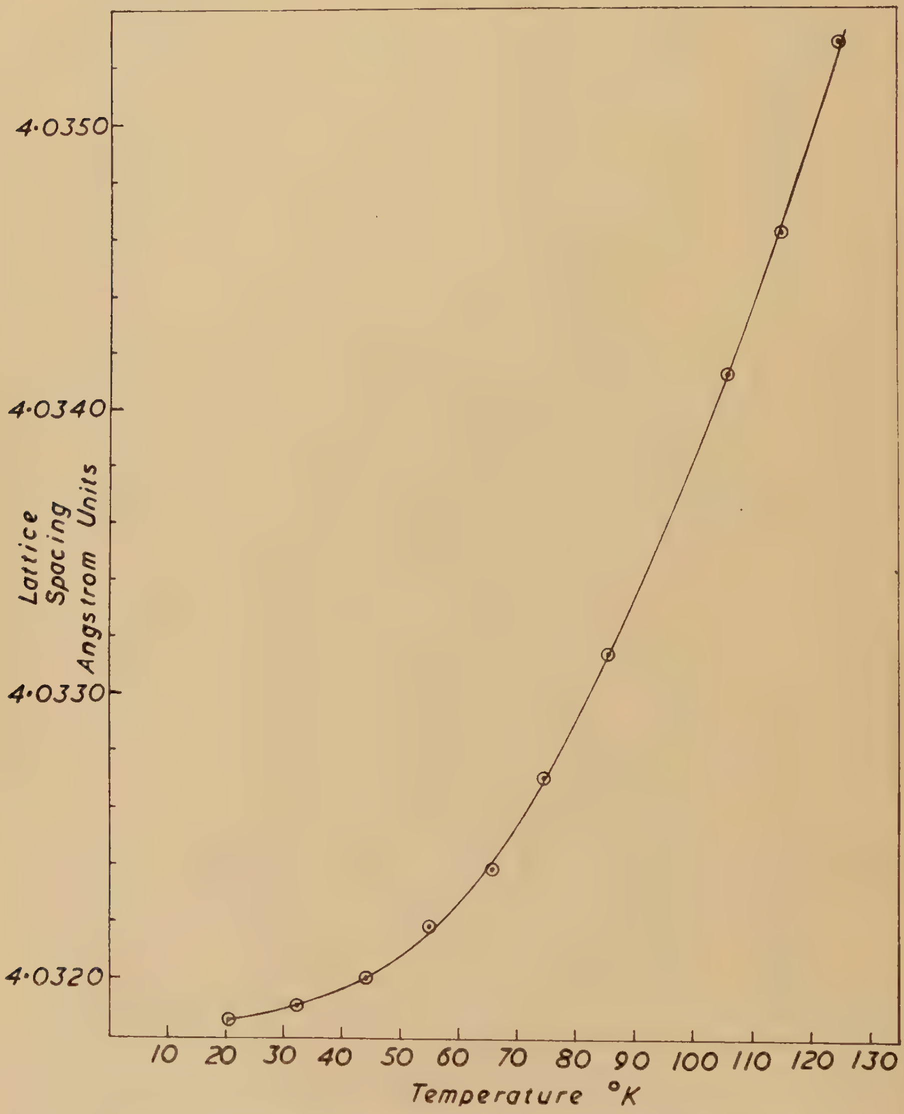

Lattice parameter of aluminium as a function of temperature.

Our results therefore represent a nearly constant value of γ, with a deviation corresponding to an increase in γ at the lowest temperatures. Since the expansivity and specific heat vary approximately as the cube of the temperature in this region, it is hardly possible from the present data to define accurate values of γ at these lower temperatures. It does appear however that our results indicate an increase in γ as the temperature is lowered.

Fig. 4

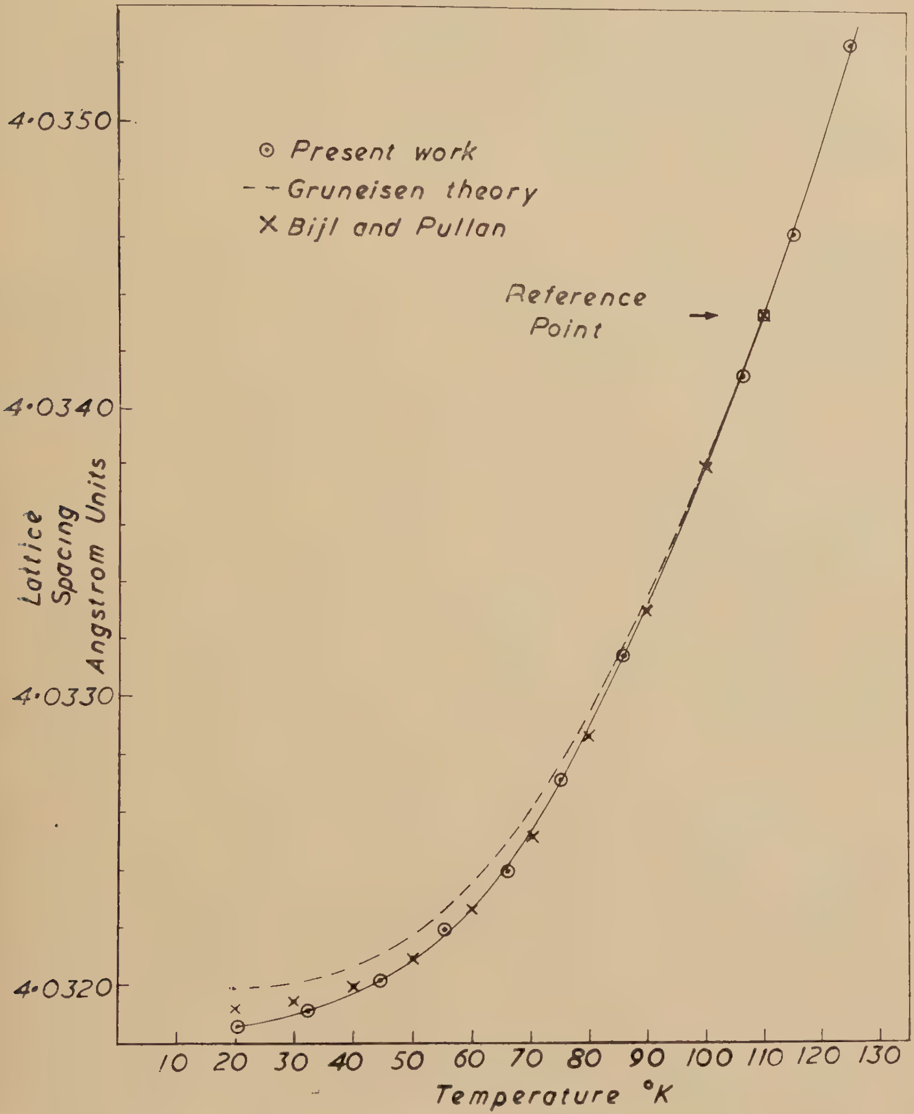

Comparison of experimental results and Grüneisen theory.

The present results do not give sufficient information about the detailed variation of α at the lowest temperatures for comparison with Barron's theory, except that they appear to indicate an increase in γ as opposed to the decrease which his theory predicts. We believe still greater accuracy may be possible by the x-ray method, and experiments are proceeding.

ACKNOWLEDGMENTS

We wish to acknowledge the assistance of Mr C. D. Murray and the generous loan of equipment by Messrs. Hilger and Watts Ltd. The aluminium wire was kindly given us by Messrs. Johnson, Matthey. One of us (B. F. F.) is indebted to the British Oxygen Co. for a Research Fellowship, and the work has been assisted by a grant-in-aid from the D.S.I.R.

REFERENCES

ADAMS, L. H., 1926, *Int. Crit. Tab.*, **1,** 58.
BARRON, T. H. K., 1955, *Phil. Mag.*, **46,** 720.
BIJL, D., and PULLAN, H., 1954, *Phil. Mag.*, **45,** 290; 1955, *Physica,* **21,** 285.
EBERT, H., 1928, *Z. Phys.*, **47,** 712.
EDMUNDS, I. G., LIPSON, H., and STEEPLE, H., 1955, *X-ray Diffraction by Polycrystalline Materials* (London: Institute of Physics), p. 366.
GIAUQUE, W. F., and MEADS, P. F., 1941, *J. Amer. Chem. Soc.*, **63,** 1899.
IEVINS, A., and STRAUMANIS, M., 1936, *Z. Phys. Chem.* B, **34,** 402.
JETTE, E. R., and FOOTE, F., 1935, *J. Chem. Phys.*, **3,** 605.
JONES, G. O., 1955, *Proc. Phys. Soc.* B, **68,** 320.
KEESOM, W. H., VAN AGT, F. P. G. A. J., and JANSEN, A. F. J., 1926, *Leiden Commun.* 182 a.
LIPSON, H., and WILSON, A. J., 1941, *J. Sci. Instr.*, **18,** 144.
LONSDALE, K., 1955, *X-ray Diffraction by Polycrystalline Materials* (London: Institute of Physics), p. 654.
NELSON, J. B., and RILEY, D. P., 1945, *Proc. Phys. Soc.*, **57,** 160.
NIX, F. C., and MACNAIR, D., 1941, *Phys. Rev.*, **60,** 597.
RUBIN, T., ALTMAN, H. W., and JOHNSTON, H. L., 1954, *J. Amer. Chem. Soc.*, **76,** 5289.
SCOTT, R. B., 1941, *Temperature: Its Measurement and Control in Science and Industry* (New York: Reinhold), p. 210.
SIMON, F., 1922, *Ann. d. Phys.*, **68,** 241.
SMAKULA, A., and KALNAJS, J., 1955, *Phys. Rev.*, **99,** 1737.
VAN ARKEL, A. E., 1926, *Physica,* **6,** 64.
VAN BERGEN, H., 1941, *Ann d. Phys.*, **37,** 583.
WILSON, A. J. C., 1941, *Proc. Phys. Soc.*, **53,** 235; 1942, *Ibid.*, **54,** 487.

LXXVII. *Soft X-Ray Spectroscopy of Solid Solutions of Aluminium and Magnesium*

By B. Gale† and J. Trotter

(Communication from National Physical Laboratory)

[Received January 28, 1956]

Summary

Soft x-ray L_{23} bands of aluminium and magnesium when each is dissolved in the other have been examined photographically. The widths and shapes of the solute bands differ considerably both from those of the solvents and the corresponding pure metals. An attempt has been made to correlate some of the changes in terms of a Thomas–Fermi treatment of the fields around impurity atoms.

§ 1. Introduction

Considerable theoretical interest has been shown recently in the distribution of electrons in metallic solid solutions. Friedel's work (1952) which uses both a wave-mechanical treatment and simple energy considerations, suggests that the valency electrons of the solute and solvent atoms in a dilute solid solution are not shared in a common valency band. This general idea appears to be supported by soft x-ray emission spectra, e.g., Cu–Zn alloys (Bearden and Friedman 1940), Al–Ni and Al–Cu alloys (Farineau 1939), Cu–Al (Yoshida 1936) and Cu–Al, Cu–Be and Al–Be alloys (Skinner and Johnston 1938), for if complete sharing occurs the solute and solvent bands would be identical. Only in the observations of the K-spectra from the intermetallic compounds Mg_2Al_3 and Mg_3Al_2 (Farineau 1937) is there any such evidence ; but even here some subsequent observations by Das Gupta and Wood (1955) of the L-spectra of similar alloys makes this case rather doubtful.

In the case when the solute atoms have a higher valency than the solvent atoms the donation of the excess charge to the common valency band would leave a positive charge on the solute ion cores. Calculation of the electrical resistance of such ionic lattices (Mott and Jones 1936) shows that the value would be infinite unless the ion core charge is shielded. This shielding is formed by a perturbation of the energy levels of the valency band in the neighbourhood of the solute ion. When this is sufficiently strong, one or more energy levels may be subtracted from the bottom of the band and these will be closely asscoiated with atomic orbitals. In such cases the charge configuration is specified by the appropriate wave-functions of the free atom.

---

† Now at Massachusetts Institute of Technology.

It is evident from transition probability considerations that only those electrons close to an excited atom will contribute to the soft x-ray spectra. Thus the solvent emission band should be little changed at low concentrations and will give a close representation of the lattice electron energies. The solute emission band on the other hand will reflect the energies of only those electrons within approximately a solute atomic cell. In the work described here an attempt has been made to deduce the behaviour of the electrons about aluminium and magnesium when each is dissolved in the other from their L-emission spectra. Some work on the soft x-ray bands of alloys in this system has recently been published (Das Gupta and Wood 1955); but this is mainly a general survey of the system without special attention to the solid solutions.

§ 2. EXPERIMENTAL TECHNIQUE

The spectrograph used is essentially similar to that described by Skinner (1940). The x-ray tube is made of glass to facilitate cleaning and observations. To minimize contamination two liquid air traps are built in; one very close to the anticathode and the other in the pumping line from the diffusion pump. The tube is sealed to the spectrograph by wax between a flange on each part so that adjustment of the anticathode axis relative to the spectrograph slit system is quite easy. The anticathode is a square sectioned copper tube, of 12·5 mm side, mounted vertically in a glass cone so that it can be rotated to expose each face in turn to electron bombardment. An electron gun consisting of a barium and strontium oxide coated nickel filament set vertically in a nickel focusing shield is mounted close to the anticathode and bombards an area of about 15 mm by 5 mm. With this type of filament it was found difficult to avoid traces of the barium lines and in some cases also the strontium lines. However, in the present work no difficulties from overlap with the bands to be investigated were experienced. On the opposite side of the anticathode there is an evaporator used for depositing pure metals. To prepare the x-ray tube for an exposure it is pumped out overnight to a pressure of about 10^{-5} mm. The anticathode is then degassed, after filling it with water, by heating with electron bombardment. With liquid air in the traps pumping is continued until a pressure of about 5×10^{-7} mm is reached. If then required a layer of metal is evaporated on the anticathode which, for long exposures, is renewed at intervals. Under these conditions an electron current of up to 100 mA at 2·5 kv is obtainable. Radiation from the anticathode passes through two slits before impinging on the grating. The first of these has a width of 0·03 mm and a height of 15 mm and the second is of the same height, width 1·5 mm and set 3 cm nearer the grating. A diverging beam of x-rays is then incident on the grating at an angle of about 6° and irradiates the whole of the 3·7 cm width of rulings. Thus the geometry does not comply with the resolution criterion of Mack *et al.* (1932). It does however increase the intensity of the spectra though with an inappreciable reduction of resolution. The diffracted beam is focused on to a photographic plate mounted on a carriage and set to lie in the Rowland circle of the grating. To do this, preliminary focusing was done by direct measurement of the geometry of the system. This was followed by a process of trial and error to produce optimum sharpness of the L_3 edge of magnesium. The range of wavelengths detectable for one fixed setting of the spectrograph is about 400Å and a shutter in front of the photographic plate enables up to five separate exposures to be recorded. A dispersion curve was determined from the positions of the barium, strontium and magnesium first and second order spectra (Skinner 1940, Seigbahn and Magnusson 1934).

Two types of specimen were used in this work. For the pure magnesium and aluminium spectra, evaporated specimens were mainly used, while for the alloys and some of the pure magnesium spectra, strips of rolled cast material were soldered to the copper anticathode. These strips, having dimensions 4 cm × 1·2 cm × 0·1 cm, were prepared by press-forging and hot rolling at approximately 400°c followed by annealing for about 24 hours at the same temperature. The composition of these strips was determined chemically but as a check on the actual amount of aluminium going into solid solution their lattice parameters were measured using a Geiger counter diffractometer. The inaccuracy of measurement was about ±0·0005 Å; this is large, since only (0002) and (0004) lines were measurable due to marked preferred orientation. By comparing these parameters with those obtained by Hume–Rothery and Raynor (1938) the concentration of aluminium could be estimated to an accuracy of ±0·2 atomic %.

Photometry of the plates was done on a Moll recording photometer and the resolution of the traces as estimated from the resolutions of the spectrograph and the photometer is about 0·3 Å in the wavelength range studied. The Ilford Q1 plates used saturate easily so that calibration of their photographic response was necessary. To do this, evaporated magnesium spectra were recorded with three different exposures and by comparing the blackenings of corresponding points on each of them a photographic response curve was constructed. In this way a magnesium spectrum was obtained which, as a standard, was used to relate the spectra from the alloys. For the alloys each spectrum was accompanied by a spectrum of magnesium subsequently evaporated on its surface. This magnesium curve was corrected using the original response curve and compared with the standard spectrum. The ordinates of the corrected spectra agreed to within about 3% of those of the standard when scaled to fit at one point. Reproducibility of features on the spectra as measured from several plates is also about ±3% so that the accuracy of the intensity or $N'(E)$ ordinates of any one spectrum in fig. 2 should be about ±6%.

§ 3. Experimental Results

(i) *Aluminium in Magnesium*

Alloys with chemical compositions 0, 4·05, 6·63, and 11·39 atomic % of aluminium were used. The highest composition corresponds to approximately the maximum solubility of aluminium in magnesium. x-ray parameter measurements gave corresponding composition values of 0, 3·6, 6·6 and 9·3 atomic %, the latter value being very close to the limit of solubility at 400°c. Thus the metallurgical condition of the materials may be specified as follows: 4·05 and 6·63%, complete solid solutions ; 11·39%, saturated solid solution with about 5% by weight of the intermetallic compound $Mg_{17}Al_{12}$.

For convenience in describing the results, the following definitions adopted by Skinner are used : the wavelength of the emission edge is the position where the intensity is half the peak value and the 'empirical breadth' of the band is the distance from this edge to the position where a linear extrapolation of the intensity curve near the tail intersects the background intensity. The alloy spectra obtained show two distinct main bands corresponding to transitions of the type ($L_{23}V$) for the magnesium and aluminium atoms respectively. These will be dealt with in turn.

An example of the actual microphotometer records of a Mg ($L_{23}V$) band is shown in fig. 1. After making the photographic response correction the intensity ordinates $I(\lambda)$ of the L_3 component are multiplied by the factor λ_3. This is done to obtain curves $N'_{s+d}(E)$ shown in fig. 2 (*a*) which are proportional to the density of states of s- and d-type electrons. The general shape and the empirical width (7·4±0·2 ev) of the magnesium band agrees well with the data obtained by Skinner (1940). Comparison of spectra obtained from both evaporated layers and block specimens of magnesium showed no significant difference. With increasing aluminium concentration it is evident that there is a progressive change in the band shape. But to be more explicit about these changes it is desirable to compare the relative intensities of these bands. Attempts were made to do this by comparing the alloy bands with magnesium bands obtained on the same plate with the same experimental conditions, namely, unaltered anticathode position and the same total power dissipation in the x-ray tube. The results obtained were reproducible only to within about 20% due probably to absorption by thin layers of contamination on the anticathode. The alternative procedure adopted therefore was to assume part of the distribution to be invariant and to scale the curves to fit accordingly. In the curves shown it is assumed that the lower energy electrons are unaltered, that is to say, they are scaled to fit in the range 40 to 47 ev. On this basis the effect of alloying appears as a 'rounding off and increase of the intensity of the node', associated with zone overlap together with a slight increase in the height of the peak. This is only marked in the 11·5% alloy but there is a hint of it in the lower concentrations. No changes in either the position of the sharp cut-off or in the width of the band outside the respective errors of ±0·05 and ±0·02 ev were observed.

The aluminium (L^3V) bands of the alloys as shown in fig. 2 (*b*) are not reproduced on the same scale as the magnesium, since in order to show the lowest concentration band up clearly considerable over exposure of the magnesium spectrum was necessary. For clarity therefore the $N'(E)$ scale for these bands is five times that for the magnesium bands. The relative accuracy of the $N'(E)$ ordinate is evidently somewhat lower and by examination of traces from different plates is estimated to be about ±10%. To this must be added the estimated accuracy of the scaling factors so that the accuracy of the $N'(E)$ curves relative to each other is of the order of ±15%. To add to the difficulty of studying these bands the long wavelength end is overlapped by the magnesium–L_3 (L_{23}) V–satellite with band head at 195·7 Å. It is clear however that the band is quite unlike that of pure aluminium both in shape and in breadth. The empirical width does not appear to change with composition and when allowance is made for the magnesium satellite the value is probably well over 9 ev and thus rather greater than that of magnesium. It is considerably smaller than the value of 13·2±0·5 ev measured for pure aluminium. The widths of the emission edges of these bands are not significantly broader than those observed in the pure aluminium spectra. However, there is a small but significant change in the wavelength of the edges. For pure aluminium the value obtained is 170·8±0·2 Å, agreeing well with Skinner's (1940) value of 170·6 Å, whereas for the alloys the value is 171·8±0·2 Å and does not appear to change with composition.

(ii) *Magnesium in Aluminium*

Only one alloy in this solid solution phase was investigated, namely one near to the phase boundary at 400°c. The same procedure was followed as for the magnesium-rich solid solution spectra, many plates being exposed before obtaining a satisfactory record of both spectra. The composition as determined by comparing the x-ray parameter with those determined by Savickij and Tylkina (1949) was 11·0±0·2 wt.% compared with the chemically determined value of 12·2 wt.%. Thus in this specimen there should only be about 5% by weight of the complex β-phase. The solute and solvent bands are shown in fig. 3. It is evident that the aluminium band shows only a slight change in shape. The wavelength of the edge does not change by any observable amount but there is evidence that the node corresponding to the first zone overlap is 'rounded off', though the effect is not so marked as in magnesium-rich solid solutions. In addition the second zone overlap node appears to disappear. As before the most marked change is in the solute band. The wavelength of the edge is changed from 250·5±0·2 to 249·5±0·2 Å while the width of 9·5±0·5 ev is again between that of pure solute and solvent bands.

Fig. 2 (*a*)

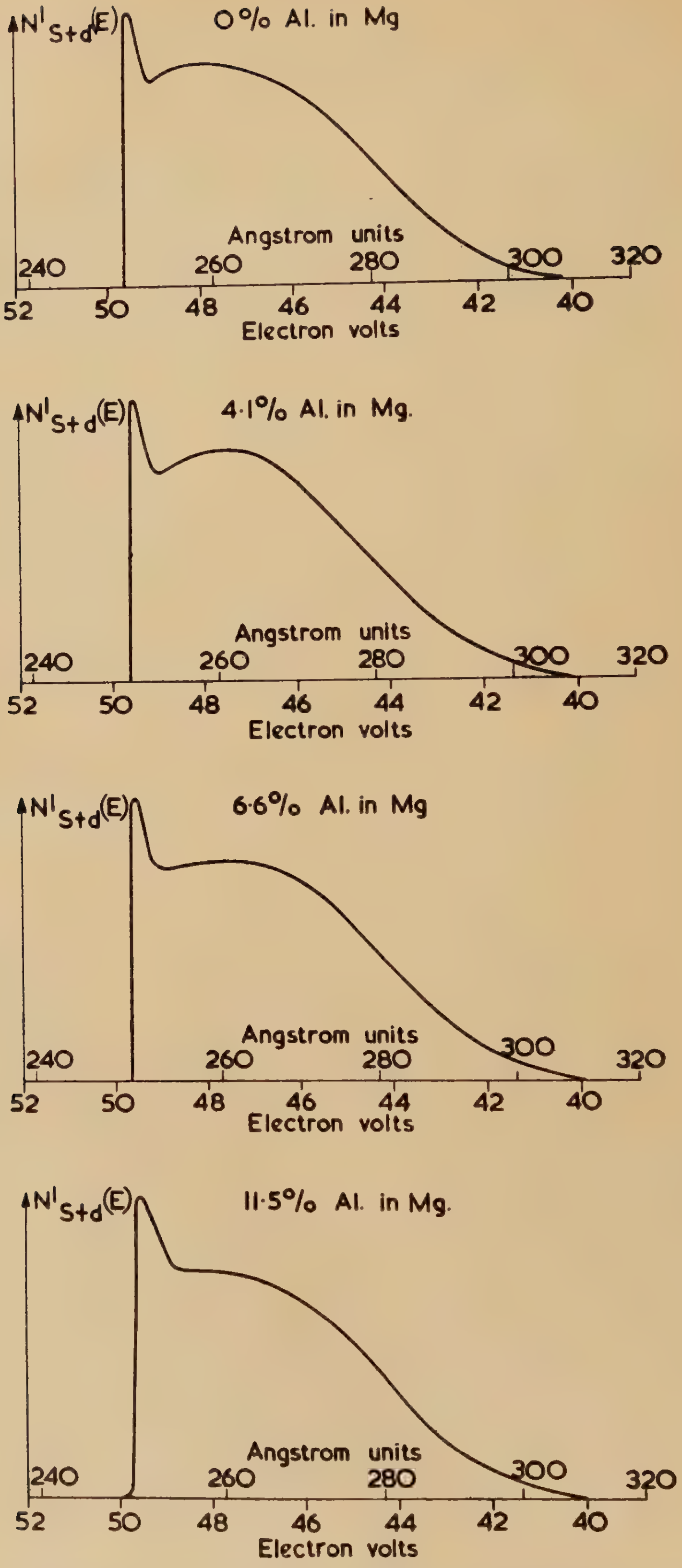

Density of states curves for the s- and d-symmetry electrons derived from the magnesium $L_{23}(V)$ bands in the magnesium-rich solutions.

Fig. 2 (*b*)

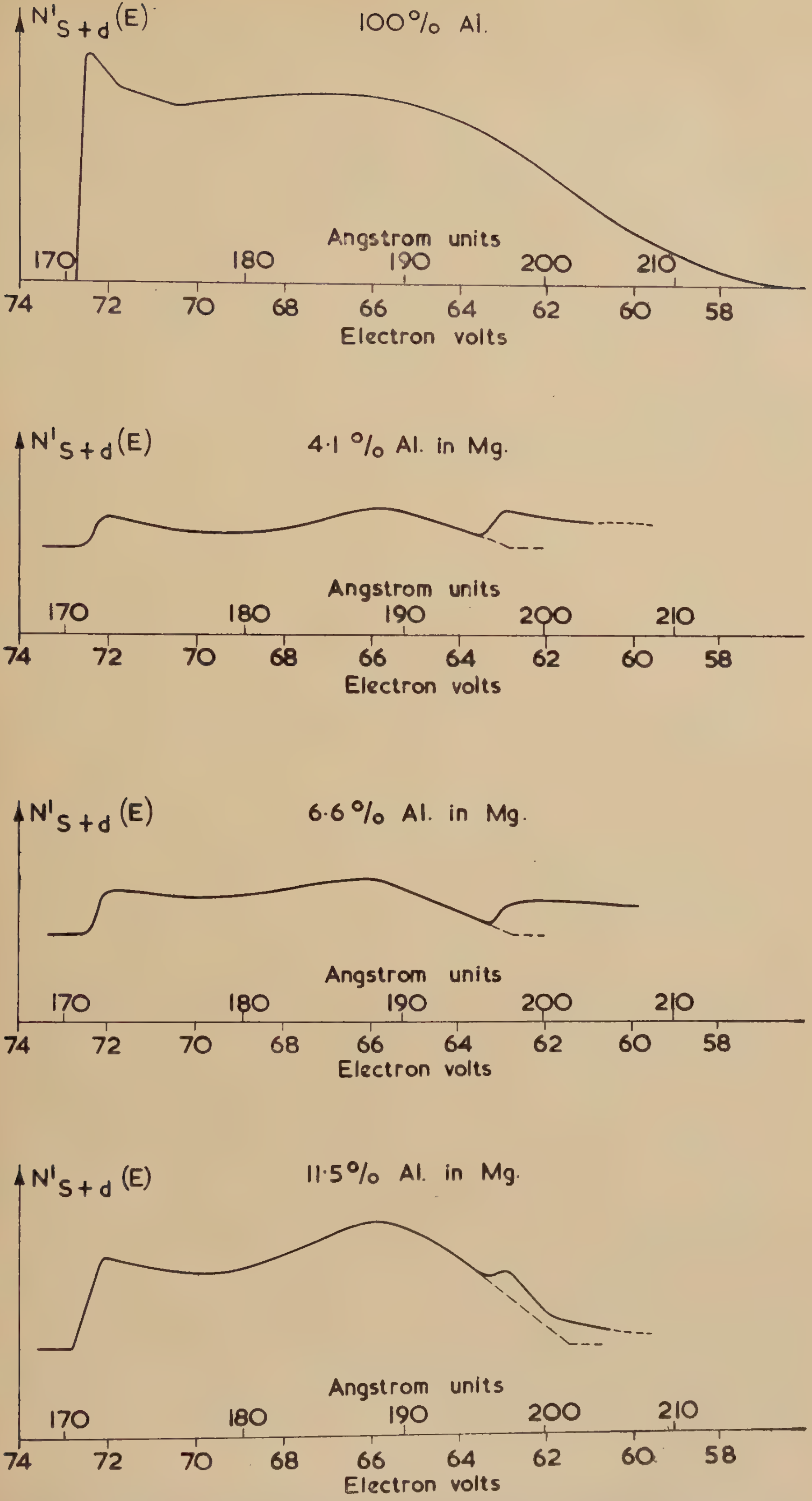

Density of states curves for the s- and d-symmetry electrons derived from the aluminium ($L_{23}V$) bands in the magnesium-rich solutions. The peak at approximately 196Å is the edge of the magnesium $L_3(L_{23})V$ satellite.

Fig. 3

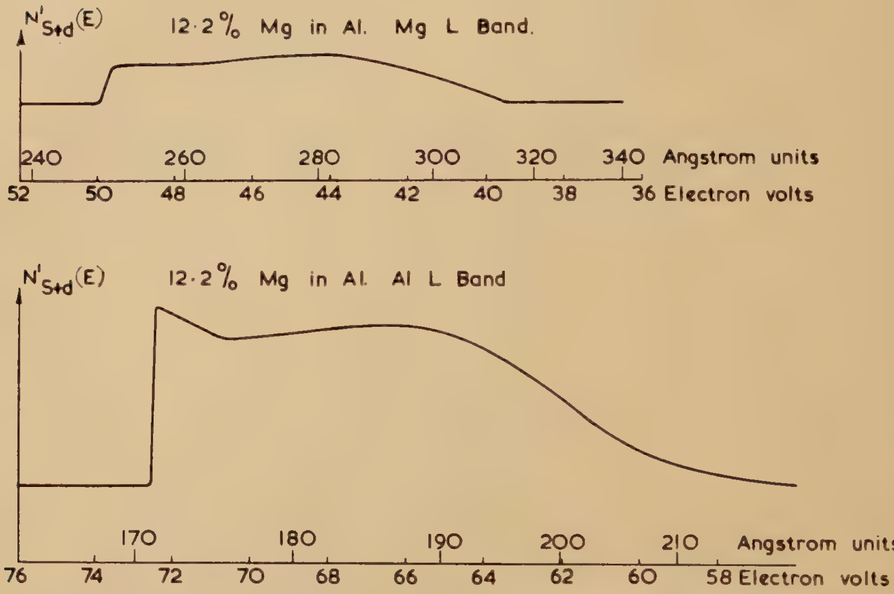

Density of states curves for the s- and d-symmetry electrons derived from the magnesium and aluminium ($L_{23}V$) spectra in the 12·2% solution of magnesium in aluminium.

§ 4. Discussion

In the attempt to interpret numerically the energies of soft x-ray spectra, it is apparent that when one of the atoms is excited there will be a necessity for charge shielding, and this, in general, appears to be by a bound electron. The maximum energy associated with the subsequent x-ray emission can be regarded as that of a two electron process, the electron from the top of the valency band going into the vacant x-ray level and the shielding electron replacing it. The resultant energy change would be, for the magnesium L-spectrum, closely equivalent to the excitation energy for the transition $2p^6 \rightarrow 2p^5 3s$ in Mg^{++}. The value given in *Atomic Energy Levels* (1949) is about 52·5 ev compared with the ($L_{23}V$) soft x-ray emission edges at 49·4 ev ; and the difference between the two values seems, in the main, to be accounted for by the exchange and coulomb energies between the bound electrons and the conduction band (Friedel 1954 b). Shielding by an electron other than of 3s symmetry could in principle give rise to satellite bands. However, as has been pointed out by Skinner *et al.* (1954), these alternatives are unlikely due to Auger transitions to the 3s level. Thus the interpretation of the magnesium satellite as a transition involving a doubly ionized x-ray level (denoted by $L_3(L_{23})V$) (Skinner 1940), is still the most likely explanation.

It is interesting to compare the aluminium bands of the dilute aluminium alloys with those obtained by other authors in different systems. There is a superficial resemblance to the Al–K bands of Cu–Al alloys obtained by Yoshida (1936), Farineau (1939) and Cauchois (1950) in that the band appears to have two components, especially for higher percentages. However there does not seem to be any evidence in the alloys we have studied of the disappearance of the emission edge as the concentration is reduced observed by Skinner and Johnston (1938). A two component structure is not however so marked in the aluminium band from Ni–Al alloys (Farineau 1939) but it is very conspicuous in the Be bands from Cu–Be alloys (Skinner and Johnston 1938).

Friedel (1952) has put forward an explanation of the aluminium doublet bands in which two of the three Al-valency electrons are in 3s-orbitals. That this might be so was suggested by a simple energy criterion, namely that if the energy levels of solute valence electron atomic orbitals lie below the bottom of the solvent conduction band there will be electrons in these orbitals. In making this comparison he has assumed that the effect of the lattice field on the energy of bound electrons is negligible and that therefore their energies are given by the appropriate ionization potentials in the free atom.

Applying these ideas to the Mg–Al system it is evident that no bound electrons occur in the aluminium-rich phase. However since the second and third ionization potentials of aluminium, 18·8 and 27·9 ev respectively, are numerically greater than the minimum energy of the magnesium conduction band, approximately −15 ev (Raimes 1950), one or two aluminium valency electrons should be bound in the magnesium-rich phase. These two possibilities can be checked experimentally.

If two electrons are bound in the 3s orbitals the aluminium band should consist of two overlapping components if the excitation of the x-ray level produces a further bound 3 p electron. They correspond to the two transitions :—(i) An electron from the valency band jumps into the 2 p hole while at the same time the shielding 3 p electron goes to the top of the conduction band. (ii) Similar to and stronger than (i), involving the 3 s shielding electrons. But this transition will be broadened by the 3 p→3 s Auger transition. Thus the band will have an edge followed by a broad hump displaced towards low energies by the energy associated with the $3\ s^2 \rightarrow 3s\ 3p$ transition in the free Al^+ atom. The value observed for this separation is about 6·5 ev which is much greater than the 4·6 ev of the Al^+ transition (*Atomic Energy Levels*, 1949). In the aluminium spectrum from Cu–Al however (Cauchois 1950) the two components are separated by about 5·0 ev and this has been taken to indicate two bound electrons in that solid solution.

If instead one electron is bound the unpaired spin would make the alloy strongly paramagnetic. An approximate value for this contribution to the mass susceptibility, calculated from Langevin's formlua, is 2×10^{-6} for 4 atomic % of aluminium. The values measured for pure magnesium and this alloy were $0{\cdot}53\times10^{-6}$ and $0{\cdot}48\times10^{-6}$ ($\pm2\%$), the iron contents being 0·0007% and 0·0018% respectively. This result would thus also appear to invalidate the energy criterion which is very much in favour of this case. Presumably the assumption that the bound atomic orbitals overlap insufficiently for their energy to be greatly different from their ionization potentials is incorrect.

In Mg–Al it is evident that the shielding charge around the aluminium solute does not have a precise atomic configuration. All that can really be deduced is that some of the valency charge is attracted by the positive aluminium core perturbing potential and remains in 'quasi-atomic orbitals', whereas when the solute is magnesium valence charge is repelled leading to a diminution of band width. The small changes in emission edge are probably only indirectly connected with these band width changes, in view of the remarks made at the beginning of the discussion. Instead the small increase in wavelength of the aluminium solute emission edge is produced by the decrease in the Coulomb interaction energy of the valency charge and the x-ray emission screening charge. For the magnesium solute the sign of this wavelength change is reversed but in neither case is it at present possible to give any reliable numerical estimate.

Some details of the solvent bands can be deduced from a Thomas–Fermi treatment of the solute ion perturbing potentials. Treating the solute atoms as point sources of a coulomb field superimposed on the lattice field, it has been shown (Friedel 1954 a) that to a first approximation the density of states curve will be moved bodily to lower energies. To a second order approximation the movement of any part of the curve will also depend on the slope at that point. Thus at the node of the magnesium curve, where the first and second zones overlap, the shifts are of such sign as to decrease its depth. An approximate value for the energy shift ΔE was obtained from the formula deduced from this treatment:

$$\Delta E \simeq \frac{2Zq'}{q'C^{1/3}r_s} \exp\,(q'C^{1/3}r_s)$$

where

$$q' = q + {}^{1/2}\frac{\pi dN(E)}{dE},$$

C is the atomic concentration, r_s is the equivalent atomic radius of magnesium, Z is the difference of ion core charges for magnesium and aluminium and $q^2=4\pi N(E)$. In general the greater the slopes of the nodal arcs the greater will be their relative movement.

In applying this analysis to the magnesium solvent spectrum an experimental $N(E)$ curve was constructed by scaling it to fit the free electron relation at low energies. At the node the proportion of s- and p-type wave functions are equal in the treatment by Jones *et al.* (1934) so that in that region $N(E)$ is known. The resultant relative movement of the two components of the node would then appear to be about 0·3 ev which is of the right order to explain the observed effect. The relative movement for the first zone overlap in the aluminium solvent is less than 0·1 ev and is barely discernible; it is however sufficiently large, about 0·2 ev, to account for the apparent disappearance of the second overlap.

A change in width of the solvent bands would also be predicted in this treatment, of magnitude $3ZC/q^2r_s^3$ which is equivalent to that predicted from the usual free electron common band model if the effective electron mass is unity. Taking q to be 1 and $C=0{\cdot}1$ these changes will be $\simeq +0{\cdot}15$ ev and $-0{\cdot}30$ ev for magnesium and aluminium respectively. These values are unfortunately too close to the experimental accuracies for any reliable comparison to be made.

The general simple picture which emerges from this work is that the energy band is strongly perturbed in the neighbourhood of the solute ions. These can be regarded as sources of a coulomb field partially screened by a 'piling up' or repulsion of lattice electrons and with a sign depending on the relative valency of the solute and solvent atoms. It is interesting to note that for the beryllium bands in dilute **Cu**Be and **Al**Be obtained by Skinner and Johnston (1938) the difference in the solute and solvent bands was explained in terms of a 'sorting function' $S(E)$: thus

$$N(E)\text{—solute}=S(E)\,N(E)\text{—lattice}$$

where $0 \leqslant S(E) \leqslant 1$ and represents the probability that a lattice electron of energy E can penetrate into the solute atom. Such an analysis would apply, as in their spectra, only when the solute band width is equal to or less than that of the solvent. But the idea that the lattice electrons are scattered by the solute ions implicit in their work is of general validity and is especially marked in our results.

ACKNOWLEDGMENTS

The work described above has been carried out as part of the General Research Programme of the National Physical Laboratory, and this paper is published by permission of the Director of the Laboratory.

The authors wish to acknowledge the continued assistance and encouragement of Dr. N. P. Allen and Dr. E. A. Calnan. The apparatus was designed by Mr. W. F. Atkins of Metrology Division, N.P.L. and Mr. D. A. Briers of the Radar Research Establishment, Malvern. It was constructed in the Metrology Division, N.P.L. by Mr. J. R. White.

REFERENCES

NATIONAL BUREAU OF STANDARDS, 1949, *Atomic Energy Levels.*
CAUCHOIS, Y., 1950, *Comptes Rendus*, **231,** 574.
BEARDEN, J. A., and FRIEDMAN, H., 1940, *Phys. Rev.*, **58,** 387.
FARINEAU, J., 1937, *Comptes Rendus*, **205,** 365.
FARINEAU, J., 1939, *J. Phys. Rad.*, **10,** 327.
FRIEDEL, J., 1952, *Phil. Mag.*, **43,** 153; 1954 a, *Advances in Physics*, **3,** 446; 1954 b, *Ann. de Physique*, **9,** 181.

Das Gupta, K., and Wood, E., 1955, *Phil. Mag.*, **46,** 77.

Jones, H., Mott, N. F., and Skinner, H. W. B., 1934, *Phys. Rev.*, **45,** 379.

Mott, N. F., and Jones, H., 1936, *Metals and Alloys* (Oxford : University Press).

Mack, J. E., Stehn, J. R., Edlen, B., 1932, *J. Optical Soc. Amer.*, **22,** 245.

Parratt. L. G., and Jossem, E. L., 1955, *Phys., Rev.*, **97,** 916.

Raimes, S., 1950, *Phil. Mag.*, **41,** 568.

Hume-Rothery, W. and Raynor, G. V., 1938, *J. Inst. Metals*, **63,** 201.

Savickij, E. M. and Tylkina, M. A., 1949, *Doklady Akad. Nauk, SSSR*, **67,** 81.

von Siegbahn, M., and Magnusson, T., 1934, *Z. Physik*, **88,** 559.

Skinner, H. W. B., 1940, *Phil. Trans. Roy. Soc.*, **239,** 95.

Skinner, H. W. B., Bullen, T. G., and Johnston, J. E., 1954, *Phil. Mag.*, **45,** 1070.

Skinner, H. W. B., and Johnston, J. E., 1938, *Proc. Camb. Phil. Soc.*, **34,** 109.

Yoshida, S., 1936, *Sci. Papers Tokyo*, **28,** 243.

LXXVIII. *Remanent Magnetism of some Dolerites, Basalts and Volcanic Tuffs from Tasmania*

By MARY ALMOND and J. A. CLEGG
Department of Physics, Imperial College of Science & Technology, London

and

J. C. JAEGER
Department of Geophysics, Australia National University, Canberra, A.T.C.†

[Received May 23, 1956]

ABSTRACT

Magnetic measurements have been made on a number of samples of Tasmanian dolerites, basalts, and tuffs, varying in age from the Triassic to the early Tertiary, which were obtained by diamond drill coring. The magnetic dips of all these rocks were found to be very considerably greater than the present dip in Tasmania, and this result is believed to furnish strong evidence to support the hypothesis that a relative movement has occurred between the land mass of Tasmania and the geographical poles since the early part of the Tertiary period. Magnetic reversals were found to occur over certain ranges of depth in both the dolerites and the tuffs. The possible implications of these reversals are discussed in detail.

§ 1. INTRODUCTION

WE have recently investigated the remanent magnetization of a number of samples of Tasmanian rocks obtained by diamond drill coring. The specimens, all of which were intrusive or volcanic in origin, were obtained from bore holes in the Great Lake area, and were supplied to one of us (J.C.J.) by courtesy of the Hydroelectric Commission of Tasmania. In the region concerned a number of sills of quartz dolerite (Tholeiite) occur.‡ These sills, some of which have a thickness greater than 1000 feet, are believed to be Jurassic or Cretaceous, and to have an age of 90 to 120 million years. A number of samples from different sill complexes were taken from four bore holes and were shipped to London for measurement at various times. The cores, which were $\frac{7}{8}$ in. in diameter, were cut into cylindrical specimens approximately $\frac{7}{8}$ in. in length, and the direction and intensity of magnetization of each specimen was measured using an astatic magnetometer in the way described by Blackett (1952). No attempt had been made during the drilling operations to orient the cores horizontally so that no information could be obtained as the the magnetic declination of the rocks, but since there was good reason to believe that the bore holes remained vertical throughout their entire length, the dip measurements can be taken to be reliable. The individual lengths of core were supplied with markings to distinguish between their upper and lower ends, so that it was also possible to find the sense of the magnetic dip.

---

† Communicated by Dr. J. A. Clegg.

‡ These sills were intruded into Upper Triassic (Rhaetic) sediments. Subsequently, there was a long interval of erosion and peneplanation during which the roof rocks of most of the sills were stripped off and a mature lateritized peneplain was developed in the dolerites, which are more than ordinarily resistant to erosion. Subsequently, again, there was an epoch of block faulting and, later, Tertiary sediments and basalts appear, together with some limestones which are certainly Lower Miocene and possibly Oligocene. Allowing for the long time involved in peneplanation, it is considered that the possible time range of the dolerites is from late Rhaetic to Lower Cretaceous.

Of the four cores examined, the first, which was distinguished by the code number 5001, was taken from a tholeiite sill believed to be 2000 feet thick, and specimens were obtained at intervals of approximately 50 feet down to a depth of 1000 feet. The second core, number 5002, was taken from what is believed to be another portion of the same sill as 5001. It yielded specimens of dolerite down to a depth of 146 feet, and passed below this level into a volcanic tuff which will be described later. In the remaining two cores, numbers 8102 and 8103, the sills were overlaid by 500 feet of tertiary basalt lava and samples of dolerite were obtained from depths of 500 to 700 feet.

Measurements were made initially on the doleritic sills, and were extended later to the basalts and the tuffs.

§ 2. MEASUREMENTS ON DOLERITES

In all a total of 57 cylinders of dolerite were cut from cores 5001, 5002, and 8102. The first set of samples to be examined were from core 5001 and were taken from depths ranging from 1 to 947 feet. A detailed account of the results obtained for this core has already been given by Jaeger and Joplin (1955) and will not be repeated here. Briefly, the most significant feature was the consistent steepness of the magnetic dips, only one specimen having a direction of magnetization deviating by more than 7° from the vertical. It was also found that while the majority of the cylinders were magnetized normally (i.e. upwards), a proportion amounting to about one-fifth of the total number had reverse magnetization. These findings have since been confirmed by a further series of measurements made on the same core in Canberra by Jaeger and Joplin (1955) who, on combining the two sets of results, and giving consideration to the possibility of errors in the marking of the cores, conclude that the upper 700 feet of this particular sill is magnetized normally, while the lower part is reversed.

Following the measurements on this core, two further series of dolerite samples were obtained from cores 5002 and 8102. The results, which have not previously been published, are tabulated below.

These measurements agree very closely with those described previously for core 5001. The only specimen with a dip shallower than 75° was taken from the uppermost part of core 5002, and may well have been affected by lightning or other surface phenomena. In all, the mean value obtained for the inclination form the measurements made on all three cores is 85·5°. This is significantly greater than the present magnetic dip in Tasmania, which has a value of 70°, while the dip corresponding to an axial dipole field is 60°. The measurements therefore suggest that a relative movement has occurred between the land mass and the geographical poles at some time since the Jurassic period.

Table 1. Core 5002

Depth (feet)	Dip (+ve dip up)	Intensity ($\times 10^3$c.g.s.u.)
8	−44°	2·7
13	+86	0·91
30	+84	1·05
49	+86	0·27
71	+80	0·90
92	+82	0·38
125	+84	0·50
152	+84	0·031

Table 2. Core 8102

Depth (feet)	Dip (+ve dip up)	Intensity ($\times 10^3$c.g.s.u.)
500	+90°	4·93
518	+89	2·92
540	+83	5·20
562	+88	6·96
575	+75	7·67
598	+88	6·29
615	+89	9·20
636	+87	7·40

With regard to the magnetic reversal found at a depth of some 700 feet in the first core (no. 5001), it is possible that the rocks of the upper and lower parts of the site were injected at different times and that the Earth's field underwent a reversal in the intervening period. On the other hand, a very careful search for any geological evidence of multiple intrusion has been made and none has been found: it is considered that the sill was emplaced in a single act of intrusion. A second possibility is that the Earth's field reversed during the cooling of the sill: if this were the case it must have done so in an extremely short time. It can be calculated that for a sill 2000 feet thick of rock with a melting range of 1000–800°c, latent heat of solidification 100 cal/gm, thermal conductivity 0·005, specific heat 0·25, and density 2·8 (units calorie and c.g.s., °c) intruded at 1000°c into country rock with the same thermal properties, it will take about 2200 years for a Curie point of 500°c to progress from the contact to the centre of the sill and about 150 years for it to move between the distances of 650 and 750 feet from the contact. Since the region above 650 feet appears to be normal, and that below 750 feet to be reversed, it seems that if a reversal of the Earth's field were 'trapped' in the sill in this way, it must have taken place in the improbably short time of less than 150 years. Finally, of course, there remains the possibility that the apparent reversal is due to some physio-chemical effect in the rocks themselves.

§ 3. MEASUREMENTS ON BASALTS

In addition to the study of the dolerites described above, other sections of the cores were also examined. In particular, a limited number of samples of the tertiary basalt overlying the dolerite were obtained from borings 8102 and 8103. Both these holes penetrate through a number of flows and the cores consist of massive portions interspersed with highly vesicular and much altered material. Measurements were made on eight specimens taken from the massive sections, and the results are tabulated below.

Table 3. Cores 8102 and 8103. Massive Basalts

Core No.	Depth (feet)	Dip (+ve dip up)	Intensity ($\times 10^3$c.g.s.u.)
8103	21	+82°	12·5
8103	155	+84	9·9
8103	191	−85	4·6
8103	285	+80	5·7
8103	360	+89	20·8
8102	416	+83	9·3
8102	444	+85	15·9
8102	469	+77	5·4

Samples taken from the vesicular layers between the massive portions had a much lower magnetic intensity and more widely scattered directions of magnetization, and the results for these sections have not been included in the table.

Despite the small number of specimens measured, it is evident that the magnetic dips correspond closely to those of the older tholeiite sills. There appears to be a single case of magnetic reversal at a depth of 191 feet, but with the limited amount of material available for measurement the possibility of this being spurious, due to an error in marking one of the core sections, cannot be precluded.

§ 4. MEASUREMENTS ON VOLCANIC TUFFS

Of greater interest were the results of the investigation of the tuffs underlying the tholeiite sill in core number 5002, which are probably Triassic in age. They are greyish white in colour and have a rather coarse texture, containing abundant grains of quartz and felspar set in a friable white matrix. Although they have the characteristic features of volcanic tuffs, their precise origin is highly speculative, but the fact that a proportion of the grains are rounded suggest that they may have been transported over considerable distances, and the abundance of clay present, indicates that they were probably deposited in water. We first measured three specimens of these rocks, taken from 175 feet, 185 feet and 195 feet below the present Earth's surface. They were considerably less strongly magnetized than the dolerites and basalts, having a mean magnetic intensity of $4{\cdot}8 \times 10^{-6}$ c.g.s. units, but their directions of polarization again lay close to the vertical. It was found, however, that while the first two specimens were magnetized in a normal upward direction, the third and lowest had a downward dip. This suggested the presence of a magnetic reversal at some depth between 185 feet and 195 feet, and since a fairly complete length of core was available, we decided to investigate the variation of magnetization over this range of depths in greater detail. We, therefore, measured a number of cylinders cut at approximately one foot intervals between 174 feet and 195 feet with the following results :

Table 4. Core 5002. Tuffs

Depth (feet) below surface	Dip (+ve dip upwards)	Intensity of Magnetization ($\times 10^6$ c.g.s.u.)
174·5	+84°	17·3
175	+78	9·0
175·5	+85	19·9
176·5	+84	6·8
177·5	+83	6·8
178·5	−80	8·2
179·5	+81	15·7
180·5	+79	8·9
181·5	+84	3·8
185	+80	4·0
186	+81	4·4
187	+79	14·0
188	+85	8·0
189	+82	5·6
190	+78	15·6
191	+81	2·6
195	−85	0·87

It can be seen from the table that in addition to the reversely magnetized cylinder obtained previously from a depth of 195 feet, a second case of downward dip occurs at 178·5 feet. Now, in the latter instance, the particular specimen concerned had been taken from a continuous section of core, approximately 5 feet in extent, which had been carefully marked over the whole of its length before cutting in the laboratory. The normally magnetized specimens found immediately above and below, at depths of 177·5 feet and 179·5 feet, were also from the same 5 foot section, so that there was no possibility in this case of the reversal being spurious. In order to examine the variation of inclination with depth over the particular region concerned in greater detail, the whole of the 5 foot length was cut into a continuous sequence of thin disks, which were measured separately. We found the inverse magnetization to be confined to a single 5 in. length of core, around 178 feet 4 inches, throughout which the dip had a mean value of 83°, and was directed downwards: the remainder of the section, above and below this, had a mean dip of 82° but was magnetized in an upward sense. The transition from downward to upward polarization at the upper and lower extremities of this 5 in. portion was very sharp, and there was no indication of any continuous systematic variation in the direction of magnetization in passing from the reversed to the normal regions. In fig. 1 the vertical component of the intensity of magnetization is plotted as a function of depth. There is no significant change in intensity close to the ends of the reversed portion, and the specimens showing reverse and normal polarization are, on the whole, equally strongly magnetized. It is evident, therefore that over a range of depths extending from 178 feet 1·5 inches to 178 feet 6·5 inches, the magnetic polarization undergoes a total inversion, and that the transition occurs in a space of a few millimeters, corresponding to the width of a saw cut.

Fig. 1

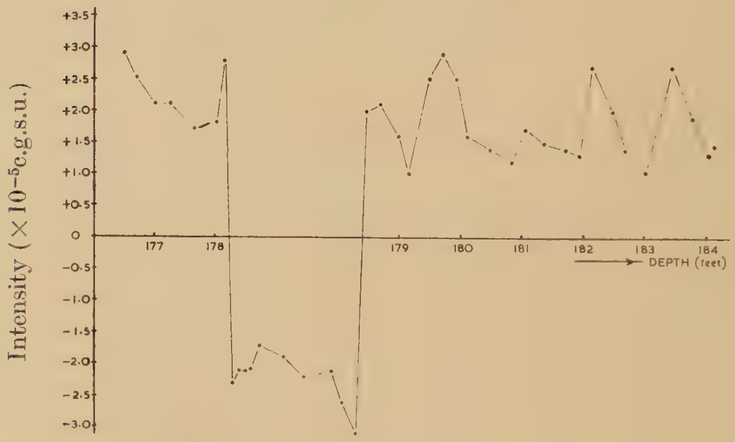

Scale of depth over reversed 5 in. (178 ft. $1\frac{1}{2}$ in.–178 ft. $8\frac{1}{2}$ in.) increased by factor 3.

We subjected a number of specimens to a series of demagnetization and other tests. The demagnetization curves for steady and alternating fields were similar for both normal and reversed specimens, both of which had a natural coercive force of approximately 300 oersteds, and were completely demagnetized in a 50 cycle per second alternating field of about 700 oersteds. In a steady field, of the order of 10 oersteds, there was a time delay effect similar to that described previously by Clegg *et al.* (1954). The rate of rise of magnetization with time of application of field, and the rate of decay after removal of the field were the same for the reversed and normal rocks. We saturated a number of specimens of both kinds in fields of the order of 4000 oersteds, and again we found no difference in behaviour: there was a linear relationship between saturated intensity, J_s, natural remanent magnetization, J_n, the ratio J_s/J_n having a mean value of 15 for normal and reversed samples alike. The remanent coercive force after saturation was the same in both cases.

We are indebted to Mr. J. H. Leng who measured the thermal demagnetization of the rocks, and made an x-ray analysis of the separated magnetic fraction. The demagnetization curves obtained by heating normal and reversed specimens in zero magnetic field were in good agreement, and both were found to have a Curie temperature of 380°. This corresponds well with the Curie point of pyrrhotite (Fe_7S_8), and subsequent x-ray examination of the magnetic component showed it to have the expected hexagonal structure, with a lattice spacing approximating closely to that of the pyrrhotite crystal.

Reviewing the foreging results we conclude that these tuffs contain a single ferromagnetic component, with the crystal structure and magnetic behaviour of pyrrhotite, and that by none of the tests which we applied was it possible to distinguish any difference in the magnetic properties of the normal and reversed specimens.

§ 5. DISCUSSION OF RESULTS OBTAINED FOR VOLCANIC TUFFS

This magnetic reversal, occurring over a narrow range of depths in the volcanic tuffs, poses a number of interesting geophysical problems. The issue is complicated by the uncertainty as to the mechanism whereby the rocks were originally magnetized. They could evidently have acquired their present polarization in one of three ways, viz.:

(i) by orientation of the magnetic particles before consolidation,

(ii) by heating of the magnetic fraction above the Curie temperature during the intrusion of the overlying dolerite sills, or

(iii) by some more subtle physical process at an unspecified intermediate period.

These three possibilities will be considered separately.

(i) *Magnetization before Consolidation*

If the rocks had been produced by a process of slow sedimentation in calm water we might have supposed the reversely polarized section to have been formed, and acquired its magnetization, during a period when the Earth's field was reversed. But these tuffs were produced as a result of volcanic activity, and were laid down rapidly. To account for the result in terms of a change in direction of the Earth's field during deposition it would therefore be necessary to assume that the 5 in. layer showing inverse polarization, and the normally magnetized layers immediately above and immediately below, were the product of three separate volcanic eruptions, between each of which the field underwent a reversal. Now the appearance of this particular portion of the core suggests strongly that it was the product of continuous uninterrupted deposition. The whole of the 5 foot length, including the reversed portion, is uniform in mineral composition and grain size, and there is no trace of bedding planes such as would be expected if considerable intervals of time had elapsed between the deposition of different layers.

It is also possible to explain a magnetic reversal such as this in terms of relative movement between different parts of the sedimentary mass shortly after deposition. It is well known that a recently formed and unconsolidated sediment which has been laid down on a sloping surface may be subject to a considerable degree of slumping, and that this is often so pronounced that certain portions become completely inverted. Now Irving (1954) has shown that the magnetization of some slumped beds is exactly parallel in direction to that in neighbouring undeformed layers, whereas in other slumped beds the magnetic directions are widely scattered, sometimes randomly, suggesting that the magnetization may be fixed in an unconsolidated sediment prior to the deformation. In this latter case, if slumping took the form of a straight inversion, a reversal of magnetization would result. However, there is no sign of any such movements having taken place in these rocks and, even if they had occurred, it would be strange if slumping, which is regarded by geologists as a highly complicated process, should produce an exact 180° inversion without some intermediate directions as well.

(ii) *Magnetization by Heating*

Rejecting tentatively the hypotheses of changes in the Earth's field during deposition, and of slumping, there is an alternative possibility that the present magnetization of these rocks may be due to heating of the tuffs at the time when the overlying dolerite was intruded. Calculations for an intrusion with the physical properties described earlier (see § 2) show that the country rock, whose distance from the contact is less than 0·4 of the thickness of the sill, will be heated above 380°c (the observed Curie point of the present magnetic material). In the present instance there is now 140 feet of dolerite above the tuff, so that it may be expected that the latter was heated above its Curie temperature to within a distance of 56 feet below the contact. The distance may be greater than this since some of the original dolerite has been removed by weathering. The length of core in which this reversal occurs was obtained from a depth of only 30 feet below the floor of the sill, so that it is possible that it acquired a thermoremanent magnetization at the time of injection. Indeed, since there is carbonaceous matter, and so probably sulphur, present in the tuff, it is possible that the pyrrhotite itself was actually formed during heating by the intrusion.

The observed magnetic reversal could evidently have occurred as a result of this heating. It is well known that Néel (1952) has shown on theoretical grounds how it is possible for an igneous rock to acquire a magnetization in a direction opposite to that of the Earth's field at the time of cooling. He suggested four mechanisms whereby such an effect might occur, and his predictions have been brilliantly justified by Nagata's (1953) discovery of self reversing lavas and by Gorter's (1954) synthesis of self reversing ferrites. If, however, such an effect was responsible for the observed reversal in these tuffs, there must have been some physical difference between the directly and inversely magnetized rocks at the time of cooling. That we have been unable to detect any difference in behaviour between the normal and reversed specimens, by our laboratory measurements, may be because the differences which once existed have been obliterated. Alternatively, it may be that the differences still exist but that our tests were not sufficiently sensitive to detect them.

(iii) *Magnetization by some Long Period Process*

An alternative possibility is that the whole rock mass became magnetized uniformly, either before consolidation or by subsequent heating, but that owing to some physical or chemical process which occurred at a later period, the direction of magnetization was changed over a certain range of depths. Changes such as this could take place in either of two ways: they may be due to long period relaxation effects of the kind suggested by Néel (1950, 1951) and detected in igneous rocks by Buddington and Balsley (1954) and by Asami (1954), which would cause the direction of magnetization in the rock to follow the Earth's magnetic field over long intervals of time; or they may be caused by a modification of one of the Néel self-reversing mechanisms already mentioned in a way similar to that described by Graham (1953). These alternatives will be considered separately.

If the reversal is to be explained in the first of the ways suggested, we must assume that the direction of magnetization was initially uniform throughout the whole rock mass, but that owing to long period magnetic instability, it tended to follow the variations in the Earth's field throughout subsequent geological ages. It has been shown by Néel (1950, 1951) that the relaxation times for such long period phenomena depend very critically on the grain size and on the composition of the magnetic minerals present in the rock, so that it is possible, owing to very small differences in constitution, for different sections of the same rock mass to follow the changes in the external field with vastly different time lags, and therefore to have different polarizations at the present time.

The effect of this must be considered in relation to the period of secular variation of the Earth's field, which is of the order of a thousand years, and to the average time interval elapsing between reversals of the Earth's dipole field. If we accept the estimates of Hospers (1954) and of Roche (1950), and take the latter to be of the order of a million years, we must suppose many such reversals to have occurred since these rocks were formed in Triassic times. We will assume for the purpose of the present argument that the field was reversed at the time of formation, and that while the reversely polarized section has relaxation time large in comparison with a million years, and therefore gives a true indication of the magnetic dip at that time, the normal specimens have suffered subsequent changes due to greater instability. We can examine two particular possibilities :

(*a*) If the magnetic relaxation time of the unstable rocks were small in comparison with a thousand years their magnetic directions would lie along the present Earth's field, in which case the dips would have a value of 70°. Since the measured dip (82°) of the normally polarized rocks is significantly greater than this we can discard the possibility.

(*b*) If the relaxation time were considerably longer than a thousand years, but less than a million years, we would expect the polarizations to correspond closely to that of the present axial dipole field, in which case the dips would be of the order of 60°. But if the measured dip of 82° is in fact related to the direction of the dipole field at some time in the past, this would imply that the latitude of Tasmania must then have been 74° South. Thus, if the present magnetic directions of the normally magnetized rocks have been acquired by a relaxation mechanism of this time period, we must assume the postulated Northward movement of Tasmania to have occurred since the most recent reversal of the Earth's field—conceivably within the last million years.

An alternative possibility is that the rocks may have been initially unstable but that the stability has increased at some time in the past. If, for example, the relaxation time immediately after formation was of the order of several thousand years, and if some subsequent physical or chemical change in the magnetic material caused it to increase to many millions of years, the magnetization would become 'frozen' in the direction of the dipole field at the time when the change took place. Such changes need not necessarily occur simultaneously throughout the whole of the rock mass, and if the times of freezing of different parts extened over a number of field reversals we might expect different sections to have diametrically opposite polarizations.

Owing to the great experimental difficulties encountered in obtaining reliable information concerning these long period relaxation phenomena, and the paucity of the present knowledge on the subject, it is not feasible to make any clear estimate of the extent to which the remanent magnetism of these rocks can be attributed to such causes.

Turning now to the possibility that the inversely polarized rocks were magnetized by a long period self reversing process which may have taken place at some time since they acquired their original remanent magnetism, Graham (1953) has put forward a plausible suggestion, based on a consideration of one of Néel's (1952) mechanisms, to show how it might be possible for certain red sandstones to suffer reversal as a result of chemical action after deposition ; and it is possible to visualise other variants of the Néel processes which might cause self reversals to occur in sedimentary rocks. We cannot preclude the possibility of some such magnetic change having occurred in the volcanic tuffs under consideration here, and our results could be explained on the assumption that the rocks were laid down at a time when the Earth's field had the same sense as it has today, and that they became uniformly magnetized in that direction, but that at some later period a magnetic self reversal occurred throughout a particular layer 5 in. in depth. If such were the case, there must evidently have been a difference between the magnetic condition of the layer in which the change took place and the layers above and below which retained their original polarity. As pointed out previously, however, we have been unable to detect any such difference.

Finally, therefore, it seems impossible, on the basis of the present experimental measurements, to form any definite conclusion as to how the observed magnetic reversal occurred in these tuffs. The results, however, do serve to underline the uncertainties attending any discussion of field reversal. There is strong presumptive evidence to support the belief that the Earth's magnetic field has reversed at times during past geological ages. The best of this evidence is furnished by the experiments carried out by Hospers (1954) by Nagata (1953), by Kato *et al.* (1955), and more recently by Leng (1956), on the magnetization of baked rocks surrounding igneous dykes. In these instances, the geological conditions were such that there could be little doubt as to how and when the magnetization was acquired. But in the present case the magnetic history of the material is by no means certain, and it has been shown that there are at least two possible explanations, based on the hypotheses of slumping, and of a self reversing mechanism, which could account for the observed results without stipulating any change in the Earth's dipole field in past ages. It may be that with the development of more searching laboratory tests in the future, some of the present obscurities will disappear. In the meantime every case of magnetic reversal in rocks must be treated on its own merits, and its implications must be considered with reserve.

ACKNOWLEDGMENTS

We gratefully acknowledge the help and advice we have received on this work from Professor P. M. S. Blackett. We are indebted to Mr. P. H. S. Stubbs and Mr. E. Irving for their criticism and discussion of our conclusions. We also wish to thank Mr. A. H. Chapman who was responsible for a number of the experimental measurements, and Dr. J. H. Leng who carried out the thermal and x-ray tests on the specimens. The rock cores were supplied by courtesy of the Hydroelectric Commission of Tasmania.

REFERENCES

ASAMI, E., 1954, *J. Geomag. Geodec.*, **6,** 145.

BALSLEY, J. R., and BUDDINGTON, A. F., 1954, *Tech. Comm. Paleomagnetism*, Xth Assembly, ATME, IUGG, Rome.

BLACKETT, P. M. S., 1952, *Phil. Trans. Roy. Soc.*, **245,** 309, 1952.

CLEGG, J. A., ALMOND, Mary, and STUBBS, P. H. S., 1954, *Phil. Mag.*, **45,** 583.

GORTER, E. W., 1954, *Thesis*, University of Leiden.

GRAHAM, 1953, *J. Geoph. Res.*, **58,** 243.

HOSPERS, J., 1953, *Proc. Kon. Ned. Acad. Wet.* B, **56,** 467 ; 1954, *Ibid.*, **67,** 112.

IRVING, E., 1954, *Ph.D. Thesis*, Cambridge.

JAEGER, J. C., and JOPLIN, G., 1955, *Geol. Soc. Australia*, **2,** 1.

KATO, Y., TAHAGI A., and KATO, I., *J. Geomag. Geodec.*, *Kysto*, **6.**

LENG, J. H., 1956 *Ph.D. Thesis*, Imperial College, London.

NAGATA, T., 1953, *Nature, Lond.*, **172,** 850.

NÉEL, L., 1952, *Phys. et Rad.*, **11,** 49 ; 1951, *Ibid.*, **12,** 339 ; 1952, *Ibid.*, **13,** 249.

ROCHE, A., 1950, *Comptes Rendus*, **230,** 1608.

LXXIX. CORRESPONDENCE

The Migration of Copper Atoms on the Surface of Silver

By R. B. Kehoe,[†] R. C. Newman[‡] and D. W. Pashley[§]
Physics Department, Imperial College, London[||]

[Received May 23, 1956 ; in revised form June 25, 1956]

The phenomenon of epitaxy in thin metal layers deposited by evaporation on to single crystal subtrates is well known. It was first demonstrated by Lassen and Bruck (1935) who deposited silver on to the cleavage face of rocksalt and examined the deposit by electron diffraction. Further studies have been made almost exclusively by this method (for a summary, see Pashley 1956). The mode of growth of these epitaxial deposits has been the subject of much conjecture (e.g. Elleman and Wilman 1948 and Frank and van der Merwe 1949, 1949–50) but there is no direct experimental evidence for any particular mechanism.

We have recently carried out a number of experiments in which copper was condensed on to a smooth (111) silver surface, which had been formed by deposition on to heated mica. The silver surface was maintained at about 270°c during the growth of the copper which was deposited at about 5 Å $\sec^{-1}$ in a vacuum of better than 10^{-4} mm Hg. Electron diffraction examination of the layer during its growth showed that the copper was oriented in double positioning with its (111) plane parallel to the silver surface (Kehoe, Newman and Pashley 1956). The deposits were subsequently examined in an optical microscope. In general, the copper had formed as a number of isolated crystallites which could barely be resolved. However, one particular specimen with a copper deposit of about 200 Å thickness showed some remarkable features which may throw light on the growth mechanism.

(i) The copper had grown in the form of a large number of isolated crystallites with pronounced triangular bases (see fig. 1), the edges of which were parallel to the silver $[1\bar{1}0]$ directions. The size distribution of the crystallites is given in the table. If it is assumed that the crystallites are triangular pyramids with cube side faces, the mean thickness can be calculated as 220 Å, in good agreement with the thickness estimated from the amount of copper deposited.

(ii) There were several line irregularities in the silver surface, initiated by the cleavage steps in the mica substrate. The copper crystallites had grown preferentially along these irregularities. This is shown in fig. 2, which also shows clearly on either side of the irregularity a band of silver on which no copper crystallites had formed.

[†] Now at the G.E.C. Research Laboratories, Wembley.

[‡] Now at the A.E.I. Research Laboratory, Aldermaston.

[§] Now at the Tube Investments Research Laboratories, Hinxton Hall, Cambridge.

[||] Communicated by the Authors.

These observations would be explained qualitatively by the growth mechanism suggested by Frenkel (1923). After deposition the copper atoms retain a certain mobility and move over the surface as a two-dimensional gas. By collision with each other, the copper atoms form mobile aggregates which eventually come to rest in the form of oriented crystallites as energy is lost to the substrate lattice. These act as nuclei for further growth by the direct impact of other mobile atoms or aggregates.

It is reasonable to suppose that the irregularities in the surface would act as traps for these mobile aggregates ; this would lead to preferential growth along the irregularities, resulting in a lowering of the density of the completed crystallites in the immediate neighbourhood of the imperfection. This effect is well illustrated in fig. 2. From the width of the lowly populated region, it follows that copper can migrate a distance of at least 10 μ at the substrate temperature of 270°c. Large migration distances of metal atoms on glass surfaces have been observed by Andrade (1935).

Crystallite edge length (μ)	Number per cm^2
$<0{\cdot}6$	510×10^4
0·6–1·2	294×10^4
1·2–1·8	81×10^4
1·8–2·4	89×10^4
2·4–3·0	46×10^4
3·0–3·6	6×10^4

According to the above growth mechanism, the orientation of a completed crystallite is determined by the initial very small aggregate of atoms which forms a nucleus probably at some preferred point on the substrate. Other atoms added to the nucleus simply continue its structure. It is the orientation of the initial nucleus that should be considered in any theory of orientation.

The electron diffraction examination showed that between the visible crystallites there was no monatomic or thicker coherent copper layer. This indicates that the growth cannot have been by the mechanism suggested by Frank and van der Merwe (1949, 1949–50).

Why the specimen described above behaved differently from the rest is not clear, but is presumably due to differences either in the surface cleanliness or the local surface structure. All of the silver substrates were prepared in a vacuum of better than 10^{-4} mm Hg, and then stored in corked bottles for periods of up to several days before use. Normally, such storage did not influence the mode of growth of the copper in any detectable manner. It is therefore assumed that the specimen described above became contaminated in some way, either during this storage or during manipulation. It seems possible that this contamination influenced the mobility, without affecting the basic growth mechanism. An electron microscope investigation of the normal specimens would be of interest, as a check on this point.

ACKNOWLEDGMENTS

The authors wish to express their gratitude to Dr. M. Blackman for helpful discussions.

Two of the authors (R. B. K. and R. C. N.) are indebted to the University of London for Postgraduate Studentships, and the former also to the Department of Scientific and Industrial Research for a maintenance grant. The third author (D. W. P.) is an I.C.I. Research Fellow of the University of London.

REFERENCES

ANDRADE, E. N. DA C., 1935, *Trans. Faraday Soc.*, **31,** 1137.
ELLEMAN, A. J., and WILMAN, H., 1948, *Proc. Phys. Soc.*, **61,** 164.
FRANK, F. C., and VAN DER MERWE, J. H., 1949, *Proc. Roy. Soc.* A, **198,** 205; 1949–50, *Ibid.*, **200,** 125.
FRENKEL, J., 1923, *Z. Phys.*, **26,** 117.
KEHOE, R. B., NEWMAN, R. C., and PASHLEY, D. W., 1956, *Brit. J. Appl. Phys.*, **7,** 29.
LASSEN, H., and BRUCK, L., 1935, *Ann. Phys., Lpz.*, **22,** 65.
PASHLEY, D. W., 1956, *Advances in Physics*, in the press.

Evidence for Direct Emission of a Pair of γ-Rays from the Point of Decay of a K-Meson

By M. S. SINHA and N. C. DAS
Bose Institute, Calcutta

Until now six different modes of K-meson decay are known, namely, $K_{\mu2}$, $K_{\pi2}$, K_{e3}, $K_{\mu3}$, τ and τ' ($K_{\pi3}$) (Ritson *et al.* 1956). The authors in the above reference suggested for $K_{\mu3}$ a decay scheme of the type $K_{\mu3}\rightarrow\mu+\pi^{\circ}+\nu$ to explain satisfactorily their observed results. Hoang *et al.* (1956) of Rochester University have also shown evidence for the same decay scheme of $K_{\mu3}$. We reproduce here a cloud chamber picture (Pl. 40) which, however, appears to show an alternative mode of decay for $K_{\mu3}$. The electron pairs E_1 and E_2 produced at the tenth and ninth plates respectively (plates used are all aluminium of vertical thickness 2·64 gm/cm²) are clearly associated with the decay point O of the particle PP_1O which undergoes a nuclear scattering in the last (eleventh) plate and shows itself above the plate with more than four times minimum ionization. The particle traverses within the chamber over 45 cm at about minimum ionization and also about 1 cm after scattering, and as such its life time is not inconsistent with the value of 1×10^{-8} sec (Hoang *et al.* 1956, Iloff *et al.* 1955). The charged secondary OS is produced at minimum ionization and remains minimum after passing through 8 gm/cm^2 of aluminium. It is interesting to note that the electron pairs E_1 and E_2 are observed in the stereo projection, to lie within experimental errors, in the same plane as the charged primary and the secondary.

We face a serious difficulty in the intrepretation of this event if we consider the two γ-rays to have resulted from a neutral π-meson. The opening angle θ of the two γ-rays as measured by joining the axes of the electron pairs in stereoprojection comes out to be $8^\circ\pm1^\circ$, and on the assumption that the available momentum is equally shared by the two γ's between themselves it leads to a minimum momentum of 1·9 Bev/c in the laboratory system for the π° supposed to be emitted from the point of decay. The charged secondary makes an angle of 68° with the primary and the two γ's 63° and 71° respectively. So if we assume a two-body decay, the momentum of the charged secondary in the laboratory system also comes out to be about 1·9 Bev/c which is quite inconsistent with the ionization of the parent particle before decaying. The charged secondary must have a moderately low momentum and in order to balance this momentum with the momenta of the two γ-rays we have to give up the assumption that the two γ's are produced from a π° emitted at the point of decay. We therefore suggest the following decay scheme for this event:

$$\mathrm{K}_{\mu3}\rightarrow\mu+\gamma+\gamma.$$

Now since we are not in a position to make an exact identification of the charged secondary of the K-meson decay, there also remains the possibility of the decay scheme $\mathrm{K}_{e3}\rightarrow e+\gamma+\gamma$. Either of these two decay schemes, however, makes the parent particle a Fermion. But if all K-particles are assumed to be Bosons (Hoang *et al.* 1956) the charged secondary has to be a π-meson, which is also consistent with the fact that the parent K-particle has suffered a nuclear scattering in the last plate.

The opening angles of the electron pairs E_1 and E_2 as seen after they have emerged from the aluminium plates (less than 0·5° and 0·8° respectively) lead to a rough estimate of the K-meson mass as 1462 m_e. But since multiple scattering of the electrons in passing through the aluminium plates results in a great uncertainty in the values of these opening angles, the above mass value is not very reliable. We cannot definitely say that the mass of this K-particle is different from that of a τ-meson of mass 965 m_e or that of a $\mathrm{K}_{\mu2}$ of mass 941 m_e (Leprince-Ringuet *et al.* 1955), although the high ionization of the parent particle and small opening angles of the electron pairs suggest a mass near about 1462 m_e.

ACKNOWLEDGMENTS

We wish to thank the Atomic Energy Commission, Government of India, for generous support and to Prof. D. M. Bose for constant encouragement and advice and also for offering facilities to work at the High Altitude Research Station of the Bose Institute at Darjeeling.

REFERENCES

HOANG, T. F., *et al.*, 1956, *Phys. Rev.*, **101,** 1834.
ILOFF, E., CHUPP, W. W., *et al.*, 1955, *Phys. Rev.*, **99,** 1617.
LEPRINCE-RINGUET, 1955, *Proc. of the Fifth Annual Rochester Conf.*, 75.
RITSON, D. M., *et al.*, 1956, *Phys. Rev.*, **101,** 1085.

LXXX. REVIEWS OF BOOKS

Reactor Physics. By D. J. Littler and J. F. Raffle. (Permagon Press.) [Pp. 196.] Price 25*s*.

This little book will be welcome to the growing number of nuclear engineers which our atomic age requires.

About the first quarter of it is an exposition in simple terms of atomic and nuclear physics, with a minimum of mathematics. A certain amount of calculus is unavoidably used in the later chapters which deal with neutron diffusion theory, calculation of lattice constants and critical sizes, the effect of air gaps, reflectors and delayed neutrons. Problems of shielding and radiation damage are discussed as well as relevant measuring techniques.

The book is written in an attractive straightforward style and illustrated with many well-designed diagrams. O.R.F.

Electric Dipole Moments. By J. W. Smith. (London: Butterworths Scientific Publications.) [Pp. 370.] Price 42*s*.

This book sets out to describe the principles underlying the various methods of measuring permanent molecular dipole moments and the interpretation of the results in terms of modern theories of electronic structure.

The classical method for the determination of dipole moments based on temperature dependence of dielectric constant of a gas or a dilute solution is historically most important and receives most attention, experimental methods and the analysis of data being described in some detail. Less attention is given to the recent development of more accurate microwave methods based on the Stark effect.

In dealing with interpretation the author adopts the general approach of dividing the total moment into bond moments and then allowing for various corrections due to factors such as lone pairs and inductive and mesomeric displacements. This is a satisfactory procedure provided the reader keeps in mind the essentially arbitrary nature of the separation into bond moments, which are not in themselves observable. There is a long discussion of the dipole moment of the C–H bond, for example, comparing various proposed values and the attempts of various experimentalists to measure it, but no clear definition of what is meant by the concept. Nevertheless, if the basic qualitative idea is accepted, subsequent chapters on the effect of various electronic factors form an interesting account of the use of a physical property of a molecule in interpreting its chemical behaviour. There are final chapters on the information dipole moment data gives about restricted rotation and molecular association.

One missing feature that might have been expected is an adequate table of measured values of dipole moments. Many values are quoted at various points in the text to illustrate particular points but a systematic compilation of the more important measurements in an appendix would have added to the value of the book as a work of reference. J.A.P.

[*The Editors do not hold themselves responsible for the views expressed by their correspondents.*]

Fig. 5

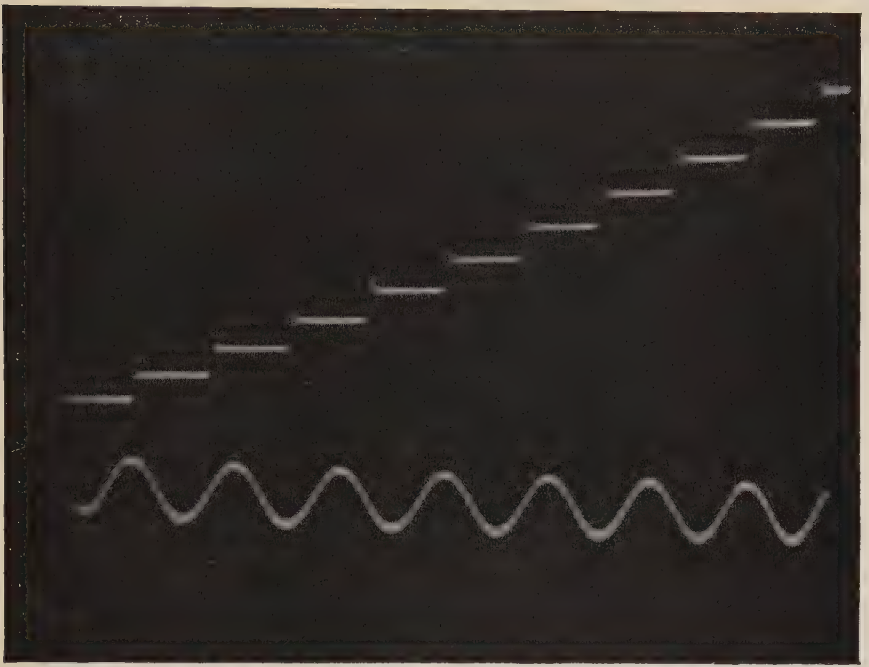

Oscillograph record of displacement of end of steel rod 1 metre long and 1·25 cm in diameter when 0·01 grams of lead azide have been detonated at the opposite end. (Period of timing wave 500 microseconds.)

Fig. 6

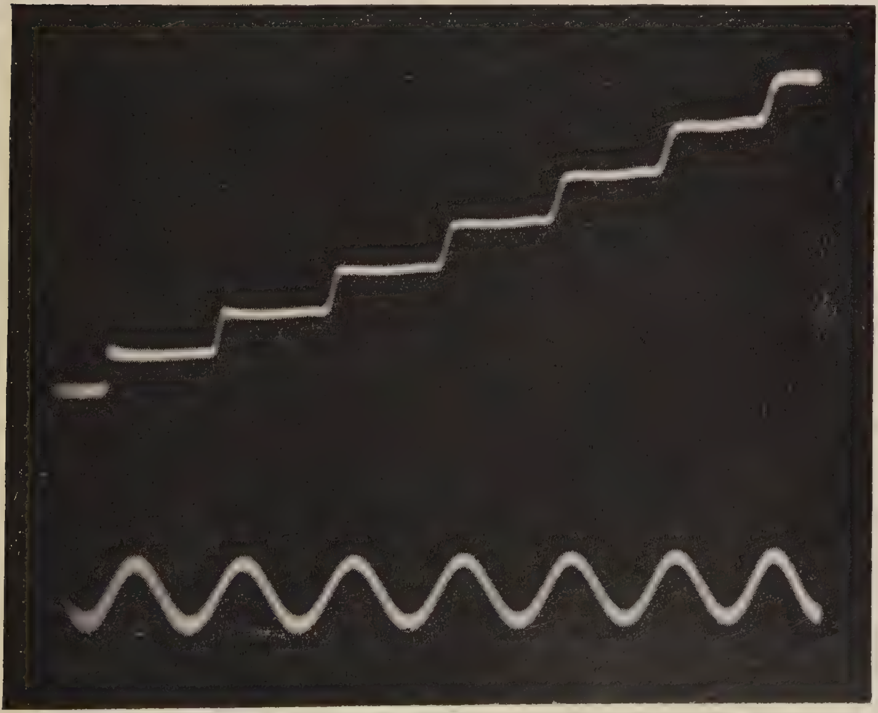

Oscillograph record of displacement of end of polystyrene rod 50 cm long and 1·25 cm in diameter when 0·005 grams of lead azide have been detonated at the opposite end. (Period of timing wave 500 microseconds.)

Fig. 7

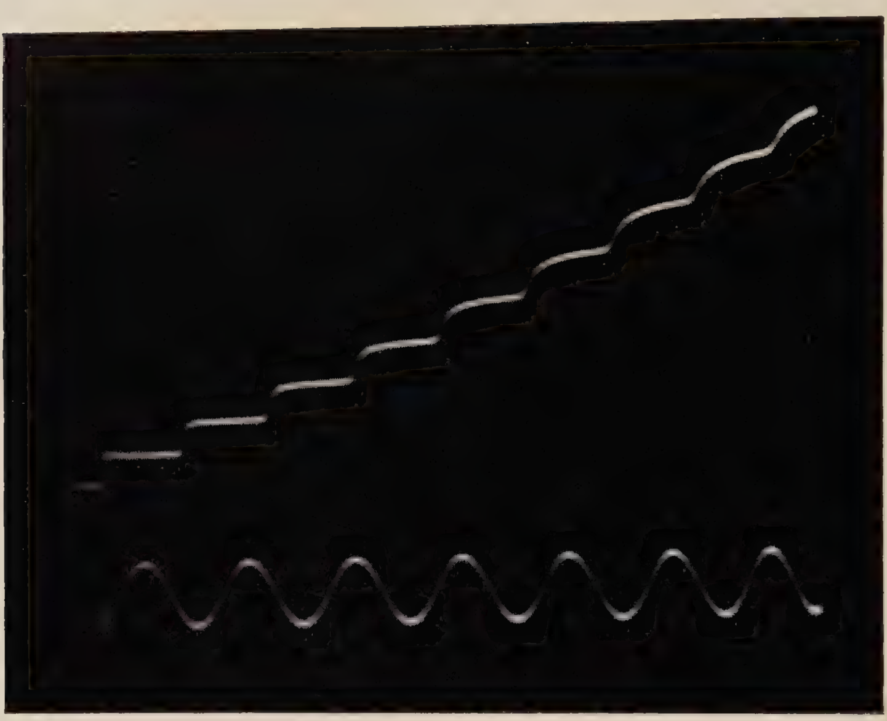

Oscillograph record of displacement of end of polymethylmethacrylate rod 46 cm long and 1·25 cm in diameter when 0·005 grams of lead azide have been detonated at the opposite end. (Period of timing wave 500 microseconds.)

Fig. 8

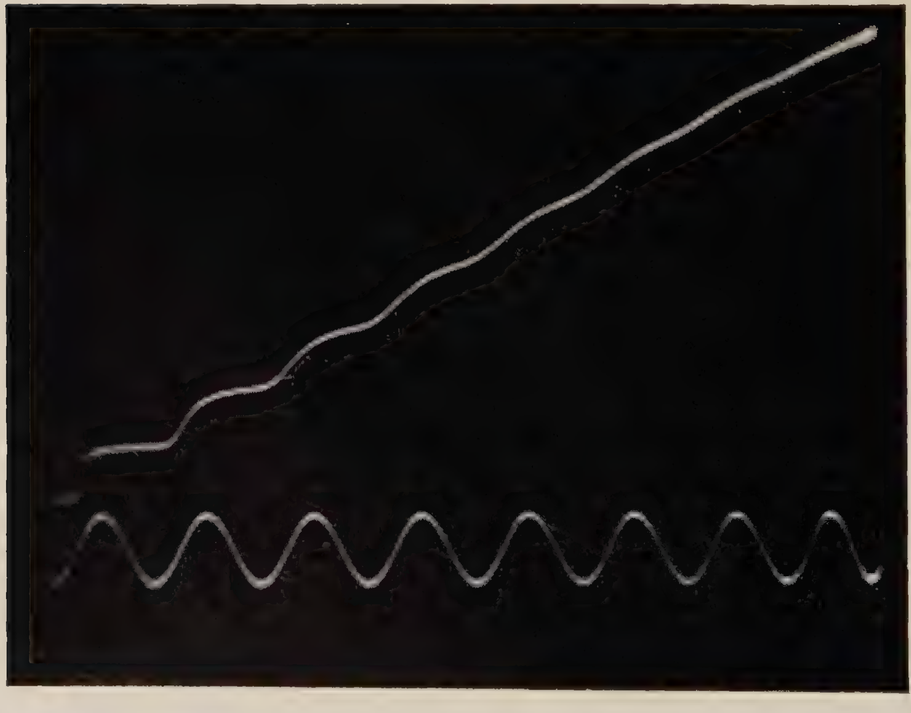

Oscillograph record of displacement of end of polythene rod 20 cm long and 1·25 cm in diameter when 0·005 grams of lead azide have been detonated at the opposite end. (Period of timing wave 500 microseconds.)

Fig. 1

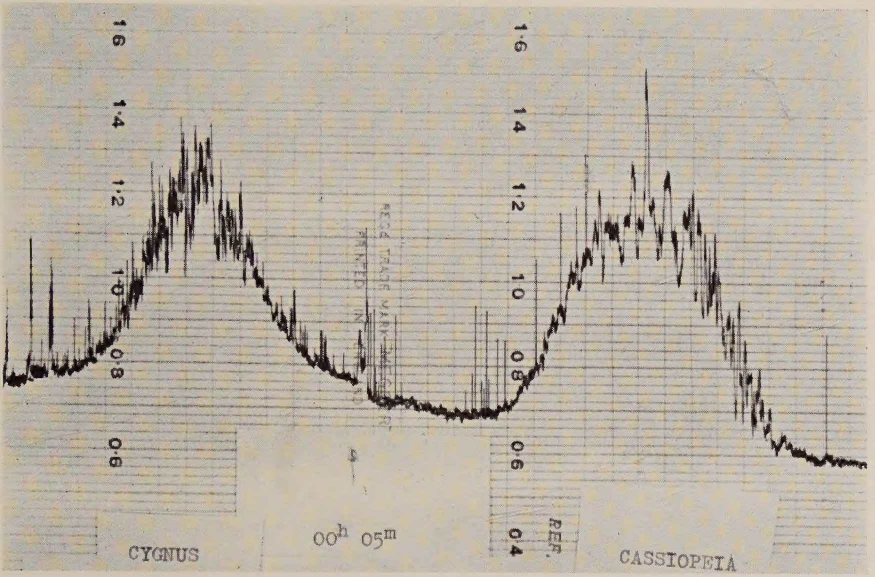

Facsimile of the record of the transit of Cygnus and Cassiopeia on 1955 August 11th–12th, showing scintillations. Radio frequency 30 Mc/s.

Fig. 4

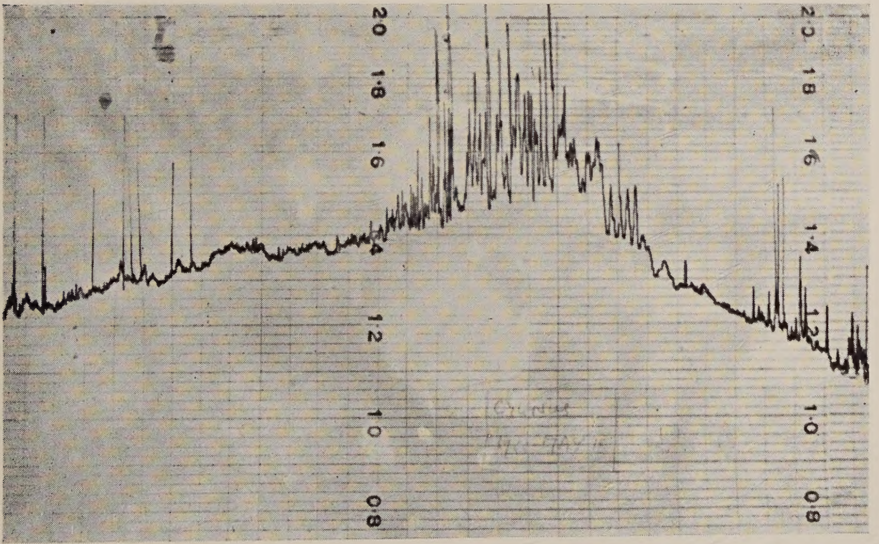

Facsimile of the record of the transit of Cygnus on 1955 May 18th. Radio frequency 22·6 Mc/s.

Fig. 1

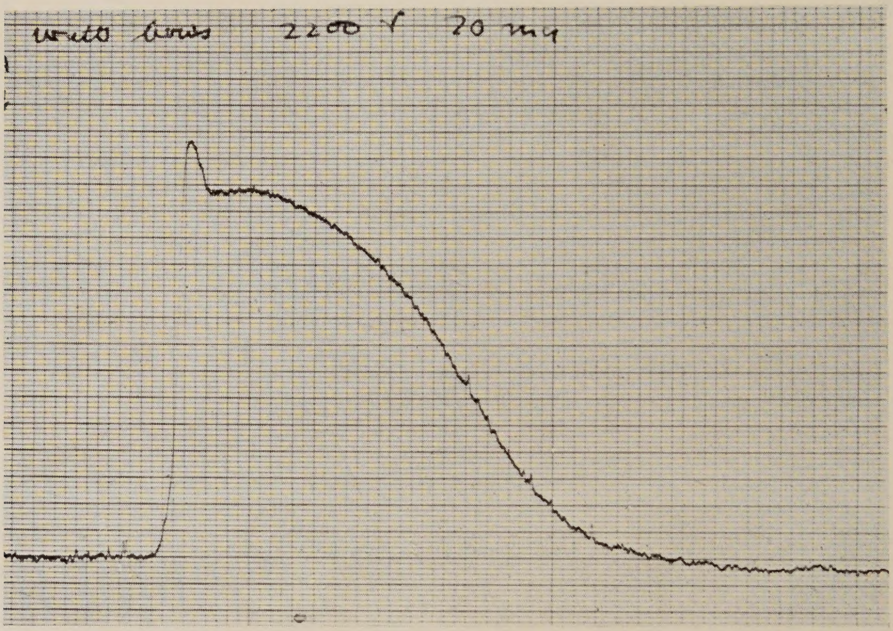

Microphotometer record of Mg ($L_{23}V$) Band.

Fig. 1

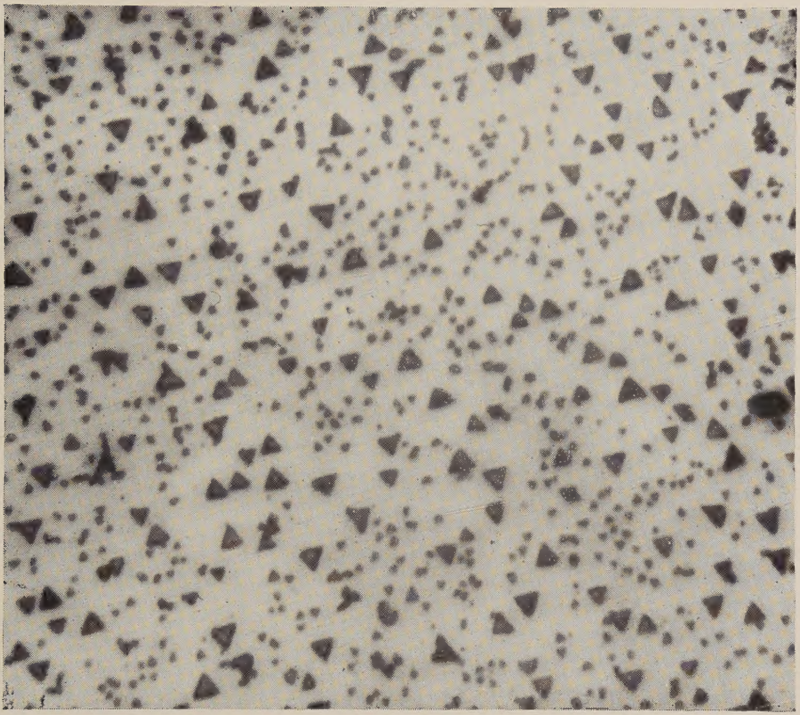

Triangular-based copper crystallites. Magnification ×1000.

Fig. 2

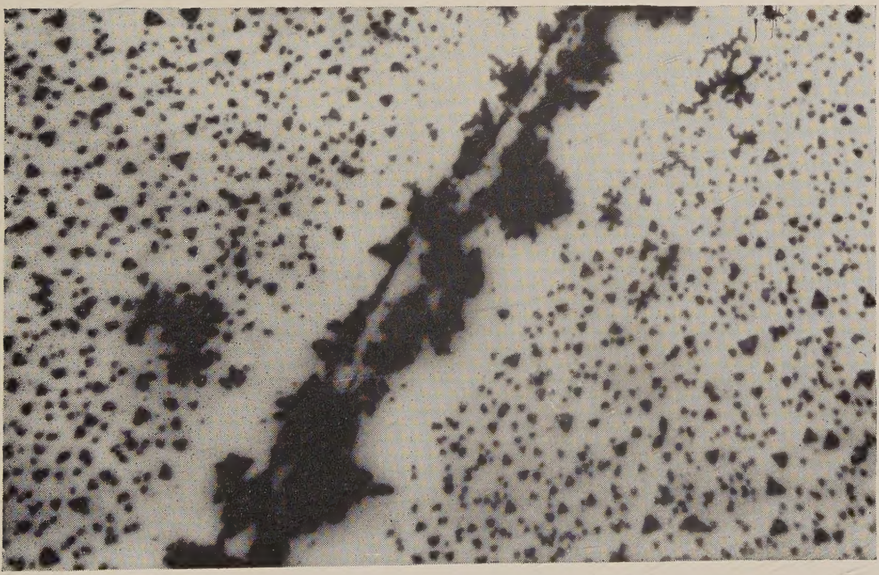

Mode of growth of copper crystallites in the neighbourhood of a surface irregularity. Magnification ×750.

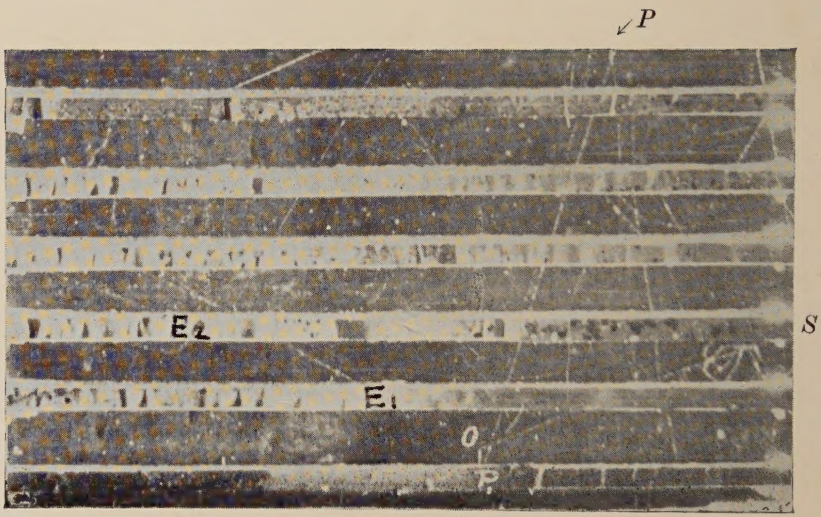
P
E_2
S
E_1
O
P